# Differentiating between types of meningitis in a paediatric population using $^{1}$H-NMR metabolomics


## CDW van Zyl

orcid.org 0000-0001-8883-471X


Dissertation accepted in partial fulfilment of the requirements for the degree *Master of Science in Biochemistry* at the North-West University

| | |
|---|---|
| Supervisor: | Dr SW Mason |
| Co-Supervisor: | Prof DT Loots |
| Assistant Supervisor: | Dr RS Solomons |

Graduation October 2020

22130438

# PREFACE

Through the journey of this study I have gained an abundance of experience in my personal life and in my professional career. Thank you to Dr. Shayne Mason for all the assistance, patience, motivation and guidance throughout this journey it is deeply appreciated. Prof Du Toit Loots for the valuable inputs and guidance. Thank you to my family and friends who stood by me when the going got tough. When approaching any new prospect in life always stay flexible and fluid, don't become complacent, always keep growing and becoming a better version of yourself.

## SUMMARY

Meningitis is a disease characterized by the inflammation of the meninges and spinal cord that is most commonly caused by viruses and bacteria and can be classified into two categories. 1) Acute meningitis (rapid onset), the most common form of meningitis, is caused by infectious agents such as viruses (i.e. enteroviruses, herpes simplex viruses, and mumps virus) and bacteria (i.e. *Streptococcus pneumoniae*, *Neisseria meningitidis*). 2) Chronic meningitis is characterized by gradual (delayed) symptoms over weeks to months. The most common form of chronic meningitis in the South African paediatric population of the Western Cape province is tuberculous meningitis (TBM), caused by the endemic bacillus *Mycobacterium tuberculosis* (*M.tb*).

Metabolomics is the science of analysing the small molecules (metabolites) in a biological system. Proton nuclear magnetic resonance ($^{1}$H-NMR) spectroscopy is a method that does not require prior separation of metabolites, and is able to simultaneously detect and determine the concentration of all types of metabolites, above the detection limit of 1 µM, that are present in a complex biological sample. It is well-known that the $^{1}$H-NMR analytical platform is highly repeatable, due to calibration steps performed prior to each sample analysed. Since the technical variation can be considered negligible, the analytical variation – analyst repeatability – was assessed (Chapter 3). An artificial cerebrospinal fluid (CSF) sample was created by mimicking the natural salt and buffering capacity and spiking with nine of the most common CSF metabolites. Repeat analyses was performed on three levels – low (50%), medium (100%) and high (150%) concentrations of normal reference ranges. From the acceptable repeatability results it was concluded that the analyst (myself) is competent and repeatable, capable of producing reliable $^{1}$H-NMR data.

$^{1}$H-NMR metabolomics can be a valuable approach to expand upon existing knowledge of meningitis, however, only a few $^{1}$H-NMR metabolomics studies are available in the literature to aid in the metabolic characterization of meningitis. A gap exists in the literature where the possibility of a CSF metabolic profile can be used to identify differences between types of meningitis. Hence, $^{1}$H-NMR metabolomics was used in this study to analyse the CSF of a South African paediatric cohort to better characterise cases with acute and chronic meningitis.

Firstly, CSF of a TBM sample set was compared to that of CSF from a control sample set (Chapter 4). After strict exclusion criteria, quality control checks and data filtering, statistical analyses identified markers that differentiated TBM from controls. Herein lies the strength of our study – we started with ~100 TBM and ~97 control cases, more than any other study, and we were able to refine them into a well-defined TBM group (n=23) and a homogenous control group (n=33).

Initial analysis revealed that the dominating discriminators were decreased glucose and elevated lactate in TBM cases. Removal of the NMR spectral regions representing glucose and lactate allowed us to examine the remaining metabolic profile more closely. The main differentiating metabolites identified were: acetate, alanine, choline, citrate, creatinine, isoleucine, lysine, myo-inositol, pyruvate, valine, 2-hydroxybutyrate, carnitine, creatine, creatine phosphate, glutamate, glutamine, guanadinoacetate, and proline. Of these 18 metabolites, the first 10 overlap with other studies in the literature, while the last eight metabolites are unique to this study. These eight unique metabolites led to the identification of five metabolic pathways that are significantly altered in a brain infected by *M.tb,* namely: uncontrolled glucose metabolism, increased carnitine, upregulated proline and creatine metabolism, and disrupted glutamate-glutamine cycle TBM cases. Associated with oxidative stress and chronic neuroinflammation, our findings cumulatively contribute toward destabilization of the blood brain barrier (BBB); hence, increasing BBB permeability, which is associated with increased intra-cranial pressure – a clinical hallmark of advanced meningitis, particularly in TBM.

Lastly, a comparison was also made between the CSF metabolic profile for viral (acute) meningitis (VM) to that of a control CSF sample set and that of a TBM sample set (Chapter 5). Following the same $^{1}$H-NMR metabolomics workflow, it was found that the VM and control groups did not distinguish form each other and led to the postulation that, in our paediatric cohort, VM has the same CSF metabolic profile as controls. This postulation was supported by the findings when comparing TBM and VM metabolic profiles, which were very similar to the comparison of TBM to controls. The metabolites differentiating TBM from VM were: valine, alanine, glutamine, lysine, choline, carnitine, creatine, isoleucine, proline, myo-inositol and guanadinoacetate. Thus, VM has the same metabolic profile as controls, as very similar metabolites were identified to be of statistical significance when cross comparison was done.

The metabolic insights gained from this investigation improve upon our understanding of TBM, and contribute toward the metabolic characterization of TBM to aid in future diagnostic and possibly therapeutic research. Furthermore, this study opens up a vast number of future directives for TBM research, some of which are listed at the end of my thesis.

Keywords: cerebrospinal fluid (CSF), proton magnetic resonance ($^{1}$H-NMR) spectroscopy, tuberculous meningitis (TBM), paediatrics, metabolomics, metabolic characterization, viral meningitis (VM).

# TABLE OF CONTENTS

# LIST OF TABLES

# LIST OF FIGURES

# CHAPTER 1 INTRODUCTION

## 1.1 Background

Meningitis is an inflammation of the meninges caused by foreign pathogens that cross the blood-brain barrier (BBB) and elicits an immune response. The most common pathogens of meningitis are of viral and bacterial origin. People of any age can contract meningitis, however, people of a young age (≤12 years) are more vulnerable to contracting meningitis as their immune systems are not fully developed yet and are unable to fight of the foreign pathogen systemically, resulting in increased risk of it crossing the BBB, resulting in meningitis. Viral meningitis is the most common form of meningitis and can be caused by enteroviruses, mumps and herpesviruses, and is also known as an acute/aseptic form of meningitis. Bacterial meningitis is a less common form of meningitis, caused by a wide range of bacteria. Infants are especially susceptible to this and can lead to various developmental issues. In South Africa, a higher than normal instance of tuberculous meningitis exists due to the high prevalence of pulmonary tuberculosis in the country. Tuberculous meningitis is the most severe manifestation of tuberculosis and is known as a chronic form of meningitis as it develops over a long period resulting in severe neurological complications, and with delayed treatment can lead to death. Tuberculous meningitis is difficult and time intensive to diagnose and distinguish from other types of meningitis as the initial symptoms of all meningitis are very similar. Diagnostic clinical tests take a long time as culturing is needed for a definitive result. Thus a need exists for more rapid and definitive diagnostic methodologies.

Metabolomics of meningitis is still a relatively unexplored field of research, especially in a paediatric population. Considering the above, metabolomic profiling of various meningitis types can be beneficial in the expansion of existing knowledge of meningitis, and improve upon diagnostic efficiency, resulting in faster treatment and lower mortalities.

## 1.2 Aims and objectives

### 1.2.1 Aims

Characterize the CSF metabolic profile of chronic (TBM) meningitis and acute (VM) in a South Africa paediatric population, in order to identify markers that better characterise the disease and possibly assist in an early, differential diagnosis.

### 1.2.2 Objectives

1) Analyst competency training – learning relevant SOPs within NWU Centre for Human Metabolomics (CHM) and perform repeatability studies on the NMR to ensure minimal analytical variation from the analyst (myself) (Chapter 3).
    - Create a synthetic quality control CSF sample containing at least nine metabolites at high (150 % of normal), normal (100%) and low (50 % of normal) concentration values.
    - Analyse repeatability of synthetic quality control CSF samples to determine analyst competency.

2) Perform an untargeted $^{1}$H-NMR metabolomics analysis on collected patient CSF samples and use univariate and multivariate statistics to:

    - 2.1 Characterise CSF metabolic profile for chronic (TBM) meningitis by comparison to that of a control CSF sample set (Chapter 4).
    - 2.2 Characterise CSF metabolic profile for acute (VM) meningitis by comparison to that of a control CSF sample set and that of a TBM sample set (Chapter 5).

## 1.3 Structure of dissertation and research outputs

Chapter 1 (current chapter) is a brief background of this study outlining the aims and objectives. Chapter 2 is a literature overview of viral, bacterial and tuberculous meningitis, and an overview of $^{1}$H-NMR metabolomics and existing $^{1}$H-NMR metabolomics studies on meningitis in the literature. Chapter 3 explains the process of how objective one was achieved – ascertaining analyst competency and repeatability. Chapter 4 is the main output of this study – addressing objective 2.1 by comparing CSF metabolic profiles of TBM cases to that of controls, and is presented in the form of a manuscript submitted to the Journal of Infection for peer-review, and, eventually, publication. Chapter 5 addresses objective 2.2 by comparing the metabolic profiles of VM to that of TBM and controls. Chapter 6 is the final conclusion summarizing the results in context of the aim/objectives and gives directives for future research.

## 1.4 Author contributions

The primary author/investigator is C.D.W. van Zyl. C.D.W. van Zyl was responsible for project planning, sample analysis, data analyses and writing of this dissertation, as well as all other documentation and the publication associated with this study. Dr S. Mason served as supervisor, and supervised all aspects of this study, including the project design, planning, sample analysis, and writing of this dissertation, as well as all other documentation and the

publication associated with this study. Prof D.T. Loots served as co-supervisor, and supervised aspects relating to project design, planning, and critical feedback on the dissertation, as well as all other documentation and the publication associated with this study.

I declare that my role in this study, as indicated above, is a representation of my actual contribution, and I hereby give my consent that this work may be published as part of the M.Sc. dissertation of C.D.W. van Zyl.



C.D.W. van Zyl Dr. S. Mason Prof. D.T. Loots

# CHAPTER 2 LITERATURE OVERVIEW

## 2.1 Introduction

Meningitis is a disease characterized by the inflammation of the meninges and spinal cord. The meninges consists of three layers of membrane (dura mater, arachnoid mater and pia mater) that surrounds the brain and spinal cord in order to protect it. The space between the meninges is known as the subarachnoid space, through which cerebrospinal fluid (CSF) is able to flow. CSF is a highly regulated bio-fluid produced in the ventricles of the brain, and serves a similar purpose as blood. Meningitis is usually caused by an infection, however, it can also occur as a response to non-infectious agents that are introduced into the subarachnoid space. Non-infectious meningitis is a rare occurrence in comparison to the prevalence of infectious meningitis, since the latter is able to spread more readily from person to person (Tunkel & Scheld, 1993). Infectious meningitis, can occur at any age, and is a serious disease of the central nervous system (CNS), that is characterised by inflammation of the meninges due to an immune response elicited against the invading microbial infection.

Meningitis is most commonly caused by viruses (i.e. enteroviruses, herpes simplex viruses (HSV), and mumps virus) and bacteria (i.e. *Streptococcus pneumoniae*, *Neisseria meningitidis*), although rare parasites and fungi may also be considered causative agents of such (Torpy *et al.*, 2007). Acute meningitis is the most common form of meningitis and is characterised by a rapid onset, while chronic meningitis is characterised by delayed symptoms over many weeks to months. Some patients may also present with some of the acute meningitis symptoms, however, the onset of the symptoms may be more gradual. Chronic meningitis can be caused by *Mycobacterium tuberculosis* (*M.tb*), *Cryptococcus neoformans*, *Candida* spp., and Coccidioides (Tunkel & Scheld, 1993). In this study I will be focusing on the more commonly occurring form of paediatric bacterial meningitis in the Western Cape of South Africa, namely tuberculous meningitis (TBM) — induced by *M.tb* (Wolzak *et al.*, 2012).

The clinical presentation of meningitis typically varies from individual to individual, and largely depends on the virulence of the causative agent, the spread to the CNS, and the area of CNS infected. Headache, fever, stiff neck, vomiting and confusion are all symptoms and are common to many types of meningitis (i.e., bacterial and viral). Definitive diagnosis of meningitis however, is made by analysis of CSF culture and/or polymerase chain reaction (PCR) from a lumbar puncture (LP), which may take several days or even weeks to accomplish. The remainder of this literature overview will briefly cover the causative agents,

clinical symptoms, pathological ranges, pathological tests and current diagnostic measures for viral meningitis (VM), bacterial meningitis (BM), and TBM.

## 2.2 Viral meningitis

### 2.2.1 Background

Viral meningitis (VM), also known as aseptic meningitis, is defined by patients presenting with symptoms (e.g., headache, arthralgia, nausea and photo-sensitivity) and signs (e.g., fever, neck stiffness and vomiting) of meningitis where the bacterial cultures of CSF are negative. Viral meningitis is considered an acute form of meningitis, whereas TBM is considered chronic. Although viral meningitis can occur at any age, it is more prevalent in younger children and infants, since they are the more susceptible to infections, due to their immune systems not yet being fully developed.

The transmission of VM occurs via droplet infection and close personal contact and these viruses can enter the CNS via several mechanisms (Pokorn, 2004). Many viruses replicate outside the CNS and then enter the CNS either by viral particles passing directly across the blood-brain barrier (BBB), or are carried across via infected leukocytes (mumps or herpes viruses), or via exposed peripheral and cranial nerves (Wright *et al.*, 2019). Once the virus is within the CNS, it spreads throughout the subarachnoid space, leading to an inflammatory response, resulting in meningitis. Viruses can also spread directly to neurons and glial cells through the neural tissues or via infected leukocytes.

The most common pathogens associated with VM are of enterovirus origin, however, other diseases such as mumps and herpesviruses have also been associated with such.

- Enteroviruses

Human enteroviruses cause a wide spectrum of disease, including, but not limited to: 1) hand, foot and mouth disease, 2) myocarditis, 3) polio and 4) aseptic meningitis such as VM. Enteroviruses most commonly affect children (Huang *et al.*, 1999; Henquell *et al.*, 2001).

- Mumps

The mumps virus, is the most common cause of VM, with an estimated occurrence in 10-30% of people in populations not immunized against mumps, and males have a risk factor of 25 times greater than that of females for such (Chadwick, 2005).

- Herpesviruses

Herpes simplex virus (HSV) ranks second among the causes of viral meningitis in adolescents and adults in developed countries (Kupila *et al.*, 2006). The most common HSVs that cause CNS infections are HSV type 1 (HSV-1) and HSV type 2 (HSV-2) (Tyler, 2004).

### 2.2.2 Clinical symptoms

The most common symptoms of VM are fever, headache, neck stiffness, vomiting and diarrhoea; however, these are nonspecific signs and could be caused by various other factors also. Mental status is usually not as severely affected in VM patients as with other types of meningitis. Infants usually present with additional symptoms, namely: rash, feeding difficulties and irritability. Photophobia can also occur in about one-third of patients (Jaijakul *et al.*, 2012; Rice, 2017)

### 2.2.3 Pathological ranges

A feature of VM is pleocytosis, with a CSF white blood cell count >5 cells/mm$^3$ (Khetsuriani *et al.*, 2006). The most frequently observed pathological ranges can be found in Table 2.1 for the various causes of VM. Glucose levels in the CSF are reduced while the lactate concentration remains fairly unchanged (Wright *et al.*, 2019), unlike in other types of meningitis.

**Table 2-1 Viral meningitis CSF ranges**

| | Normal CSF | EV | HSV | Mumps |
|---|---|---|---|---|
| White blood cell count | <5 cells/mm$^3$ | 9–2590 cells/mm$^3$ | 46–1860 cells/mm$^3$ | 77–1600 cells/mm$^3$ |
| Glucose | 2.5–4.4 mM | 2.5–4.4 mM | 1.7–4.4 mM | NR |
| Protein | 15–45 mg/dL | 277–1540 mg/dL | 404–3215 mg/dL | 40–74 mg/dL |
| Lymphocytes | 0-30 % | 24–100 % | 80–100 % | 77–100 % |
| Lactate | 0.9–2.7 mM | < 2mM (within normal range) | | |

Abbreviations: EV, enteroviruses; HSV, herpes simplex virus; NR=not reported. Adapted from (Wright et al., 2019), data collected from 10 studies between 1986 and 2016.

### 2.2.4 Pathological tests

The diagnosis of VM requires CSF to be collected from the patient via LP. CSF microscopy was the conventional means of diagnosis, however, this process takes some time, and, often is not sensitive enough to produce definitive results. In recent years however, nucleic acid sequence-based amplification tests (NAAT), such as PCR and reverse transcription PCR (RT-PCR), has enhanced the capability of detecting viral pathogens and have been established as

the new gold standard for the diagnosis of VM (Han *et al.*, 2016; Nolte *et al.*, 2011; Seme *et al.*, 2008).

### 2.2.5 Current diagnosis

A 'probable' case definition of VM is allocated when PCR results demonstrate a viral pathogen. Although considered the gold standard today, PCR is not very sensitive, therefore, a negative test result cannot be used to completely rule out that there is no evidence of viral pathogen(s) (Hristea *et al.*, 2012).

A 'definite' case definition of VM includes: 1) clinical evidence of acute meningitis, such as fever, headache, vomiting, bulging fontanelle, nuchal rigidity or other signs of meningeal irritation and CSF pleocytosis (>5 leucocytes/$mm^3$ if older than 2 months of age, or >15 leucocytes/$mm^3$ if younger than 2 months of age (Hristea *et al.*, 2012)), and 2) absence of any microorganism on gram stain of CSF and negative routine bacterial culture of CSF if antibiotics were not administered prior to the first LP.

## 2.3 Bacterial meningitis

### 2.3.1 Background

Bacterial meningitis (BM) is an acute form of meningitis. Early diagnosis and treatment of BM are essential. Any delay in the initiation of antimicrobial therapy results in poor outcomes such as long-term neurological deficits and potentially death. The most common causes of BM differ by age, as shown in Table 2.2. New-borns face unique risk factors, as shown in Table 2.3 (Thigpen *et al.*, 2011). *E. coli* is the agent most commonly responsible for BM in new-borns. Prematurely new-borns, with a low/very low birth weight, are at an increased risk of infection (Unhanand *et al.*, 1993). The most common causes of BM in a healthy, fully immunized paediatric population are, *Streptococcus pneumoniae* and *Neisseria meningitides* (Nigrovic *et al.*, 2008). Before a vaccine for *Haemophilus influenzea* type b (Hib) existed, Hib was the most common cause of BM. However, since then, the incidence of Hib as a cause of BM has dropped by 95% (Schuchat *et al.*, 1997). Patients who underwent or experienced recent neurological trauma, such as surgery, are at higher risk to develop BM, as the barriers that provide the first line of defence against bacteria are disrupted and do not provide optimal protection.

The typical sequence of events leading to BM is as follows: (1) colonization of the nasopharyngeal mucosa, (2) invasion of bacteria across the mucosa into the bloodstream, (3)

haematogenous seeding and replication in the subarachnoid space, and (4) development of an acute inflammatory response in the subarachnoid space that leads to meningitis (Leib & Tauber, 1999). Once bacteria enter the subarachnoid space, they replicate rapidly due to the innate immune response, which is however, not sufficient to inhibit the proliferation (Simberkoff *et al.*, 1980; Tunkel & Scheld, 1993). A combination of the infecting bacteria and the resulting tissue injury, subsequently initiates an inflammatory cascade, that results in the recruitment of immune cells, specifically: neutrophils and leukocytes, to the infection site.

**Table 2-2 Typical causes of BM by age**

| Age | Bacteria |
|---|---|
| Newborn < 1 month | *Streptococcus agalactiae* (group *B.streptococcus*)<br>*Escherichia coli*<br>Other aerobic gram-negative bacilli including *Citrobacter koseri*<br>*Listeria monocytogenes* |
| 1-3 months | *S. agalactiae* (group B streptococcus)<br>*Streptococcus pneumoniae*<br>*Neisseria meningitidis*<br>*Haemophilus influenzae* type b |
| 3 months – 5 years | *Streptococcus pneumoniae*<br>*Neisseria meningitidis*<br>*Haemophilus influenzae* type b (incompletely immunized) |
| 6-17 years and young adults | *S. pneumoniae*<br>*N. meningitides* |

Adapted from Huang *et al.,* 2019 and Greenberg & Herrera, 2019.

**Table 2-3 Risk factors for BM in newborns**

| Predisposing risk factor(s) | Typical pathogen(s) |
|---|---|
| Prematurity | *S. agalactiae* (group B streptococcus)<br>*Escherichia coli*<br>Other aerobic gram-negative Bacilli |
| Very low birthweight (<1500 g) and extremely low birthweight (<1000 g) | *S. agalactiae*<br>Enterococcus species<br>Coagulase-negative<br>Staphylococci |
| Maternal colonization with *S. agalactiae* | *S. agalactiae* |
| Traumatic delivery | *Escherichia coli*<br>Other aerobic gram-negative<br>Bacilli |
| Maternal consumption of pasteurized dairy products, deli meats, or contaminated produce | *Listeria monocytogenes* |

Adapted from Huang *et al.,* 2019 and Greenberg & Herrera, 2019.

### 2.3.2 Clinical symptoms

There are three basic combinations of clinical symptoms associated with BM: (1) a fever that gets worse over time, accompanied by a variety other non-specific symptoms, (2) clear signs of meningitis, such as fever, headache and neck stiffness, that develop rapidly over a few days, (3) septic shock with rapid clinical decompression over a few hours (Curtis *et al.*, 2010). Paediatric populations present other symptoms additionally, such as temperature instability, hypothermia, lethargy, poor feeding and higher irritability, with uncharacteristic high pitched cries (Curtis *et al.*, 2010). Physical examination of infants may show that the patient is irritable due to meningeal irritation with additional signs that include apnoea, tachycardia, and tachypnea (Gaschignard *et al.*, 2011). Nausea and vomiting are also frequently noticed. Seizures occur in up to 7% of all patients before any medical intervention is administered (Green *et al.*, 1993) as a result of increased intracranial pressure, brain edema, and/or bacterial toxins. Anticonvulsant therapy or prophylaxis may be used in the particular acute setting (Tunkel & Scheld, 1993).

### 2.3.3 Pathological ranges

Biochemical markers of BM are listed in Table 2.4. Significantly elevated CSF lactate concentrations, in combination with decreased glucose levels, are a hallmark of BM.

**Table 2-4 Bacterial meningitis CSF ranges**

| | Normal | Bacterial Meningitis |
|---|---|---|
| Glucose | 2.5–4.4mM | <1.8mM |
| Protein | 15–45 mg/dl | >100 mg/dl |
| Leucocytes | <5 cells/$mm^3$ | >2000 cells/$mm^3$ |
| Neutrophils | <5 cells/$mm^3$ | >1180 cells/$mm^3$ |
| Lactate | 0.45–2.1 mM | >1.7–8 mM |

Adapted from Huang *et al*., 2019.

### 2.3.4 Pathological tests

All patients with suspected BM should undergo a LP for the collection of CSF, unless it is unsafe to do so, for example when the patient is severely ill and/or cardiorespiratory compromised, or a skin infection is present at or near the site of collection (Greenberg & Herrera, 2019). During the LP, the appearance of healthy CSF will be clear, however, it can be cloudy due to the increased concentration of white blood cells (WBC) and/or protein — hallmarks of BM. The presence of red blood cells (RBC) in collected CSF indicates that the sample has been contaminated.

CSF is also required to perform a gram stain, which may reveal bacteria and their general morphology, if they are present. For a definitive identification of BM, a CSF culture needs to be done. Additional tests, similar to VM, include acid-fast tests, NAAT and RT-PCR panels, which are more sensitive and specific (Thwaites & Tran, 2005).

All patients who present with fever, nuchal rigidity, headache, and vomiting, should be suspected of having BM until proven otherwise (Huang et al., 2019).

### 2.3.5 Current diagnosis

'Probable' BM is defined by the literature as any child with sudden onset of fever, > 38.5 °C rectal or 38.0 °C axillary, and one or more of the following symptoms: neck stiffness, altered consciousness or other meningeal signs (e.g. meningeal irritation or inflammation). In addition, the CSF examination must show at least one of the following: turbid appearance, leucocytosis of >100 cells/$mm^3$ in isolation, or leucocytosis 10-100 cells/ $mm^3$ in combination with either elevated protein (>1 g/L) or reduced glucose (CSF glucose value <1.8mM or <50% of plasma glucose (Solomons *et al.,* 2014).

'Definite' BM is defined as a case that identifies (i.e. by Gram stain, culture or antigen detection methods) a bacterial pathogen (e.g., *H. influenzae*, pneumococcus or meningococcus) in the CSF. Any patient with *H. influenzae*, pneumococcus or meningococcus, present in blood, may be reported as a confirmed case of meningitis if the clinical syndrome is that of meningitis. The culture of *H. influenzae*, meningococcus or from a non-sterile site, such as the throat, does not confirm a case of disease, since the bacteria can be isolated from other areas without causing disease (Solomons *et al.,* 2014).

## 2.4 Tuberculous meningitis

### 2.4.1 Background

Tuberculous meningitis (TBM) is a chronic form of BM and is the most common type of CNS tuberculosis (CNS-TB). TBM is the most severe manifestation of TB — a disease caused by *M.tb*, and is associated with substantial mortality and morbidity (Rohlwink *et al.,* 2019), especially in a paediatric population in a high TB-burdened country (Van & Farrar, 2014).

The *M.tb* bacilli are spread via air transmission in aerosolized droplet form, from people who suffer from active TB. The development of TBM is a two-step process, as originally described by (Rich & McCordock, 1933) and recently by (Thwaites & Tran, 2005): 1) *M.tb* invade the

host alveolar macrophages through droplet inhalation, where the bacteria can then be disseminated to other parts of the body, including the CNS, 2) at the meninges, the *M.tb* form tubercles, called Rich foci, which eventually rupture and release tubercle bacilli into the subarachnoid space, resulting in the onset of TBM.

Another potential route of entry through the BBB is via a “Trojan horse” mechanism, where *M.tb* are transported in infected cells (macrophages and neutrophils) across the BBB. Once the *M.tb* bacilli gain access to the brain, they can survive due to a compromised local innate immunity and replicate easily, resulting in the development of TB lesions (Rich & McCordock, 1933) (Thwaites & Tran, 2005). Post-mortem studies on TBM individuals suggest that, TBM is initiated when these TB lesions rupture, and release *M.tb* bacilli into the subarachnoid space, resulting in infection of the meninges (Dastur *et al.*, 1995; Donald *et al.*, 2005; Rock *et al.*, 2008). After the release of tubercle bacilli into the subarachnoid space, a dense exudate forms. This exudate surrounds arteries and nerves restricting the flow of CSF, resulting in hydrocephalus. The exudate is rich in various cells including macrophages, neutrophils and erythrocytes (Rock *et al.,* 2008).

Microglia are the primary cerebral cells that are infected by *M.tb* (Rock *et al.*, 2005) and are also involved with immune regulation, however, astrocytes and neurons may also be involved in the pathology of TBM (Rock *et al.*, 2005).

Metabolic abnormalities are common in TBM, and include: deficiencies in gonadotropin, thyrotropin, and somatotropin (More *et al.*, 2017). Hyponatremia is also commonly reported, however, the exact mechanism responsible for this is still strongly debated (Celik *et al.*, 2015), with cerebral salt wasting and a syndrome associated with abnormalities of antidiuretic hormone, possible explanations (Davis *et al.,* 2019).

The most important feature of TBM found in post-mortem studies, is the presence of a thick, gelatinous exudate in the basal cisterns and subarachnoid space of the brain, which may also extend into the spine. The predominantly basal location, has serious implications, such as 1) the exudate surrounds the major cerebral vessels originating from the base of the brain, 2) the exudate blocks the free circulation of CSF, and 3) it surrounds and compresses the local cranial nerves resulting in cranial nerve palsies (Dastur *et al.*, 1995; Shinoyama *et al.*, 2012).

### 2.4.2 **Clinical symptoms**

Fever, neck stiffness, seizures, nausea and vomiting are common symptoms of TBM (Farinha *et al.*, 2000; Yaramis *et al.*, 1998). In young children, symptoms also include poor weight gain and listlessness (Donald *et al.*, 1985), however, these are non-specific symptoms. Depending

on the severity of the infection, neurological symptoms vary from lethargy and agitation to coma. Children often develop TBM within 3 months after initial *M.tb* infection (Donald et al., 2005), hence TBM diagnosis in <3 month old infants is typically not possible. Children also develop symptoms of TBM far faster than adults do since their immune systems are not fully developed as yet. Thus, medical attention should be sought much faster.

Hydrocephalus is the most commonly occurring, serious complication of TBM. It is also more prevalent in children than adults, occurring in more than 80% of paediatric patients at admission, however, it is rarely detected in early TBM (Yaramis *et al.,* 1998). The severity of TBM is assessed by various stages as, shown in Table 2.5.

**Table 2-5 Clinical criteria for the severity of TBM**

| Stage | Criteria |
|---|---|
| 1 | Fully conscious and no focal deficits. GCS of 15* |
| 2a | Conscious but with inattention, confusion, lethargy and focal neurological signs. GCS of 14-11 |
| 2b | GCS of 15 with a focal neurological deficit |
| 3 | Stuporous or comatose, multiple cranial nerve palsies, or paralysis. GCS of 10 or less |

*GCS = Glasgow Coma Score — a neurological scoring system of eye, motor and verbal response, which aims to give a reliable and objective way of recording the state of a person's consciousness. GCS ranges from 3 to 15, with 3 being the worst score and 15 being a good score (British Medical Research Council 1948; Toorn *et al.,* 2012).

### 2.4.3 Pathological ranges

Lumbar puncture reveals an elevated opening pressure in most cases of TBM (>18.3 mmHg) (Thwaites & Tran, 2005), as a result of increased intracranial pressure. Table 2.6 highlights the main CSF biochemical features of TBM, with decreased glucose and highly elevated lactate being characteristic of TBM.

**Table 2-6 Tuberculous meningitis CSF ranges**

| | Normal | TBM |
|---|---|---|
| Glucose | 2.5–4.4 mM | <2.2 mM |
| Protein | <1 g/L | >2.5 g/L |
| Leukocytes | 10–500 cells/uL | 150–1000 cells/uL |
| Lactate | 0.45–2.1 mM | 5–10 mM |
| CSF glucose/blood ratio | >0.5 | <0.5 |

Compiled from Hoffmann *et al.*, 1993; Solomons *et al.*, 2014; Thwaites & Tran, 2005; Wilkinson *et al.*, 2017.

### 2.4.4 **Pathological tests**

The diagnosis and treatment of TBM in its earliest stage is advised in order to improve the outcome, however, several factors hinder the diagnostic process:

1) Presenting clinical features that are nonspecific.
2) Small numbers of bacilli in the CSF reduce the sensitivity of conventional bacteriological tests.
3) Chest radiography findings of active or previous evidence of TB infection can aid in diagnosis, however, these findings lack specificity, especially in areas where there is a high prevalence of pulmonary TB (Manyelo et al., 2019).
4) The gold-standard CSF culture method used for diagnosing meningitis is slow, and, it often takes up to 6–8 weeks to confirm the presence of tubercle bacilli (Hristea et al., 2012).
5) A CSF gram stain smear test is insensitive, only resulting in a positive result in about 60–90% of all culture confirmed TBM cases and hence a negative gram stain does not rule out TBM infection (Hasbun *et al.*, 2013).
6) Smear microscopy, such as the Ziehl-Neelsen stain, is a rapid diagnostic method for routine analysis that is faster than conventional methods and more cost effective to use as a routine test and has a high predictive value (Chen *et al.*, 2012), however, the Ziehl-Neelsen staining's ability to detect acid-fast bacilli is relatively low and ranges from 10-60 %.
7) Nucleic acid amplification techniques (NAATs), such as PCR, for the detection of mycobacterial DNA has been reported by (Boulware, 2013) to be more specific and rapid. NAATs can be used to confirm a diagnosis of TBM; however, they cannot be used to rule out a TBM diagnosis (Thwaites *et al.*, 2009; Van & Farrar, 2014; Wilkinson *et al.*, 2017). The Xpert M.TB/RIF assay (Cepheid, Sunnyvale, CA, USA) uses real-time PCR and is set to become the cornerstone of commercial molecular diagnosis of TB, as it potentially has the sensitivity and specificity values that are similar to the gold-standard culture method (Lawn & Nicol, 2011), however, these tests are far more expensive comparatively.

Considering the above, the only definitive diagnosis of TBM at present, requires a successful *M.tb* culture and/or staining of CSF, accompanied by meticulous microscopy and a large volume of CSF (>5 mL) (Thwaites et al., 2004).

### 2.4.5 Current diagnosis

A ‘probable’ diagnosis of TBM is assigned if two or more of the following criteria are present: 1) a history of contact with an adult that has TB, 2) a positive tuberculin skin test, 3) a CT scan or magnetic resonance image (MRI) demonstrating the characteristic features of TBM (ventricular dilatation, meningovascular enhancement and/or granuloma/s), or 4) positive microbiological identification of acid-fast bacilli from gastric washings (Hristea *et al.,* 2012; Marais *et al.,* 2010). In combination with one or more of the following: 1) suspected active pulmonary tuberculosis on the basis of chest X-ray, 2) clinical evidence of other extra-pulmonary tuberculosis or 3) acid fast bacilli found in other biofluids other than CSF (Hristea *et al.,* 2012; Marais *et al.,* 2010).

A ‘definite’ diagnosis of TBM is assigned if acid-fast bacilli are present in the CSF, *M.tb* culture is positive, and a commercial NAAT of CSF is positive (Hristea *et al.,* 2012; Marais *et al.,* 2010).

## 2.5 Summary of various types of meningitis

For comparative and quick reference purposes, all the information provided within my literature review has been summarized in Figure 2.1, including parameters for normal CSF values (Huang *et al.*, 1999; Solomons *et al.*, 2014; Thwaites & Tran, 2005; Wilkinson *et al.*, 2017; Wright *et al.*, 2019). It is evident that in a clinical setting, the biochemical information collected from CSF to differentially diagnose meningitis, is limited to lactate, glucose, total protein and cell count and type.

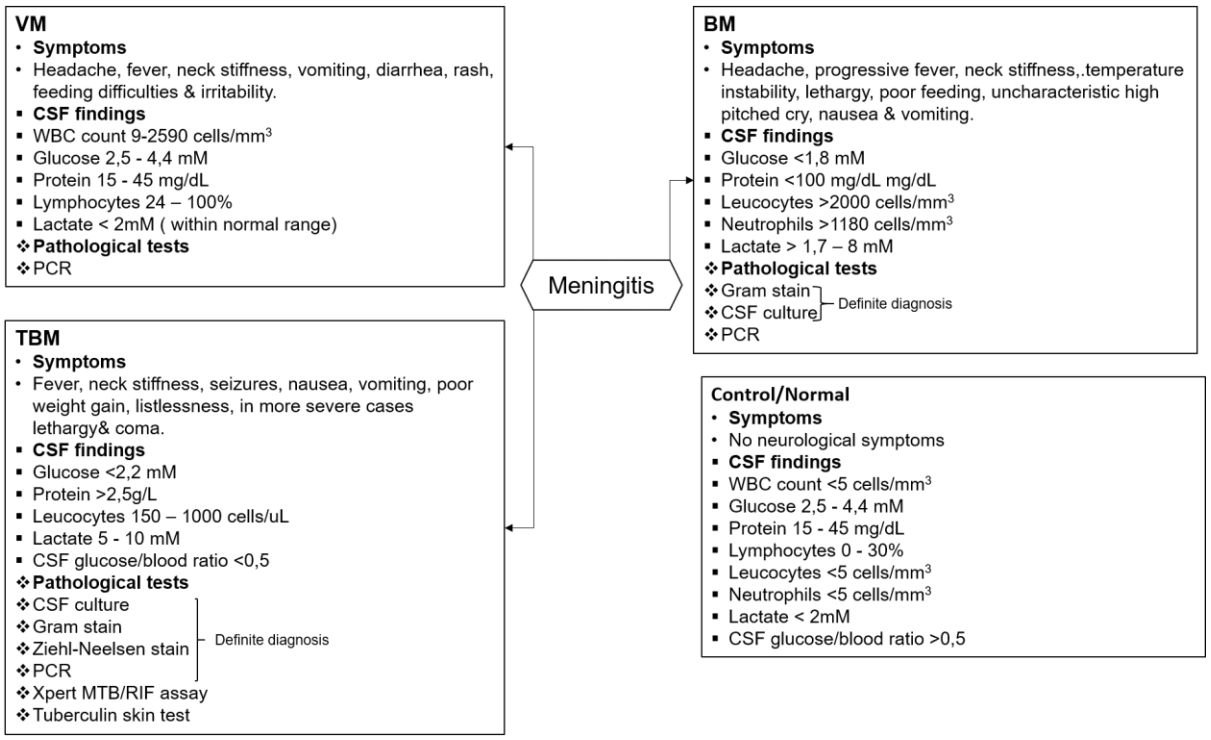


**Figure 2-1 Summary of various types of meningitis**

## 2.6 $^{1}$H-NMR metabolomics

### 2.6.1 Introduction

The term metabolomics was first introduced in 1998 by (Oliver *et al.*, 1998) to describe the relative change in concentrations of metabolites that are associated with the deletion or overexpression of a gene, and was explicitly described by (Fiehn, 2001) as the "*comprehensive and quantitative analysis of all small molecules in a biological system*".

Metabolomics offers an advantage over other parts of the 'omics' family (e.g., proteomics and transcriptomics), since metabolites are the final products of enzymatic reactions in cells. Metabolomics most accurately reflects the true cellular activity or change without the challenges of post-transcriptional or post-translational modifications that can occur within transcriptomics and proteomics, respectively, that adds complexity.

The most commonly used analytical platforms within metabolomics for the detection and analysis of metabolites are mass spectrometry (MS)-based methods and nuclear magnetic resonance (NMR). Metabolites in complex solutions can be separated by either gas chromatography (GC), liquid chromatography (LC), or capillary electrophoresis (CE), and coupled with MS for compound identification and quantification. NMR spectroscopy is a method that does not require prior separation of metabolites, and is able to simultaneously identify and determine the concentration of all types of metabolites, above the detection limit of 1 µM, present in a complex biological sample.

### 2.6.2 General metabolomics workflow

A general $^{1}$H-NMR metabolomics workflow can be seen in Figure 2.1. Correct sample collection, handling and storage, are just as crucial for metabolomics accuracy, as the actual analyses of these samples.

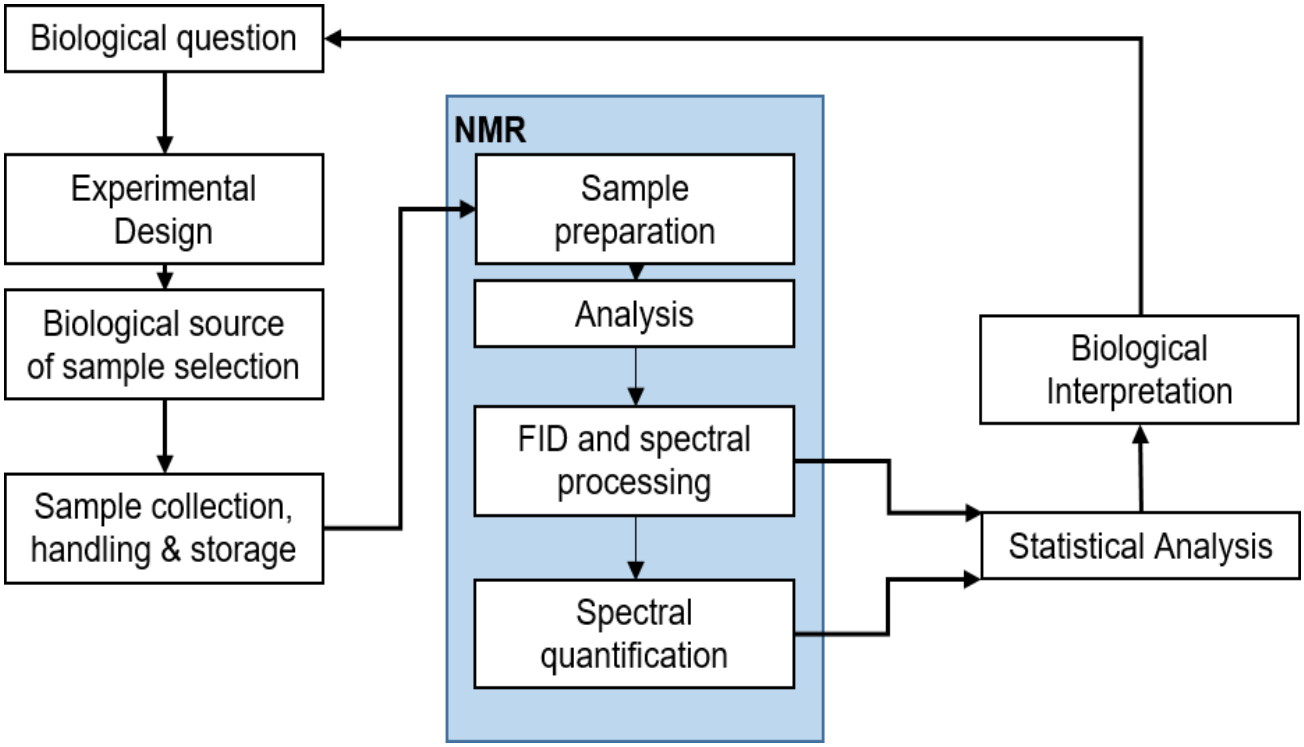


**Figure 2-2** **Summary of general $^{1}$H-NMR workflow showing the iterative flow from the biological question, sample collection, through analysis and statistics, to biological interpretation.**

### 2.6.3 Nuclear magnetic resonance

NMR is a non-destructive technique that can detect different classes of metabolites in a sample, regardless of their size, charge, volatility or stability (Dunn & Ellis, 2005). NMR is most frequently used in medical applications, such as human diagnostic metabolomics, for analysis of blood, plasma, serum, CSF and urine (Nicholson *et al.*, 1983).

The principle functioning of NMR involves the use of strong magnetic fields combined with radio frequency pulses, to produce high-energy spin states in nuclei (e.g. $^{1}$H, $^{13}$C or $^{31}$P), and it is the radiation that is emitted when these nuclei return to their lower energy spin state that is detected (Dunn & Ellis, 2005). NMR does not require the samples to be volatilized, thus it is a non-destructive analytical technique, and therefore allows the measurement of metabolite concentrations in intact tissues (Lindon *et al.*, 2003) and, most importantly, it is a technique that provides structural information about the metabolites, subsequently definite identification.

NMR offers advantages for metabolites that are difficult to ionize or derivatize, as in the case of MS, and allows for the identification of compounds that are identical in mass, with different isomers. Another advantage of NMR is that less complex sample preparation is needed prior

to analysis, and the sample is not chemically altered, as in the case of derivatization. The throughput for NMR is also higher than MS, and accurate absolute quantification can also be done. Running cost are lower when compared to other analytical techniques and it delivers more reproducible results (Guennec *et al.*, 2014).

On the downside however, NMR has a higher initial investment cost when compared to other analytical techniques. Data interpretation after analysis is also much more complicated than other chromatographic coupled MS techniques, since multiple, possibly overlapping, peaks, can represent a single metabolite. Spectral libraries of pure compounds are subsequently required for identification, and experience in interpretation of such. The main disadvantage of NMR over other chromatographic methods, is its lacking sensitivity. A summary of the comparisons between NMR and MS, as discussed above, can be found in Table 2.7.

**Table 2-7 Advantages and disadvantages of NMR compared to MS**

| | NMR | MS |
|---|---|---|
| **Reproducibility** | Highly reproducible | Compared to NMR, MS data is less reproducible |
| **Sensitivity** | Lower sensitivity, however can be improved with multiple scans, higher magnetic strength and by using a cryo-cooled probe | High sensitivity and can detect metabolites with nanomolar concentrations |
| **Selectivity** | Usually used for untargeted analysis | Can be used for targeted or untargeted analysis, when used in combination with chromatography it is a superior tool for targeted analysis |
| **Sample measurement** | Relatively fast analysis using 1H-NMR spectroscopy, where all metabolites at a detectable concentration level can be detected in one analysis | Depending on ionization method analysis can take longer |
| **Sample preparation** | Minimal sample preparation, as biofluid samples is used as is with the addition of a buffer solution and a deuterated locking solvent | More demanding, as sample needs to be derivatized for chromatography |
| **Sample recovery** | Non-destructive, thus sample can be used for several analysis and be recovered for storage | MS is a destructive technique as sample needs to be ionized, thus sample cannot be recovered. |
| **Quantitative analysis** | Inherently quantitative as the signal intensity is directly proportional to the metabolite concentrations | Intensity of the MS spectra is often not correlated with metabolite concentrations as the ionization efficiency may vary |
| **(Un)Targeted analysis** | Can be used for both targeted and untargeted analyses, however it is not commonly used for targeted analyses | GC-MS and LC-MS are preferable for targeted analysis |
| **Number of detectable metabolites** | Varies, depending on magnetic field strength and probe used, usually 50-200 metabolites can be detected and identified | Varies, depending on which technique is used, however it is possible to detect far more compounds than NMR and identify several hundred metabolites. |

Adapted from (Emwas *et al.,* 2019)

### 2.6.4 Previous CSF 1H-NMR metabolomics studies on meningitis

The first application of $^{1}$H-NMR metabolomics on CSF from meningitis cases was done in 2005 by Coen et al. Since then, five additional $^{1}$H-NMR metabolomics studies have been done on CSF samples collected from various different types of meningitis cases. Table 2-8

summarizes the results of these studies by including insights offered and the metabolic markers identified.

**Table 2-8 Insights offered and CSF metabolic markers of meningitis identified by $^{1}$H-NMR metabolomics studies**

| Reference [Human/Animal study] | Type of meningitis [n] | Insights | Metabolic markers |
|---|---|---|---|
| (Coen *et al.*, 2005) [Human] | BM [11]<br>VM [12] | This study highlights the potential that metabolomics has to aid in the rapid diagnosis of meningitis, as the NMR metabolite profiles of the CSF sample do show substantial differences between VM, BM and controls. | 3-Hydroxybutyrate<br>Acetoacetate<br>Alanine<br>Citrate<br>Creatine<br>Creatinine<br>Glucose<br>Glutamate<br>Glutamine<br>Isoleucine<br>Lactate<br>Leucine<br>Pyruvate<br>Valine |
| (Himmelreich *et al.*, 2009) [Animal] | BM [61] | This study demonstrated that for *C. neoformans* and *S. pneumonie* infections it is possible to provide a diagnosis for the causative agent without prior culture diagnosis. | Acetate↑<br>Alanine<br>Citrate^<br>Glucose↓<br>Glutamate<br>Glutamine<br>Lactate↑ |
| (Mason *et al.*, 2015) [Human] | TBM[17] | This study proposed a hypothetical astrocyte–microglia lactate shuttle that can potentially be utilized to aid in the improvement of early clinical assessment of TBM in a paediatric population. | **Control vs TBM**<br>2-Oxogluterate↓<br>3-Hydroxybutyrate↓<br>3-Hydroxyisovalerate↓<br>Acetate↑<br>Acetoacetate↓<br>Acetone↑<br>Alanine↓<br>Betaine↓<br>Choline↓<br>Citrate↓<br>Creatine↓<br>Creatinine↑<br>$DMSO_2$↑<br>Formate↓<br>Glutamine↑<br>Leucine↓ |

| | | | |
|---|---|---|---|
| | | | Lysine↓<br>Mannose↑<br>Myo-Inositol↑<br>Phenylalanine↓<br>Pyruvate↓<br>Succinate↓<br>Threonine↓<br>Tyrosine↓<br>Valine↓<br>Valine/Isoleucine↓ |
| (Chatterji *et al.*, 2016)<br>[Human] | BM [21]<br>TBM[30] | This study focused on the metabolomic differentiation of BM & TBM from healthy and disease controls using 3 sample matrices: CSF, urine & serum. It concluded that the use of NMR, coupled with stringent statistical parameters, could be used to differentiate meningitis cases from control cases based on CSF metabolic profiles. It was a pilot study that also proved the potential of using urine to differentiate meningitis cases from controls, which may provide a possible future diagnostic method that does not require invasive procedures to acquire sample for diagnostic purposes. | **BM & TBM vs Neurological disease control**<br>Citrate↑<br>Glucose↓<br>Lactate↑<br>Pyruvate↑<br>**BM vs TBM**<br>3-Hydroxyisovalerate↑<br>Formate↑<br>Isobutyrate↑ |
| (Li *et al.*, 2017)<br>[Human] | VM [20]<br>TBM[18] | This study found 25 key metabolites that were identified that may be potential biomarkers for TBM differential diagnosis when comparing to VM and are worthy of further investigation. It also provided insight into the pathogenic mechanisms of TBM and VM, and suggests that more studies need to be done with a larger sample size to evaluate the diagnostic value of this metabolomics approach. | **TBM vs VM**<br>Alanine↑<br>Asparagine↑<br>Aspartate↑<br>Betaine↓<br>Choline↑<br>Citrate↓<br>Cyclohexane↑<br>Fructose↓<br>Glucose↓<br>Glycerine↑<br>Glycine↓<br>Lactate↑<br>L-Glutamine↑<br>Lipoprotein↑<br>L-Serine↓<br>L-Threonine↓<br>L-Valine↓<br>Malonate↑<br>Malonic acid↑<br>N,N-Dimethylformamide↑<br>Putrescine↑<br>Pyruvic acid↑ |

| | | | |
|---|---|---|---|
| | | | Sucrose↓<br>Tyrosine↓ |
| (Zhang *et al.*, 2019) [Human] | VM [27]<br>BM [20]<br>TBM [25]<br>Control[28] | This study demonstrated that NMR metabolomics can differentiate TBM from other types of meningitis and controls with high reliability. Several metabolites were identified that differentiates TBM, VM and BM from each other, these metabolites can be used as potential biomarkers for future diagnostic purposes. Pathway analyses also indicated that the carbohydrate and amino acid metabolisms are the most affected in TBM cases, which correlates with finding of previous studies. | **TBM vs Control**<br>1,3-Dimethyluric acid↓<br>2-Hydroxy isovalerate↑<br>2-Oxoglutarate↑<br>3-Hydroxy butyrate↑<br>3-Hydroxy isovalerate↑<br>Acetamide↑<br>Caprate↑<br>Choline↓<br>Creatinine↓<br>Cyclohexane↓<br>Glucose↓<br>Glycine↓<br>Isobutyrate↑<br>Isovaleric acid↑<br>Lactate↑<br>L-Alanine↑<br>L-Isoleucine↑<br>L-Methionine↓<br>L-Valine↑<br>Myo-Inositol↓<br>Pyruvate↓<br>**TBM vs VM**<br>1,3-Dimethyluric acid↓<br>2-Hydroxy butyrate↑<br>2-Hydroxy isovalerate↑<br>2-Oxoglutarate↑<br>3-Hydroxy butyrate↑<br>3-Hydroxy isovalerate↑<br>Acetamide↑<br>Acetate↑<br>Caprate↑<br>Choline↓<br>Creatinine↓<br>Cyclohexane↓<br>Glucose↓<br>Isobutyrate↑<br>Iso-Valeraldehyde↑<br>Isovaleric acid↑<br>Lactate↑<br>L-Alanine↑<br>L-Isoleucine↑<br>L-Leucine↑<br>L-Serine↓<br>L-Valine↑ |

| | | | |
|---|---|---|---|
| | | | Myo-inositol↓<br>**TBM vs BM**<br>1,3-Dimethyluric acid↓<br>Acetamide↓<br>L-Alanine↓<br>L-Serine↓<br>L-Valine↓<br>Lysine↓ |

Considering the above, $^{1}$H-NMR metabolomics has provided valuable insight into the differentiation of various types of meningitis substantiating the need for further investigation into $^{1}$H-NMR metabolomics for such purposes.

## 2.7 Problem statement

Only five $^{1}$H-NMR metabolomics studies have been done to date which, provide insights into the altered metabolome induced by different of types of meningitis, and provide potential metabolic indicators of the disease (Table 2.8). Only two of these however (Li *et al.,* 2017; Zhang *et al.,* 2019) directly compare acute meningitis (VM) to chronic meningitis (TBM), as we have done, however exclusively in a population of 15 years and over. Due to the high prevalence of meningitis in various paediatric populations (≤ 12 years old) across the globe, in this investigation we chose to do an $^{1}$H-NMR metabolomics study, comparing the CSF metabolic profile of acute meningitis (VM) vs chronic meningitis (TBM) within a Western Cape paediatric population of South Africa, known for their high risk of contracting TBM (Wolzak *et al.*, 2012).

## 2.8 Aims

Characterize the CSF metabolic profile of chronic (TBM) meningitis and acute (VM) in a South Africa paediatric population, in order to identify markers that better characterise the disease and possibly assist in an early, differential diagnosis.

## 2.9 Objectives

2) Analyst competency training – learning relevant SOPs within NWU0Human Metabolomics (CHM) and perform repeatability studies on the NMR to ensure minimal analytical variation from the analyst (myself) (Chapter 3).
   - Create a synthetic quality control CSF sample containing at least nine metabolites at high (150 % of normal), normal (100%) and low (50 % of normal) concentration values.
   - Analyse repeatability of synthetic quality control CSF samples to determine analyst competency.

2) Perform an untargeted $^{1}$H-NMR metabolomics analysis on collected patient CSF samples and use univariate and multivariate statistics to:

   - 2.1 Characterise CSF metabolic profile for chronic (TBM) meningitis by comparison to that of a control CSF sample set (Chapter 4).
   - 2.2 Characterise CSF metabolic profile for acute (VM) meningitis by comparison to that of a control CSF sample set and that of a TBM sample set (Chapter 5).

## 2.10 References


Boulware, D.R. 2013. Utility of the Xpert MTB/RIF assay for diagnosis of tuberculous meningitis. PLoS Med, 10(10):e1001537.

Celik, U., Celik, T., Tolunay, O., Baspinar, H., Komur, M. & Levent, F. 2015. Cerebral salt wasting in tuberculous meningitis: Two cases and review of the literature. Case Report. Neuro Endocrinol Lett, 36(4):306-310.

Chadwick, D.R. 2005. Viral meningitis. Br Med Bull, 75-76(1):1-14.

Chatterji, T., Singh, S., Sen, M., Singh, A.K., Maurya, P.K., Husain, N., Srivastava, J.K., Mandal, S.K. & Roy, R. 2016. Comprehensive 1H NMR metabolic profiling of body fluids for differentiation of meningitis in adults. Metabolomics, 12(8):130.

Chen, P., Shi, M., Feng, G.D., Liu, J.Y., Wang, B.J., Shi, X.D., Ma, L., Liu, X.D., Yang, Y.N., Dai, W., Liu, T.T., He, Y., Li, J.G., Hao, X.K. & Zhao, G. 2012. A highly efficient Ziehl-Neelsen stain: identifying de novo intracellular Mycobacterium tuberculosis and improving detection of extracellular M. tuberculosis in cerebrospinal fluid. J Clin Microbiol, 50(4):1166-1170.

Coen, M., O'Sullivan, M., Bubb, W.A., Kuchel, P.W. & Sorrell, T. 2005. Proton nuclear magnetic resonance-based metabonomics for rapid diagnosis of meningitis and ventriculitis. Clin Infect Dis, 41(11):1582-1590.

Curtis, S., Stobart, K., Vandermeer, B., Simel, D.L. & Klassen, T. 2010. Clinical features suggestive of meningitis in children: a systematic review of prospective data. Pediatrics, 126(5):952-960.

Dastur, D.K., Manghani, D.K. & Udani, P.M. 1995. Pathology and pathogenetic mechanisms in neurotuberculosis. Radiol Clin North Am, 33(4):733-752.

Davis, A.G., Rohlwink, U.K., Proust, A., Figaji, A.A. & Wilkinson, R.J. 2019. The pathogenesis of tuberculous meningitis. J Leukoc Biol, 105(2):267-280.

Donald, P.R., Schaaf, H.S. & Schoeman, J.F. 2005. Tuberculous meningitis and miliary tuberculosis: the Rich focus revisited. J Infect, 50(3):193-195.

Donald, P.R., Schoeman, J.F. & van Schalkwyk, H.J. 1985. The 'Road to Health' card in tuberculous meningitis. J Trop Pediatr, 31(2):117-120.

Dunn, W.B. & Ellis, D.I. 2005. Metabolomics: Current analytical platforms and methodologies. Trac-Trends in Analytical Chemistry, 24(4):285-294.

Emwas, A.H., Roy, R., McKay, R.T., Tenori, L., Saccenti, E., Gowda, G.A.N., Raftery, D., Alahmari, F., Jaremko, L., Jaremko, M. & Wishart, D.S. 2019. NMR Spectroscopy for Metabolomics Research. Metabolites, 9(7).

Farinha, N.J., Razali, K.A., Holzel, H., Morgan, G. & Novelli, V.M. 2000. Tuberculosis of the central nervous system in children: a 20-year survey. J Infect, 41(1):61-68.

Fiehn, O. 2001. Combining genomics, metabolome analysis, and biochemical modelling to understand metabolic networks. Comp Funct Genomics, 2(3):155-168.

Gaschignard, J., Levy, C., Romain, O., Cohen, R., Bingen, E., Aujard, Y. & Boileau, P. 2011. Neonatal Bacterial Meningitis: 444 Cases in 7 Years. Pediatr Infect Dis J, 30(3):212-217.

Green, S.M., Rothrock, S.G., Clem, K.J., Zurcher, R.F. & Mellick, L. 1993. Can Seizures Be the Sole Manifestation of Meningitis in Febrile Children? Pediatrics, 92(4):527-534.

Greenberg, R.G. & Herrera, T.I. 2019. Chapter 8 - When to Perform Lumbar Puncture in Infants at Risk for Meningitis in the Neonatal Intensive Care Unit. (In Benitz, W.E. & Smith, P.B., eds. Infectious Disease and Pharmacology. Philadelphia: Content Repository Only! p. 87-102).

Guennec, A.L., Giraudeau, P. & Caldarelli, S. 2014. Evaluation of fast 2D NMR for metabolomics. Anal Chem, 86(12):5946-5954.

Han, S.H., Choi, H.Y., Kim, J.M., Park, K.R., Youn, Y.C. & Shin, H.W. 2016. Etiology of aseptic meningitis and clinical characteristics in immune-competent adults. J Med Virol, 88(1):175-179.

Hasbun, R., Bijlsma, M., Brouwer, M.C., Khoury, N., Hadi, C.M., van der Ende, A., Wootton, S.H., Salazar, L., Hossain, M.M., Beilke, M. & van de Beek, D. 2013. Risk score for identifying adults with CSF pleocytosis and negative CSF Gram stain at low risk for an urgent treatable cause. J Infect, 67(2):102-110.

Henquell, C., Chambon, M., Bailly, J.L., Alcaraz, S., De Champs, C., Archimbaud, C., Labbe, A., Charbonne, F. & Peigue-Lafeuille, H. 2001. Prospective analysis of 61 cases of enteroviral meningitis: interest of systematic genome detection in cerebrospinal fluid irrespective of cytologic examination results. J Clin Virol, 21(1):29-35.

Himmelreich, U., Malik, R., Kuhn, T., Daniel, H.M., Somorjai, R.L., Dolenko, B. & Sorrell, T.C. 2009. Rapid etiological classification of meningitis by NMR spectroscopy based on metabolite profiles and host response. PLoS One, 4(4):e5328.

Hoffmann, G.F., Meier-Augenstein, W., Stockler, S., Surtees, R., Rating, D. & Nyhan, W.L. 1993. Physiology and pathophysiology of organic acids in cerebrospinal fluid. J Inherit Metab Dis, 16(4):648-669.

Hristea, A., Olaru, I.D., Baicus, C., Moroti, R., Arama, V. & Ion, M. 2012. Clinical prediction rule for differentiating tuberculous from viral meningitis. Int J Tuberc Lung Dis, 16(6):793-798.

Huang, C.C., Liu, C.C., Chang, Y.C., Chen, C.Y., Wang, S.T. & Yeh, T.F. 1999. Neurologic complications in children with enterovirus 71 infection. N Engl J Med, 341(13):936-942.

Huang, F.S., Brady, R.C. & Mortensen, J. 2019. Bacterial Meningitis. (In Domachowske, J., ed. Introduction to Clinical Infectious Diseases: A Problem-Based Approach. Cham: Springer International Publishing. p. 245-257).

Jaijakul, S., Arias, C.A., Hossain, M., Arduino, R.C., Wootton, S.H. & Hasbun, R. 2012. Toscana meningoencephalitis: a comparison to other viral central nervous system infections. J Clin Virol, 55(3):204-208.

Kupila, L., Vuorinen, T., Vainionpaa, R., Hukkanen, V., Marttila, R.J. & Kotilainen, P. 2006. Etiology of aseptic meningitis and encephalitis in an adult population. Neurology, 66(1):75-80.

Lawn, S.D. & Nicol, M.P. 2011. Xpert(R) MTB/RIF assay: development, evaluation and implementation of a new rapid molecular diagnostic for tuberculosis and rifampicin resistance. Future Microbiol, 6(9):1067-1082.

Leib, S.L. & Tauber, M.G. 1999. Pathogenesis of bacterial meningitis. Infect Dis Clin North Am, 13(3):527-548, v-vi.

Li, Z., Du, B., Li, J., Zhang, J., Zheng, X., Jia, H., Xing, A., Sun, Q., Liu, F. & Zhang, Z. 2017. Cerebrospinal fluid metabolomic profiling in tuberculous and viral meningitis: Screening potential markers for differential diagnosis. Clin Chim Acta, 466:38-45.

Lindon, J.C., Holmes, E. & Nicholson, J.K. 2003. So what's the deal with metabonomics? Anal Chem, 75(17):384A-391A.

Manyelo, C.M., Solomons, R.S., Snyders, C.I., Stanley, K., Walzl, G. & Chegou, N.N. 2019. Potential of host serum protein biosignatures in the diagnosis of tuberculous meningitis in children. bioRxiv:670323.

Marais, S., Thwaites, G., Schoeman, J.F., Torok, M.E., Misra, U.K., Prasad, K., Donald, P.R., Wilkinson, R.J. & Marais, B.J. 2010. Tuberculous meningitis: a uniform case definition for use in clinical research. Lancet Infect Dis, 10(11):803-812.

Mason, S., van Furth, A.M., Mienie, L.J., Engelke, U.F., Wevers, R.A., Solomons, R. & Reinecke, C.J. 2015. A hypothetical astrocyte-microglia lactate shuttle derived from a (1)H NMR metabolomics analysis of cerebrospinal fluid from a cohort of South African children with tuberculous meningitis. Metabolomics, 11(4):822-837.

More, A., Verma, R., Garg, R.K., Malhotra, H.S., Sharma, P.K., Uniyal, R., Pandey, S. & Mittal, M. 2017. A study of neuroendocrine dysfunction in patients of tuberculous meningitis. J Neurol Sci, 379:198-206.

Nicholson, J.K., Buckingham, M.J. & Sadler, P.J. 1983. High resolution 1H n.m.r. studies of vertebrate blood and plasma. Biochem J, 211(3):605-615.

Nigrovic, L.E., Kuppermann, N., Malley, R. & Bacterial Meningitis Study Group of the Pediatric Emergency Medicine Collaborative Research Committee of the American Academy of, P. 2008. Children with bacterial meningitis presenting to the emergency department during the pneumococcal conjugate vaccine era. Acad Emerg Med, 15(6):522-528.

Nolte, F.S., Rogers, B.B., Tang, Y.W., Oberste, M.S., Robinson, C.C., Kehl, K.S., Rand, K.A., Rotbart, H.A., Romero, J.R., Nyquist, A.C. & Persing, D.H. 2011. Evaluation of a rapid and completely automated real-time reverse transcriptase PCR assay for diagnosis of enteroviral meningitis. J Clin Microbiol, 49(2):528-533.

Oliver, S.G., Winson, M.K., Kell, D.B. & Baganz, F. 1998. Systematic functional analysis of the yeast genome. Trends Biotechnol, 16(9):373-378.

Pokorn, M. 2004. Pathogenesis and Classification of Central Nervous System Infection. EJIFCC, 15(3):68-71.

Rice, P. 2017. Viral meningitis and encephalitis. Medicine, 45(11):664-669.

Rich, A., & McCordock, H. 1933. The pathogenesis of tuberculous meningitis. Bull John Hopkins Hosp, 52:5.

Rock, R.B., Hu, S., Gekker, G., Sheng, W.S., May, B., Kapur, V. & Peterson, P.K. 2005. Mycobacterium tuberculosis-induced cytokine and chemokine expression by human microglia and astrocytes: effects of dexamethasone. J Infect Dis, 192(12):2054-2058.

Rock, R.B., Olin, M., Baker, C.A., Molitor, T.W. & Peterson, P.K. 2008. Central nervous system tuberculosis: pathogenesis and clinical aspects. Clin Microbiol Rev, 21(2):243-261, table of contents.

Rohlwink, U.K., Figaji, A., Wilkinson, K.A., Horswell, S., Sesay, A.K., Deffur, A., Enslin, N., Solomons, R., Van Toorn, R., Eley, B., Levin, M., Wilkinson, R.J. & Lai, R.P.J. 2019. Tuberculous meningitis in children is characterized by compartmentalized immune responses and neural excitotoxicity. Nat Commun, 10(1):3767.

Schuchat, A., Robinson, K., Wenger, J.D., Harrison, L.H., Farley, M., Reingold, A.L., Lefkowitz, L. & Perkins, B.A. 1997. Bacterial meningitis in the United States in 1995. Active Surveillance Team. N Engl J Med, 337(14):970-976.

Seme, K., Mocilnik, T., Komlos, K.F., Doplihar, A., Persing, D.H. & Poljak, M. 2008. GeneXpert enterovirus assay: one-year experience in a routine laboratory setting and evaluation on three proficiency panels. J Clin Microbiol, 46(4):1510-1513.

Shinoyama, M., Suzuki, M. & Nomura, S. 2012. Fulminant tuberculous meningitis--autopsy case report. Neurol Med Chir (Tokyo), 52(10):761-764.

Simberkoff, M.S., Moldover, N.H. & Rahal, J., Jr. 1980. Absence of detectable bactericidal and opsonic activities in normal and infected human cerebrospinal fluids. A regional host defense deficiency. J Lab Clin Med, 95(3):362-372.

Solomons, R.S., Wessels, M., Visser, D.H., Donald, P.R., Marais, B.J., Schoeman, J.F. & van Furth, A.M. 2014. Uniform research case definition criteria differentiate tuberculous and bacterial meningitis in children. Clin Infect Dis, 59(11):1574-1578.

Thigpen, M.C., Whitney, C.G., Messonnier, N.E., Zell, E.R., Lynfield, R., Hadler, J.L., Harrison, L.H., Farley, M.M., Reingold, A., Bennett, N.M., Craig, A.S., Schaffner, W., Thomas, A., Lewis, M.M., Scallan, E., Schuchat, A. & Emerging Infections Programs, N. 2011. Bacterial meningitis in the United States, 1998-2007. N Engl J Med, 364(21):2016-2025.

Thwaites, G., Fisher, M., Hemingway, C., Scott, G., Solomon, T., Innes, J. & British Infection, S. 2009. British Infection Society guidelines for the diagnosis and treatment of tuberculosis of the central nervous system in adults and children. J Infect, 59(3):167-187.

Thwaites, G.E. & Tran, T.H. 2005. Tuberculous meningitis: many questions, too few answers. Lancet Neurol, 4(3):160-170.

Thwaites, G.E., Chau, T.T. & Farrar, J.J. 2004. Improving the bacteriological diagnosis of tuberculous meningitis. J Clin Microbiol, 42(1):378-379.

Tunkel, A.R. & Scheld, W.M. 1993. Pathogenesis and pathophysiology of bacterial meningitis. Clin Microbiol Rev, 6(2):118-136.

Tyler, K.L. 2004. Herpes simplex virus infections of the central nervous system: encephalitis and meningitis, including Mollaret's. Herpes, 11 Suppl 2:57A-64A.

Unhanand, M., Mustafa, M.M., McCracken, G.H., Jr. & Nelson, J.D. 1993. Gram-negative enteric bacillary meningitis: a twenty-one-year experience. J Pediatr, 122(1):15-21.

van der Sar, S.A., Zielman, R., Terwindt, G.M., van den Maagdenberg, A.M., Deelder, A.M., Mayboroda, O.A., Meissner, A. & Ferrari, M.D. 2015. Ethanol contamination of cerebrospinal fluid during standardized sampling and its effect on (1)H-NMR metabolomics. Anal Bioanal Chem, 407(16):4835-4839.

van Toorn, R., Springer, P., Laubscher, J.A. & Schoeman, J.F. 2012. Value of different staging systems for predicting neurological outcome in childhood tuberculous meningitis. The International Journal of Tuberculosis and Lung Disease, 16(5):628-632.

Van, T.T. & Farrar, J. 2014. Tuberculous meningitis. J Epidemiol Community Health, 68(3):195-196.

Wilkinson, R.J., Rohlwink, U., Misra, U.K., van Crevel, R., Mai, N.T.H., Dooley, K.E., Caws, M., Figaji, A., Savic, R., Solomons, R., Thwaites, G.E. & Tuberculous Meningitis International Research, C. 2017. Tuberculous meningitis. Nat Rev Neurol, 13(10):581-598

Wolzak, N.K., Cooke, M.L., Orth, H. & van Toorn, R. 2012. The changing profile of pediatric meningitis at a referral centre in Cape Town, South Africa. Journal of tropical pediatrics, 58(6):491-495.

Wright, W.F., Pinto, C.N., Palisoc, K. & Baghli, S. 2019. Viral (aseptic) meningitis: A review. J Neurol Sci, 398:176-183.

Yaramis, A., Gurkan, F., Elevli, M., Soker, M., Haspolat, K., Kirbas, G. & Tas, M.A. 1998. Central nervous system tuberculosis in children: a review of 214 cases. Pediatrics, 102(5):E49.

Zhang, P., Zhang, W., Lang, Y., Qu, Y., Chen, J. & Cui, L. 2019. (1)H nuclear magnetic resonance-based metabolic profiling of cerebrospinal fluid to identify metabolic features and markers for tuberculosis meningitis. Infect Genet Evol, 68:253-264.

# CHAPTER 3 NMR METABOLOMICS METHODOLOGY AND ANALYST REPEATABILITY

## 3.1 Introduction

Potential (unwanted) technical/analytical variation in any metabolomics experiment can come from the analytical instrument and/or analyst. NMR is an analytical platform known for its ability to produce highly repeatable and reproducible results (Emwas *et al.*, 2019). This is because the parameters for the NMR spectrometer are calibrated for each sample that is analysed, prior to analysis, which ensures minimal variation caused by the NMR spectrometer. The four calibration steps include: 1) the tuning of the probe to resonate at the precise frequency of the spectrometer (e.g., 500 MHz), 2) locking onto the deuterated solvent (deuterium oxide ($D_2O$)) in the sample, after which 3) shimming is performed ensuring that the magnetic field is accurately defined along all axes, and finally, 4) pulse calibration is performed to ensure that the radio frequency (RF) pulse is calibrated correctly to 90º, all while maintaining a constant temperature (300 K) within the instrument during analysis. Since the analytical platform (NMR) used in my study is considered repeatable, the only potential (unwanted) analytical variation can come from the analyst. Analyst repeatability thus needs to be determined to ensure optimal and accurate results are obtained – discussed in this chapter, according to objective 1.

## 3.2 Methods

### 3.2.1 Creation of artificial CSF

The creation of an artificial CSF (aCSF) was required for the analytical repeatability tests, as no commercially available aCSF was available for purchase. The use of actual patient CSF for assessing analyst repeatability has numerous ethical complications that require additional motivations to acquire for such method validation purposes.

In order to create a biological representative aCSF, a salt and buffer solution was prepared to simulate the ions and buffer capacity of CSF. For the creation of this solution, sodium chloride, potassium chloride, calcium chloride and magnesium chloride was used to represent the ions in CSF, and disodium phosphate and monosodium phosphate was used to represent the buffer in the aCSF. A 500 mL solution was made up in preparation for the addition of the metabolites afterwards, the exact concentrations and calculated weights of which can be found in Table 3-1.

**Table 3-1 Ions with their concentration and weight**

| Ion | Concentration (μM) | Weight (mg) per 500ml |
|---|---|---|
| Sodium chloride | 150.44 | 8.66 |
| Potassium chloride | 3.89 | 0.22 |
| Calcium chloride | 3.58 | 0.21 |
| Magnesium chloride | 2.83 | 0.16 |
| Disodium phosphate | 3.72 | 0.21 |
| Monosodium phosphate | 0.47 | 0.03 |

In order to identify the metabolites commonly found in CSF that are detectable and identifiable on the NMR analytical platform, Wishart *et al.*, 2008 was refered to. The metabolites selected to create the aCSF, and their average physiological concentrations according to Wishart et al. (2018), are listed in Table 3.2.

**Table 3-2 Selected metabolites and their average concentration**

| Metabolite | Average concentration (μM) |
|---|---|
| Glucose | 2960 |
| Lactate | 1651 |
| Alanine | 46 |
| Lysine | 29 |
| Valine | 19 |
| myo-Inositol | 84 |
| Pyruvate | 53 |
| Citrate | 225 |
| Glutamine | 432 |

A 200% stock solution was made up in order to create three concentrations to accurately determine analyst repeatability: a low, medium and high stock solution to represent 50%, 100% and 150% of average concentration respectively. This was done by dissolving specific weights of the metabolites in 500 mL of $H_2O$. The calculated weight of each metabolite can be found in Table 3.3.

**Table 3-3 Weight used for each metabolite to establish stock solution**

| Metabolite | Weight (mg) per 500 mL |
|---|---|
| Glucose | 919.5 |
| Lactate | 191 |
| Alanine | 4.1 |
| Lysine | 5.2 |
| Valine | 2.2 |
| myo-Inositol | 15.1 |
| Pyruvate | 18.7 |
| Citrate | 43.2 |
| Glutamine | 63.1 |

After making up the aforementioned 200% stock solution, the solution was sonicated for one hour to ensure the solution was homogenous. Serial dilutions were done from the stock solution to create the three levels (defined as low, medium and high as previously described). For the low (50% solution), 25 mL of the stock solution was aliquot into a 100 mL Schott glass bottle and 75 mL of milliq water was added to top up the solution to 100 mL. For medium (100% solution), 50 mL of the stock solution was aliquot into a 100 mL Schott glass bottle and 50 mL of milliq water was added to top up the solution to 100 mL. For high (150% solution), 75 mL of the stock solution was aliquot into a 100 mL Schott glass bottle and 25 mL of milliq water was added to top up the solution to 100 mL. Each of the solutions were split into 2 x 50 mL falcon plastic tubes, One tube was used to determine the NMR repeatability, and the other tube was stored at -80ºC for future use.

### 3.2.2 Sample preparation

Each sample was prepared, as according to the SOP protocols for analysing patient collected CSF as follows: 1) a 540 µL aliquot of each sample was transferred to a microcentrifuge tube, after which 60 µL NMR buffer solution[1] was added. Sample was then mixed under vortex to ensure completely homogenous and centrifuged at 12 000 x g for five minutes to remove any

[1] $^{1}$H-NMR buffer solution

A $^{1}$H-NMR phosphate buffer solution (1.5 M) was prepared in advance for the $^{1}$H-NMR sample preparation by dissolving 20.4 g of potassium phosphate monobasic ($KH_2PO_4$) in 80 mL of deuterium oxide ($D_2O$). A precise amount of 100 mg of our quantitative internal standard (TSP; trimethylsilyl-2,2,3,3-tetradeuteropropionic acid) was added to the solution. To prevent bacterial growth a quantity of 13 mg of sodium azide ($NaN_3$) was dissolved in 10 mL of $D_2O$ and added to the solution. The buffer solution was sonicated to ensure thorough mixing, the pH adjusted to 7.4 (by adding potassium hydroxide (KOH) pellets), and transferred to a volumetric flask to adjust the volume to 100 mL with $D_2O$.

particulates. A final volume of 550 µL was transferred to a 5mm NMR tube. This procedure was done for 10 replicates of each of the aforementioned dilutions of aCSF and repeated every day for 3 days consecutively, in order to determine the inter-day and intra-day repeatability of the analyst. Overall, this resulted in the analysis of 90 replicates (30 low, 30 medium, 30 high) in total.

### 3.2.3 $^{1}$H-NMR analysis

Samples were loaded onto a SampleXpress autosampler in a randomized order and were measured at 500 MHz on a Bruker Avance III HD NMR spectrometer equipped with a 5mm triple-resonance inverse (TXI) $^{1}$H {$^{15}$N, $^{13}$C} probe head and x, y, z gradient coils. The inner coil of the TXI probe was optimized for $^{1}$H observation, the focus of our study. $^{1}$H spectra were acquired as 128 transients in 32K data points with a spectral width of 10504 Hz and acquisition time of 5.4 sec. Receiver gain was set to 64. The sample temperature was maintained at 300 K and the $H_2O$ resonance was presaturated by single-frequency irradiation (NOESY-1D) during a relaxation delay of 4s, with a 90° excitation pulse of 8 µs. Shimming of the sample was performed automatically on the deuterium signal. Fourier transformation and phase and baseline correction were done automatically. The quality of the spectra was checked by ensuring that resonance line widths for TSP and metabolites were <1 Hz. Software used for NMR pre-processing was Bruker Topspin (V3.5) and Bruker AMIX (V3.9.14) was used for binning and metabolite identification (based upon commercial and in-house pure compound spectral libraries) and quantification. Selective binning (Cui & Churchill, 2003; De Meyer *et al.*, 2008; van den Berg *et al.*, 2006) was done to create a data matrix of the nine selected metabolites found in Table 3.2, for concentration calculation and statistical analysis.

## 3.3 Results

**Table 3-4 Calculated average lab CV of all three levels over three days**

| | Average lab CV (%) | | |
|---|---|---|---|
| **Metabolite** | **Low** | **Medium** | **High** |
| Glucose | 5,24 | 1,92 | 1,80 |
| Lactate | 5,49 | 1,84 | 1,99 |
| Alanine | 13,94 | 6,45 | 4,97 |
| Lysine | 25,23 | 12,38 | 7,83 |
| Valine | 26,27 | 11,40 | 8,74 |
| Myo-Inositol | 16,81 | 8,39 | 5,26 |
| Pyruvate | 9,08 | 3,35 | 3,36 |
| Citrate | 7,57 | 2,84 | 2,51 |
| Glutamine | 6,18 | 2,29 | 2,06 |

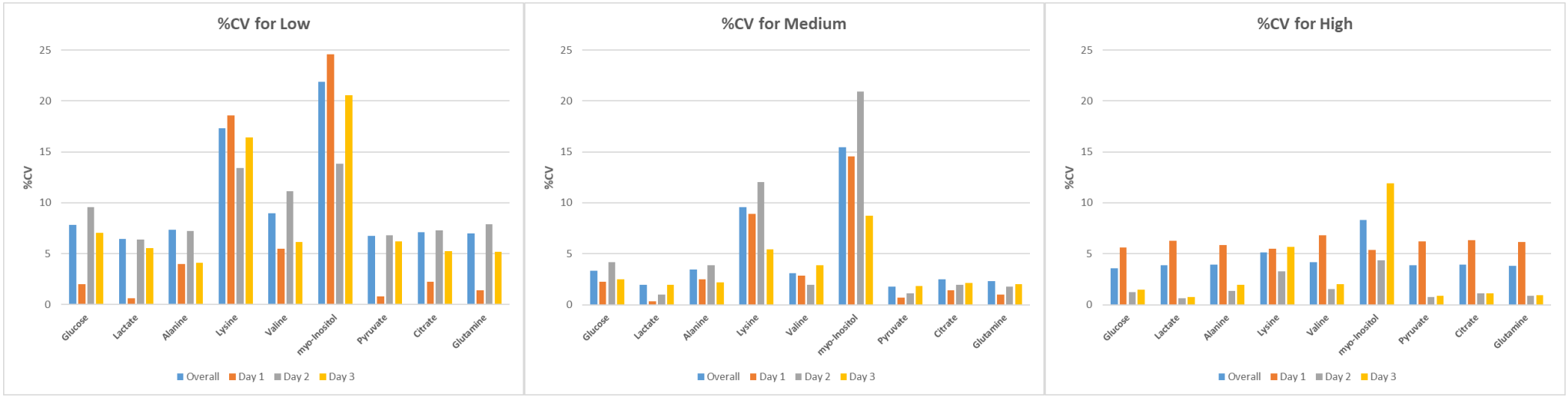


**Figure 3-1 Calculated CV plots for the nine metabolites at low, medium, and high concentrations.**

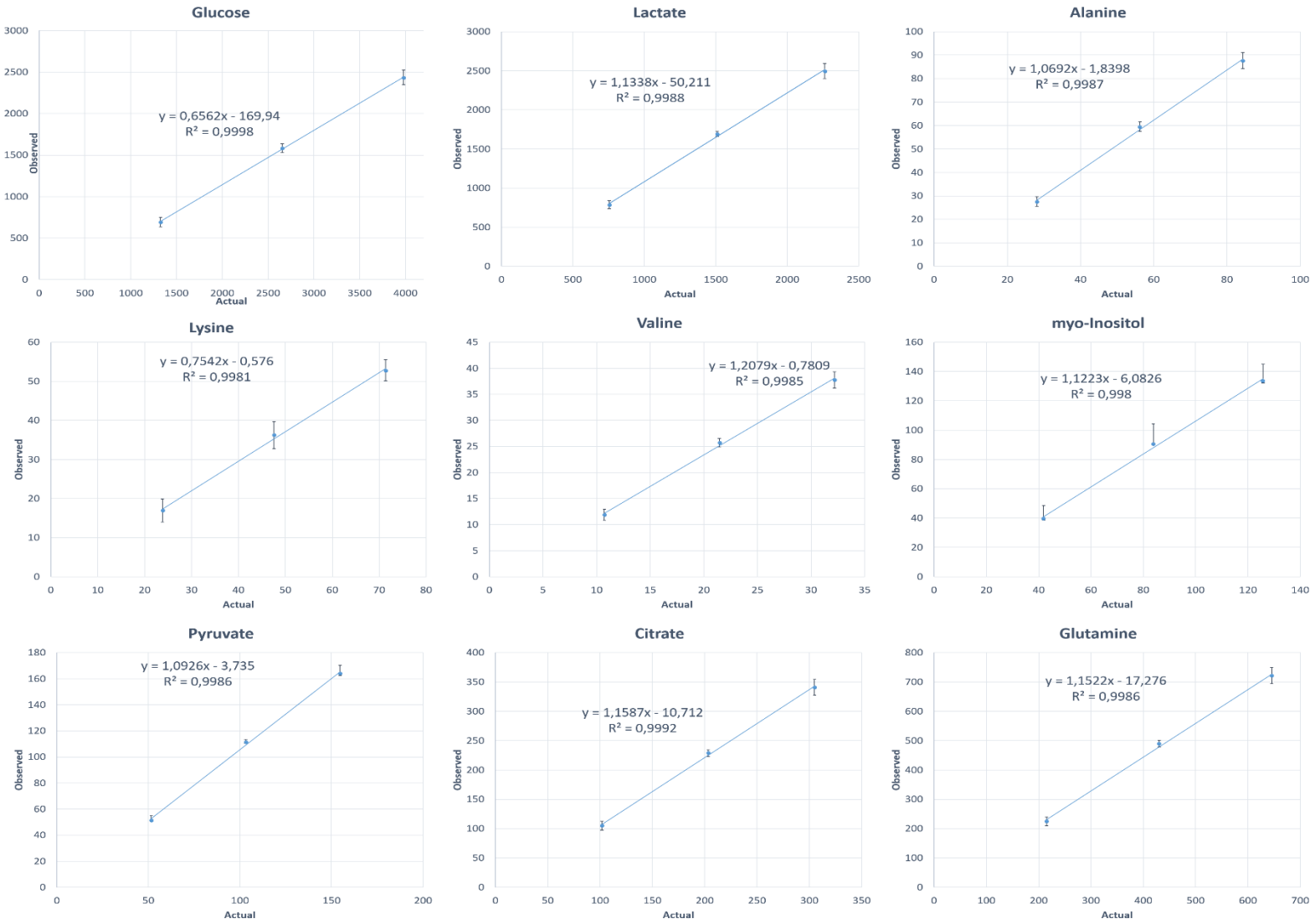


**Figure 3-2 Linearity results of the nine metabolite at low, medium and high concentration, with their respective error bars.**

### 3.3.1 Assessment of analyst repeatability

The % coefficient of variation (CV) was calculated for each day over 10 repeats for each sample concentration level over the three days and presented as graphs in Figure 3.1. The low concentration CV values were acceptable (on average <10% CV), with the exception of lysine and myo-inositol. The medium concentration CV values were acceptable as well (on average < 5% CV), again with the exception of lysine and myo-inositol. The high concentration CV values were overall all acceptable (on average <7% CV). Lysine occurs as a pentet (signal spread over five peaks) that is close to the noise level at the low and medium sample concentrations, which makes it difficult to quantify accurately as it is approaching the lower quantification limit of $^{1}$H-NMR, resulting in higher CV values. Myo-inositol is a cyclic sugar alcohol with six protons, that results in four resonance groups, a triplet located between 3.24-3.29 ppm, a double doublet located between 3.5 - 3.55 ppm, a triplet located between 3.58-3.63 ppm and a triplet located between 4.04 - 4.06 ppm at pH of 7.4. For the repeatability assessment the triplet located at 4.04-4.06 ppm was quantified as it was the only region not overlapped by other signals, however, this triplet can be affected by the suppression of the water peak at 4.72 ppm (Govindaraju *et al.*, 2000), accounting for the higher CV values.

The linearity results were calculated by plotting the observed concentration against the actual concentration. These plots are presented in Figure 3.2 and show good linearity as all nine metabolites have a $R^2$ value of > 0.99. The error bars at each point are small enough to be negligible, indicating quantification is acceptable and repeatable.

Considering the CV values for all 3 sample concentration levels and linearity plots, it can be concluded that the analyst is competent and operates in a repeatable manner, able to generate precise results, thus objective 1 was successfully completed.

## 3.4 References

Cui, X. & Churchill, G.A. 2003. Statistical tests for differential expression in cDNA microarray experiments. Genome Biology, 4(4):210.

De Meyer, T., Sinnaeve, D., Van Gasse, B., Tsiporkova, E., Rietzschel, E.R., De Buyzere, M.L., Gillebert, T.C., Bekaert, S., Martins, J.C. & Van Criekinge, W. 2008. NMR-Based Characterization of Metabolic Alterations in Hypertension Using an Adaptive, Intelligent Binning Algorithm. Analytical Chemistry, 80(10):3783-3790.

Emwas, A.H., Roy, R., McKay, R.T., Tenori, L., Saccenti, E., Gowda, G.A.N., Raftery, D., Alahmari, F., Jaremko, L., Jaremko, M. & Wishart, D.S. 2019. NMR Spectroscopy for Metabolomics Research. Metabolites, 9(7).

Govindaraju, V., Young, K. & Maudsley, A.A. 2000. Proton NMR chemical shifts and coupling constants for brain metabolites. NMR in Biomedicine, 13(3):129-153.

van den Berg, R.A., Hoefsloot, H.C., Westerhuis, J.A., Smilde, A.K. & van der Werf, M.J. 2006. Centering, scaling, and transformations: improving the biological information content of metabolomics data. BMC Genomics, 7(1):142.

Wishart, D.S., Lewis, M.J., Morrissey, J.A., Flegel, M.D., Jeroncic, K., Xiong, Y., Cheng, D., Eisner, R., Gautam, B., Tzur, D., Sawhney, S., Bamforth, F., Greiner, R. & Li, L. 2008. The human cerebrospinal fluid metabolome. J Chromatogr B Analyt Technol Biomed Life Sci, 871(2):164-173.

# CHAPTER 4 METABOLIC CHARACTERIZATION OF TUBERCULOUS MENINGITIS IN A SOUTH AFRICAN PAEDIATRIC POPULATION USING $^{1}$H-NMR METABOLOMICS

## 4.1 Metabolic characterization of tuberculous meningitis in a South African paediatric population using $^{1}$H-NMR metabolomics

Christiaan De Wet van Zyl[1], Du Toit Loots[1], Regan Solomons[2], Mari van Reenen[1], Shayne Mason[1*]

[1] Human Metabolomics, Faculty of Natural and Agricultural Sciences, North-West University, Potchefstroom, South Africa.

[2] Department of Pediatrics and Child Health, Faculty of Medicine and Health Sciences, Stellenbosch University, Tygerberg, South Africa.

*Corresponding author: Shayne Mason (https://orcid.org/0000-0002-2945-5768)

North-West University

Private Bag X6001

Potchefstroom

South Africa

2531

Email: nmr.nwu@gmail.com

Keywords: cerebrospinal fluid (CSF), proton magnetic resonance ($^{1}$H-NMR) spectroscopy, tuberculous meningitis (TBM), paediatrics, metabolomics, metabolic characterization.

Accepted for publication in the Journal of Infection (IF: 4.842) on 27 June 2020 – see Annexure 2 for journal front page of article.

### 4.1.1 **Abstract**

Objective: To better characterize the cerebrospinal fluid (CSF) metabolic profile of tuberculous meningitis (TBM) cases using a South African paediatric cohort.

Methods: $^{1}$H-NMR metabolomics was used to analyse the CSF of a South African paediatric cohort. Univariate and multivariate statistical analyses were performed to compare a homogeneous control group with a well-defined TBM group.

Results: Twenty metabolites were identified to discriminate TBM cases from controls. As expected, reduced glucose and elevated lactate were the dominating discriminators. A closer investigation of the CSF metabolic profile yielded 18 metabolites of statistical significance. Ten metabolites (acetate, alanine, choline, citrate, creatinine, isoleucine, lysine, myo-inositol, pyruvate and valine) overlapped with two other prior investigations. Eight metabolites (2-hydroxybutyrate, carnitine, creatine, creatine phosphate, glutamate, glutamine, guanidinoacetate and proline) were unique to our paediatric TBM cohort.

Conclusions: Through strict exclusion criteria, quality control checks and data filtering, eight unique CSF metabolites associated with TBM were identified for the first time and linked to: uncontrolled glucose metabolism, upregulated proline and creatine metabolism, detoxification and disrupted glutamate–glutamine cycle in the TBM samples. Associated with oxidative stress and chronic neuroinflammation, our findings collectively imply destabilization, and hence increased permeability, of the blood–brain barrier in the TBM cases.

### 4.1.2 Introduction

Tuberculous meningitis (TBM) – a disease caused by *Mycobacterium tuberculosis* (*M. tb*) – is a chronic form of bacterial meningitis, the most severe manifestation of tuberculosis (TB), and associated with substantial morbidity and mortality.[1] The paediatric population in communities with a high TB burden, such as those in the Western Cape province of South Africa, are at a high risk of TBM.[2] *M. tb* is known to cause characteristic persistent granulomatous inflammation,[3] and is one of the most common infectious causes of chronic meningitis,[4,5] defined here as at least 4 weeks of symptoms with signs of inflammation in the cerebrospinal fluid (CSF).[6,7] The pathogenesis of TBM is a two-step process, as originally described in 1933 by Rich and McCordock,[8] and more recently by Thwaites and Tran in 2005.[9] 1) *M. tb* invades the host alveolar macrophages through droplet inhalation, with subsequent dissemination to other parts of the body, including the central nervous system. 2) At the meninges, *M. tb* forms tubercles, called Rich foci, which rupture and release tubercle bacilli into the subarachnoid space, forming dense exudates, signalling the onset of TBM. This exudate, rich in macrophages, neutrophils and erythrocytes,[10] surrounds arteries and nerves, as well as restricts the flow of CSF, resulting in hydrocephalus. The microglia, whose many functions include immune regulation, are the primary cerebral cells infected by *M. tb*, although astrocytes and neurons are also affected.[11] Of the biochemical indicators of TBM, reduced CSF glucose and elevated CSF lactate have proved to be of significant importance in various studies.[12-17] However, further metabolic perturbations are also expected within the CSF.

The term metabolomics was first introduced in 1998 by Oliver et al.[18] as the relative change in concentrations of metabolites that are associated with the deletion or overexpression of a gene, and was explicitly described by Fiehn in 2001[19] to be the “comprehensive and quantitative analysis of all small molecules in a biological system”. Metabolomics offers an advantage over other parts of the ‘omics’ family – for example, proteomics and transcriptomics – as metabolites are the final products of enzymatic reactions in cells. Metabolomics most accurately reflects the true cellular activity or change without the challenges of post-transcriptional or post-translational modifications that can occur within transcriptomics and proteomics, respectively, that adds complexity. Proton nuclear magnetic resonance ($^1$H-NMR) spectroscopy is a method that does not require prior separation of metabolites, and is able simultaneously to detect and determine the concentration of all types of metabolites, above the detection limit of 1 µM, that are present in a complex biological sample. The CSF, a biofluid obtained from the site of infection in TBM, holds vast metabolic information about TBM that has yet to be fully explored. The aim of this study was to use $^1$H-NMR metabolomics to better characterize the CSF metabolic profile in a South African TBM paediatric cohort. Through strict

data filtering, in conjuncture with comprehensive meta-data accompanying the CSF samples, we were able to better define our cohort; hence, eight unique CSF metabolites, linked to five metabolic pathways, were identified in the TBM cases.

### 4.1.3 Patients and methods

#### 4.1.3.1 Patient selection, demographics and ethics

The paediatric (≤12 years old) sample group used in this investigation reside in an area endemic for TB – the Western Cape province of South Africa.[20] Each participant was referred from local regional clinics to the paediatric service at the Tygerberg Academic Hospital in Cape Town, based upon clinical signs and symptoms of meningitis. Upon admission to the hospital, each patient was assessed by the paediatric neurology team and, when they were stable enough, a CSF sample was collected via lumbar puncture for routine differential diagnostic purposes. Written, informed consent and/or assent were obtained for CSF samples to be used for research purposes. The study was approved by the Health Research Ethics Committee (HREC) of Stellenbosch University, Tygerberg Hospital (ethics approval no. N16/11/142), the Western Cape Provincial Government, as well as by the HREC of the North-West University, Potchefstroom campus (ethics approval no. NWU-00063-18-S1). The medical history of each patient was collected; a summary of the pertinent clinical demographics of the cases used for metabolic characterization in this study is given in Table 1. The main exclusion criterion for all participants was HIV-positive/unknown cases because HIV co-infection further confounds an already complex CSF metabolic profile.

**Table 4-1 Summary of mean/median ranges of various clinical results of cases investigated**

| | TBM (N = 23) | Control (N = 33) |
|---|---|---|
| | Mean (median) ± SD | Mean (median) ± SD |
| Age (months) | 52.5 (46) ± 34.6 | 42.3 (28) ± 42.2 |
| Gender | Male = 12 | Male = 23 |
| | Female = 11 | Female = 10 |
| CSF leucocytes (cells/μL) | 223.43 (93) ± 411.01 | 1.48 (0) ± 4.13 |
| CSF lymphocytes (cells/μL) | 193.48 (86) ± 313.07 | 1.38 (0.5) ± 3.38 |
| CSF PMNs (cells/μL) | 33.52 (8) ± 87.08 | 0.16 (0) ± 0.72 |
| CSF glucose (mmol/L) | 2.18 (1.85) ± 1.48 | 3.71 (3.9) ± 1.04 |

*PMN's = polymorphonuclear cells. CSF Glucose determined on-site during diagnosis via glucose oxidase assay.

#### 4.1.3.2 Experimental group definition

The two experimental groups used in this study were patients with bacteriologically confirmed TBM and non-meningitis (control) patients. The control group consisted of paediatric patients that were suspected to have meningitis based upon clinical symptoms but proved to be negative for meningitis upon final diagnosis – described in Table S1 in the supplementary information (SI), in Annexure 1. Furthermore, we excluded control patients with any indicator(s) of another form of *M. tb* infection – for example, *M. tb*-positive gastric washing or sputum, abnormal chest X-ray, close contact with family members with active TB – and neurological symptoms – such as viral encephalopathy and febrile seizures. Through these screening measures, the original number of control patients (n = 97) was reduced to a more homogeneous group (n = 36) for this study.

The number of HIV-negative patients suspected of TBM in our experimental group originally consisted of 103 paediatric cases. Cases given a final 'definite' TBM diagnosis (n = 25) were included in this study. A 'definite' diagnosis of TBM was assigned based upon a uniform case definition typically used in clinical research:[21]

1. Clinical symptoms of meningitis (headache, fever, nausea/vomiting, photophobia, meningeal irritation and/or neck stiffness) and

2. One or more of the following:

    i. Presence of acid-fast bacilli in the CSF

    ii. CSF culture positive for *M. tb*, or

    iii. *M. tb*-positive commercial NAAT (including GeneXpert) of CSF.

A ‘definite’ TBM diagnosis was also supported by: 1) a positive tuberculin skin test, 2) a computerized tomography scan or magnetic resonance image demonstrating the characteristic features of TBM (ventricular dilatation, meningovascular enhancement and/or presence of granulomas), and 3) clinical evidence of other forms of extra-pulmonary TB. A schematic workflow of our experimental design is given in Fig. 1.

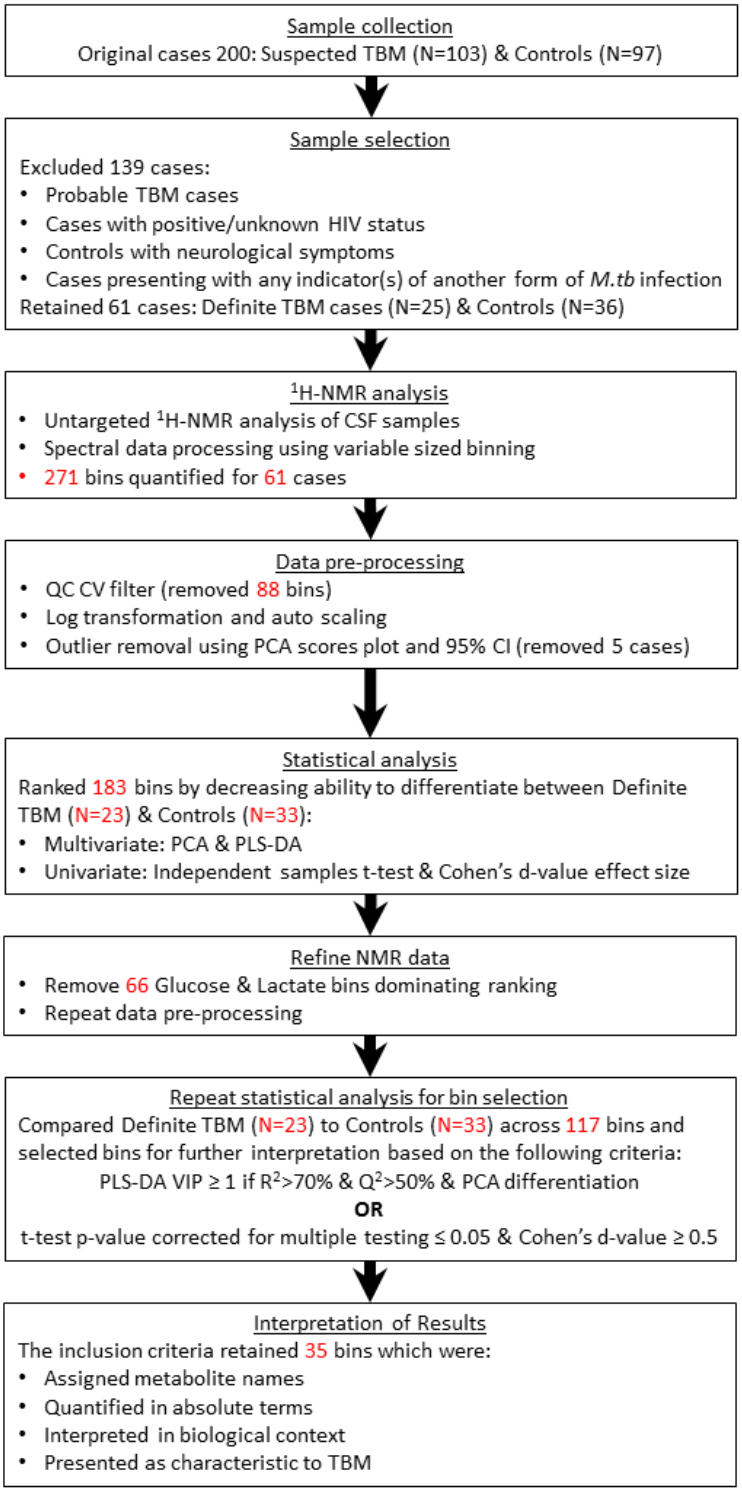


**Figure 4-1 Schematic workflow of $^{1}$H-NMR metabolomics experimental design**

#### 4.1.3.3 Sample handling and storage

All CSF samples were stored at –80°C and transported on ice to the Human Metabolomics biosafety level 3 (BSL3) lab of North-West University. A safety precaution to make sure that the CSF samples were safe for general lab use involved a 'cleaning' (filtration) procedure. All CSF samples were filtered in the BSL3 lab by using Amicon Ultra-2mL 10 000 MWCO centrifugal filters at 4500 *g* for 20 minutes to physically remove infectious bacteria and bacterial components from the sample matrix. This filtration step also had the dual purpose of physically removing interfering proteins in order to separate the low molecular weight molecules (metabolites). Each centrifugal filter unit was pre-rinsed three times using ~2 mL distilled water ($dH_2O$) and centrifuged at 4500 *g* for 10 minutes in order to remove residual amounts of glycerol from the membrane filters. Glycerol is visible on a $^1$H-NMR spectrum and exogenous amounts could interfere with surrounding NMR signals and/or cause erroneous glycerol quantification. Each sample filtrate was re-collected in clean sample collection tubes, sterilized and re-labelled as per the original sample tube, with 100 µL of each sample being aliquoted for NMR analysis and 20 µL aliquoted for a pooled quality control (QC) sample. The pooled QC sample was aliquoted into 24 equal-volume amounts. All filtered samples (including QC samples) were stored immediately at –80°C until further use.

#### 4.1.3.4 $^1$H-NMR buffer solution

A $^1$H-NMR phosphate buffer solution (1.5 M) was prepared in advance for the$^1$H-NMR sample preparation by dissolving 20.4 g of potassium phosphate monobasic ($KH_2PO_4$) in 80 mL of deuterium oxide. A precise amount of 100 mg of our quantitative internal standard (TSP; trimethylsilyl-2,2,3,3-tetradeuteropropionic acid) was added to the solution. To prevent bacterial growth, 13 mg of sodium azide was dissolved in 10 mL of $D_2O$ and added to the solution. The buffer solution was sonicated to ensure thorough mixing, the pH adjusted to 7.4 (by adding potassium hydroxide pellets), and transferred to a volumetric flask to adjust the volume to 100 mL with $D_2O$.

#### 4.1.3.5 Sample preparation

Prior to preparation, all samples were completely thawed at room temperature. A volume of 100 µL of CSF was centrifuged at 12 000 *g* for 5 minutes. The supernatant of the samples was then prepared in a 2-mm NMR tube, using an eVol® NMR digital syringe and a 180-mm-long bevel-tipped needle. The programmed pipetting sequence of the eVol® NMR digital syringe was as follows: 1) aspirate 6 µL NMR buffer solution; 2) aspirate 54 µL of the filtered sample (10%:90% ratio of $D_2O$:$H_2O$); 3) purge 60 µL (this dispenses prepared sample into 2-

mm NMR tube); 4) aspirate 60 µL; 5) purge 60 µL (mix sample once inside 2-mm NMR tube to ensure homogeneity); followed by a wash sequence; 6) aspirate 100 µL $dH_2O$; 7) purge 100 µL (waste); 8) aspirate 100 µL $dH_2O$; 9) purge 100 µL (waste); 10) aspirate 100 µL $dH_2O$; 11) purge 100 µL (waste).[22] The Bruker MATCH system was used – an adapter with a gripper to hold the 2-mm NMR tube in order to be analysed in a 5-mm NMR probe.

#### 4.1.3.6 $^{1}$H-NMR analysis

Samples were loaded onto a SampleXpress autosampler in a randomized order with QC samples interspersed periodically. Samples were measured at 500 MHz on a Bruker Avance III HD NMR spectrometer equipped with a 5 mm triple-resonance inverse (TXI) $^{1}$H {$^{15}$N, $^{13}$C} probe head and x, y, z gradient coils. The inner coil of the TXI probe was optimized for $^{1}$H observation, the focus of our study. $^{1}$H spectra were acquired as 128 transients in 32K data points with a spectral width of 6000 Hz and acquisition time of 2.72 s. Receiver gain was set to 64. The sample temperature was maintained at 300 K and the $H_2O$ resonance was presaturated by single-frequency irradiation during a relaxation delay of 4 s, with a 90° excitation pulse of 8 µs. Shimming of the sample was performed automatically on the deuterium signal. Fourier transformation and phase and baseline correction were performed automatically. The quality of the spectra was checked by ensuring that resonance line widths for TSP and metabolites were <1 Hz. Software used for NMR pre-processing was Bruker Topspin (V3.5), and Bruker AMIX (V3.9.14) was used for binning and metabolite identification (based on commercial and in-house pure compound spectral libraries) and quantification. Selective binning[23-25] between 0.76 ppm and 9.20 ppm was done to create a data matrix of 205 variably-sized bins (excluding the water region 4.20–5.30 ppm) for statistical analysis.

#### 4.1.3.7 Statistical analysis

*Data pre-processing explained*

To ensure reliable data, 24 pooled QC samples were run at set intervals throughout the batch analysis. After completion of sample analysis and spectral binning, only bins with a QC coefficient of variance (CV) below 50% were retained. Spectral intensity does not necessarily imply biological importance and so data were log transformed and auto scaled to, first, correct for skewed distributions and, second, to place bins on equal footing when presented for multivariate analysis. Finally, outliers were identified using principal component analysis (PCA) as this approach summarizes all variations in the data to fewer dimensions or principal components. Samples were then projected onto the components explaining the largest amount of variation, also referred to as a scores plot. Samples with scores outside the 95%

CI of the score centroid were considered statistical outliers and excluded. These samples also correspond to those with extreme Hotelling's T-squared values.

*Statistical analysis explained*

Two supervised statistical approaches were used to rank and iteratively select bins that differed between control and TBM cases with the aim of characterizing the latter, one being multivariate and the other univariate to provide a more comprehensive ranking. The multivariate method selected was partial least squares–discriminant analysis (PLS-DA) as it is known to be a very powerful tool for identifying even slight differences. That said, detected differences may be specific to the data set and so supportive measures were set in place. Unsupervised PCA models were used to partially validate separation achieved in PLS-DA models along with the leave-one-out predictive accuracy ($Q^2$) achieved by said models. The PCA model subsequently validated a PLS-DA if sufficient differentiation between groups was observed in a PCA scores plot of the top 3 components, PLS-DA models validated internally if predictive accuracy ($R^2$) exceeded 70% and leave-one-out predictive accuracy ($Q^2$) exceeded 50%.

The prediction accuracy thresholds set here for $R^2$ and $Q^2$ may be too low and a leave-one-out strategy too conservative to support generalizing to a predictive model. That said, the aim of this paper was to characterize better a complex disease by comparing infected with a clinically similar control group. Therefore, ranking bins according to their discriminatory ability, based on the variable importance in projection (VIP) score produced by the PLS-DA model, was considered appropriate, especially given natural separation in the PCA scores plots as an additional requirement.

The univariate method selected was the independent samples t-test (making no assumption of equal variances) and Cohen's d-value effect size to serve as validation of practical relevance and so support the aim of characterizing TBM. P-values were adjusted to correct for multiple testing. The Benjamini–Hochberg approach was implemented using the Matlab fdr script of Arnaud Delorme (2008) sourced through MathWorks (https://uk.mathworks.com/matlabcentral/fileexchange/27960-resampling-statistical-toolkit/content/statistics/fdr.m).

### 4.1.4 Results

#### 4.1.4.1 Assessment of quality of $^{1}$H-NMR metabolomics data

In order to determine the quality/reliability of the $^{1}$H-NMR metabolomics data obtained, the 24 pooled QC samples were assessed. Any bin that could not be quantified consistently across all QC observations was removed. To identify such bins the CV was calculated and, if it exceeded 50% for any given bin, the bin was removed. Subsequently, a 3D PCA scores plot comparing all experimental samples analysed with QC samples was constructed (Fig. S1). The scores plot shows that the QC samples cluster closely together, showing far less variation than the patient samples, to indicate precision in analysis and data collection. An overlay of the $^{1}$H-NMR spectra of all QC samples (Fig. S2) also indicates, qualitatively, that all QCs produced repeatable results. Based upon the assessment of these QC results, we can state that the analytical platform used in this study ($^{1}$H-NMR) produced highly repeatable data, and infer that the statistically significant differences can be ascribed to a biological origin.

#### 4.1.4.2 $^{1}$H-NMR spectral output

Representative $^{1}$H-NMR spectra of each of the two experimental groups are illustrated in Fig. 2. The spectra cover the region of 0–10 ppm, with the removal of the water peak (4.70–5.20 ppm), and are scaled to the internal standard peak (TSP: 0 ppm). Fig. 2 illustrates some of the qualitative differences, as shown in boxes A–F, between controls and TBM cases from our paediatric cohort. Metabolites were identified based upon comparison with spectral libraries of pure compounds, along with confirmation from 2D JRES and 2D COSY NMR information.

#### 4.1.4.3 Data filtering

After the QC CV filter, as described above, 183 bins remained for statistical analysis. Assessment of statistical outliers identified 5 cases (TBM: 2; controls: 3) that were removed from analysis. Univariate and multivariate statistics were performed on the 23 TBM and 33 control cases. As expected, reduced glucose and increased lactate were identified as the primary metabolites distinguishing TBM from controls. The first three principal components (Fig. S3) show an accumulated explained variance of 60%. However, our aim was to determine the more subtle metabolic differences and, in order to identify these, the 66 bins representing glucose and lactate were removed from further analysis. Hence, a final data matrix of 117 bins underwent further univariate and multivariate statistical analyses.

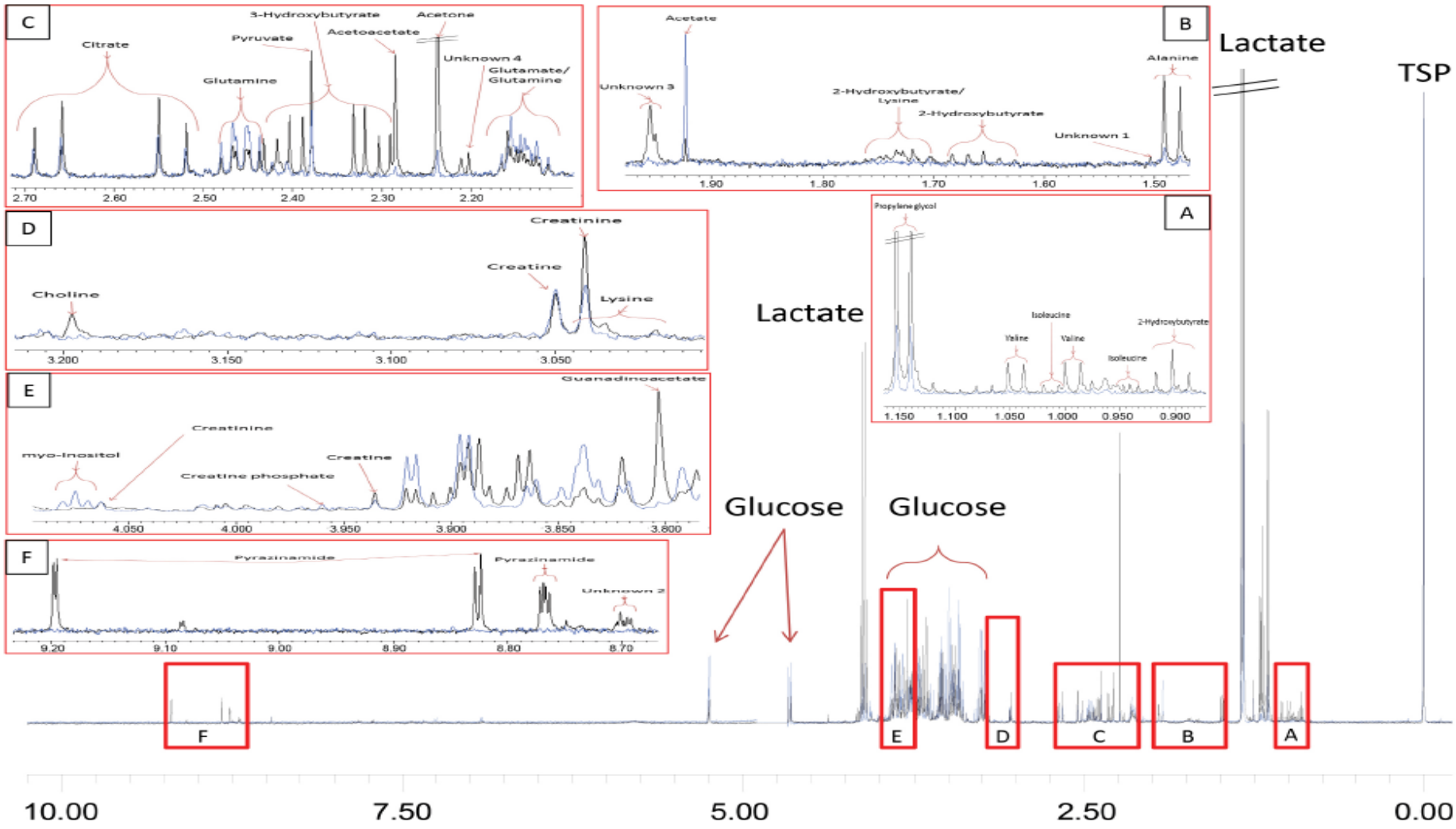


**Figure 4-2** **Representative $^{1}$H-NMR spectra scaled relative to TSP with zoomed in regions (A–F) that illustrate the qualitative difference between TBM (black) and control (blue).**

#### 4.1.4.4 Identification of statistically important metabolites

A 3D PCA scores plot of controls vs TBM cases, excluding glucose and lactate (117 bins), is shown in Fig. S4. The first three principal components show an accumulated explained variance of 54%. Unsupervised PCA of both data sets (with or without glucose and lactate) separated TBM from controls, although with some overlap. This bolsters confidence in the ability of the supervised methods to detect truly differentiating bins and avoid false discoveries. Supervised PLS-DA modelling was therefore performed. A 3D PLS-DA scores plot is shown in Fig. 3, illustrating separation of the TBM group (pink squares) from the homogeneous control group (blue dots) with a CI of 90%. This PLS-DA model has a predictive ability ($R^2$) of 71%, which cross-validated to a leave-one-out $R^2$ ($Q^2$) of 59%, indicating reliability of the multivariate model as a ranking tool.

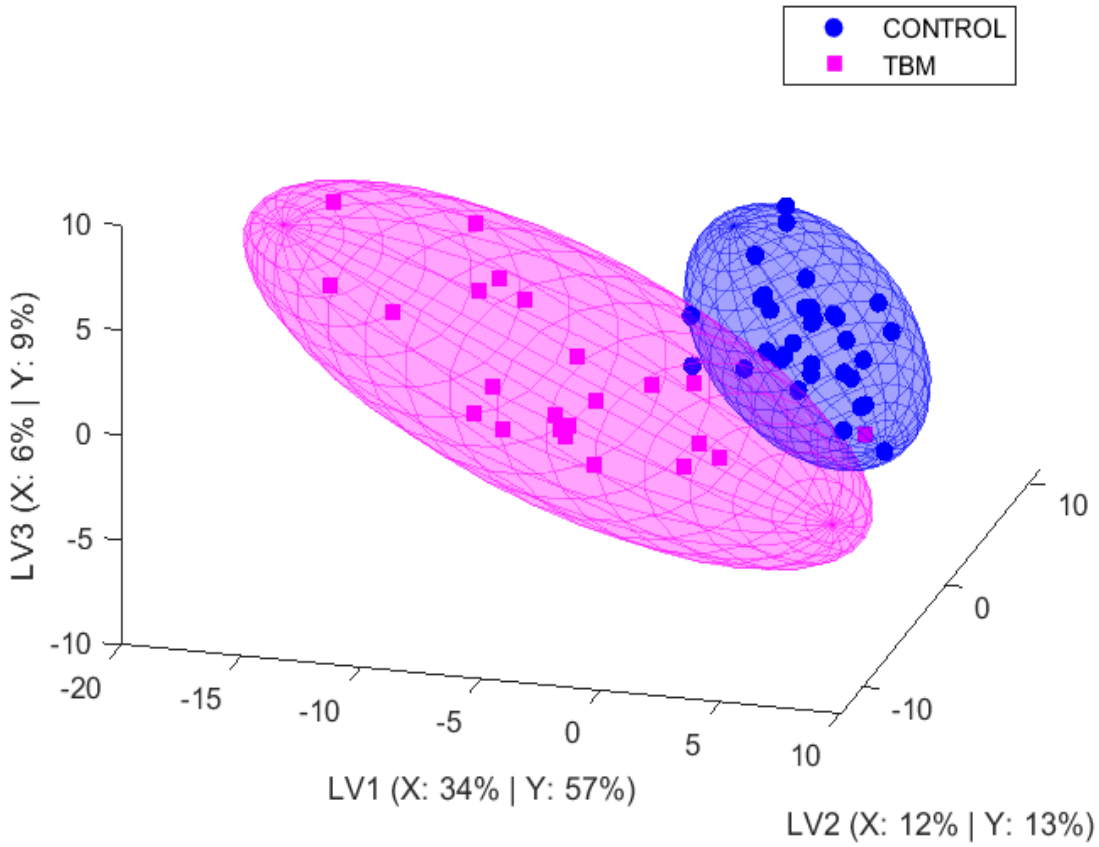


**Figure 4-3** **3D PLS-DA scores plot of controls vs TBM, excluding glucose and lactate (117 bins), with ellipsoids of 90% CI.**

The fundamental requirement for PLS-DA is to produce meaningful information that has the ability to select variables of importance. In the case of this study, this was done quantitatively

on the basis of the PLS-DA VIP score exceeding 1, as noted earlier, subject to the model proving valid for this purpose (i.e. $R^2$ > 70%; $Q^2$ > 50%, and showing PCA differentiation between groups). From the univariate data we used the cut-off criteria of t-test p-value (after adjusting for multiple testing) ≤ 0.05 and Cohen's d-value ≥ 0.5. From the 117 bin data matrix, if a bin fell within our multivariate OR univariate inclusion criteria (also shown in Fig. 2), the bin was selected as being statistically significant and practically relevant. A total of 35 bins were so selected.

Representing the 35 shortlisted bins, 18 metabolites, 1 medication (pyrazinamide[26]) and 4 unknown variables were identified. A summary of the quantitative statistical values of these 23 variables is given in Table 2. A detailed table of the chemical information and shifts for the 18 significant metabolites, as well as glucose and lactate, is given in Table S2 – Annexure 1.

**Table 4-2 Quantitative statistical data indicating the important metabolites that differentiate between controls and TBM cases, where the dominating metabolites lactate and glucose were removed**

| Metabolite | Mann–Whitney (p-value) | Effect size (d-value) | PLS-DA (VIP) |
|---|---|---|---|
| 2-Hydroxybutyrate | <0.0001 | 0.58 | 1.01 |
| Acetate | 0.4985 | 0.0007 | 1.57 |
| Alanine | <0.0001 | 0.71 | 1.60 |
| Carnitine | <0.0001 | 0.65 | 1.76 |
| Choline | <0.0001 | 0.72 | 1.95 |
| Citrate | 0.00032 | 0.53 | 1.13 |
| Creatine | <0.0001 | 0.65 | 1.62 |
| Creatinine | <0.0001 | 0.73 | 1.65 |
| Creatine phosphate | 0.007 | 0.50 | 0.91 |
| Glutamate | 0.4251 | 0.0029 | 1.10 |
| Glutamine | <0.0001 | 0.60 | 1.32 |
| Guanidinoacetate | 0.4562 | 0.0015 | 1.91 |
| Isoleucine | <0.0001 | 0.58 | 1.03 |
| Lysine | <0.0001 | 0.63 | 1.10 |
| Myo-inositol | 0.0006 | 0.51 | 0.45 |
| Proline | <0.0001 | 0.59 | 1.18 |
| Pyrazinamide | <0.0001 | 0.63 | 1.89 |
| Pyruvate | 0.4473 | 0.0018 | 1.20 |

| | | | |
|---|---|---|---|
| Valine | <0.0001 | 0.62 | 1.01 |
| Unknown 1 | <0.0001 | 0.61 | 1.62 |
| Unknown 2 | <0.0001 | 0.61 | 1.78 |
| Unknown 3 | <0.0001 | 0.69 | 1.13 |
| Unknown 4 | 0.00018 | 0.55 | 1.40 |

Since the amount of internal standard (TSP) in each sample is known, an accurate calculation of the absolute concentration of each metabolite identified was determined. A summary of the absolute concentrations of the above 18 metabolites, as well as glucose and lactate, are given as box plots in Fig. 4. For the remainder of this paper, we will refer to the significant metabolites identified to characterize the CSF metabolic profile of the paediatric cohort studied here.

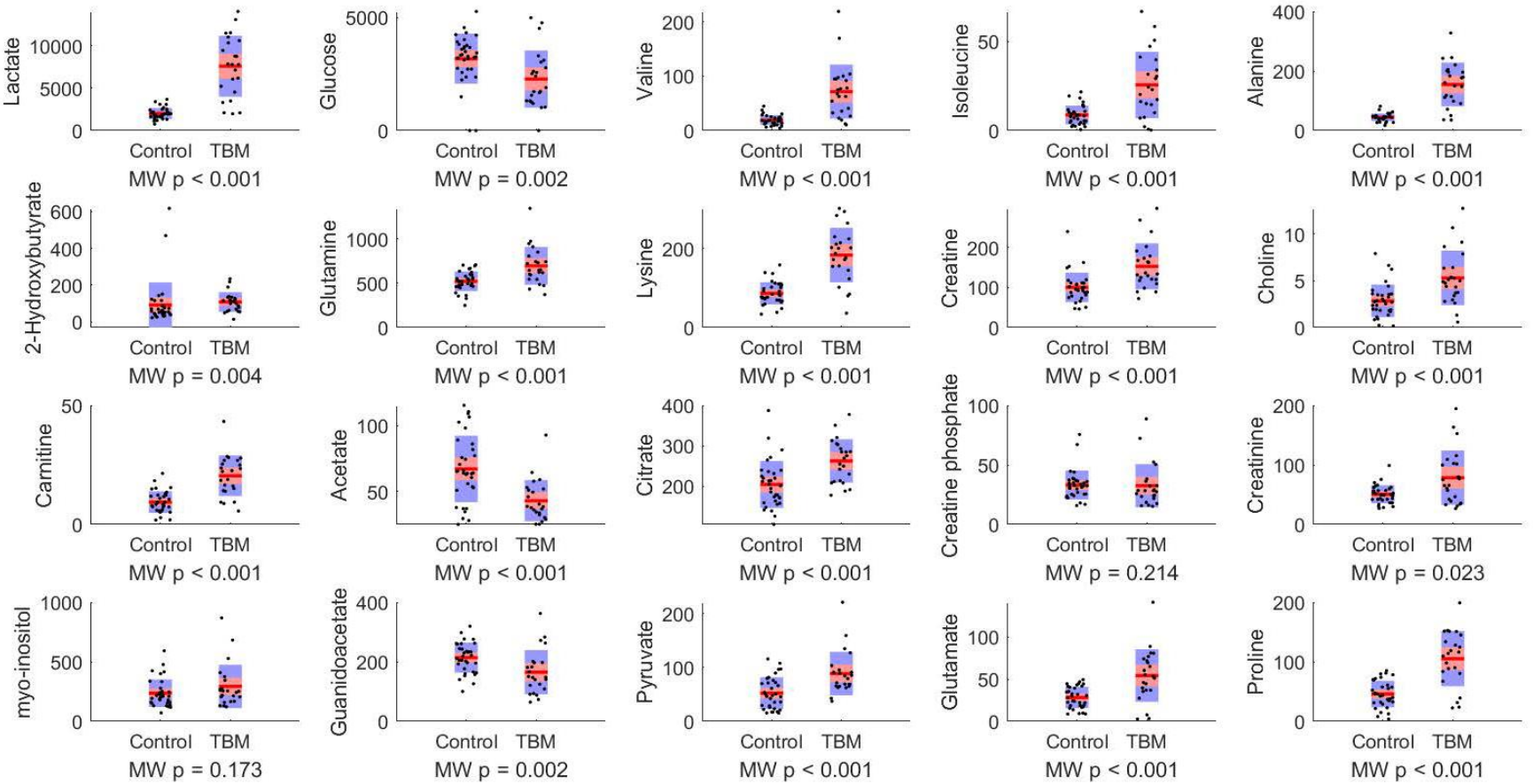


**Figure 4-4** **Box plots of the absolute concentrations (μM) of the 20 CSF metabolites identified by untargeted $^{1}$H-NMR metabolomics in our paediatric cohort. Mann–Whitney p-values given on the bottom of each box plot.**

### 4.1.5 **Discussion**

The principal metabolic changes reflected in the CSF profiles of our paediatric TBM cohort, as expected, were reduced glucose and elevated lactate concentrations. This indicates a metabolic burst that led to the increased catabolism of glucose via glycolysis to pyruvate, which was converted mostly to lactate within astrocytes. It is postulated, by the astrocyte–microglia lactate shuttle (AMLS) hypothesis,[16] that the increased lactate produced within astrocytes is transported to the extracellular space via the activated immune response. The experimental results of our NMR metabolomics study reported here support the data for the AMLS hypothesis given by Mason et al.[16] The increased lactate, together with ketones and gluconeogenic amino acids, derived from astrocytes, is directed preferentially from the neurons into microglia, where it enters the mitochondrial Krebs cycle, contributing to oxidative phosphorylation and ultimately to increased levels of ATP and reactive oxygen species required for *M. tb* degradation. The concept of a metabolic burst within the brain aligns with the angiogenesis model.[27,28] Metabolic burst is upregulated by the increased levels of vascular endothelial growth factor, now known to be an elevated immunological CSF marker of TBM.[29] Within neuropathophysiological states, the role of lactate as an energy substrate and shuttle systems in the brain are emerging as crucial in brain energy metabolism.[30] Lactate is a chemically simple metabolite, yet its dynamics within shuttling systems in neurology is profoundly complex.[31] However, the role of lactate in the brain in neuropathophysiological states has already been explored and will not be discussed here; instead, the novelty of our study lies in: 1) a well-defined (n = 23) group designated as definite TBM cases and a homogeneous control (n = 33) group being distinguished; and consequently 2) the novel recognition of discriminating metabolites in CSF that contribute to the metabolic characterization of TBM.

Two untargeted $^{1}$H-NMR metabolomics studies of CSF from TBM cases exist in the literature – Mason et al.[16] and Zhang et al.[17] The original study by Mason et al.[16] had a paediatric cohort of 63 cases (TBM patients = 33, controls = 30), whereas Zhang et al.[17] reported on a cohort of 61 adult cases (TBM = 31, controls = 30). In our study, the original paediatric cohort consisted of 200 cases (TBM = 103, controls = 97). Using the comprehensive meta-data accompanying the CSF samples, we were able to better define our cohort, as reported under ‘Experimental group definition’. Hence, owing to our strict data filtering methods, we were able to use a more-defined TBM group (n = 33) and a homogeneous control group (n = 33), in order to better characterize the CSF metabolic profile of the TBM cases. Glucose and lactate aside, 18 statistically significant metabolites were additionally identified that distinguished the CSF metabolic profiles of the definite TBM cases from controls within our paediatric cohort. Of these

18 metabolites, 7 correspond with those of the adult cohort studied by Zhang et al.[17] (alanine, choline, isoleucine, myo-inositol, pyruvate, and valine), and 10 metabolites overlap with a similar paediatric cohort investigated previously by Mason et al.[16] (acetate, alanine, choline, citrate, creatinine, isoleucine, lysine, myo-inositol, pyruvate, and valine). The proposed role(s) of these overlapping metabolites in both of the aforementioned studies were previously described and explained by Mason et al.[16]

Thus, due to the improved definition of the case phenotype, we were able to refine the metabolic characterization of the TBM cases, and identify eight additional metabolites for the first time. These eight unique CSF metabolites can be linked to five metabolic pathways, which are the focus of our discussion below, as follows: 1) uncontrolled glucose metabolism (in which 2-hydroxybutyrate plays a key role); 2) detoxification (carnitine); 3) protein metabolism (proline); 4) creatine biodegradation (creatine, creatine phosphate and guanidinoacetate); and 5) disrupted glutamate–glutamine cycle.

#### 4.1.5.1 Uncontrolled glucose metabolism

A consequence of a sustained metabolic burst, as identified above, is uncontrolled glucose metabolism. Rapid use of glucose leads to increased glycolysis, indicating that a high energy demand is present, which is expected in the case of TBM since the *M. tb* are using energy, as well as the activated immune cells of the brain cells that are fighting against the *M. tb* infection. Thus, alternative ways to generate energy in the form of ATP are needed. In our study, a significantly elevated ($p = 0.004$) metabolite identified in the CSF of TBM cases was 2-hydroxybutyrate. To our knowledge, 2-hydoxybutyrate has never been identified as a metabolite in the CSF of a *M. tb*-infected brain. In the literature, 2-hydroxybutyrate in the plasma metabolome was found to be a more sensitive marker of transient tissue ischaemia than lactate,[32] and a selective metabolite biomarker of impaired glucose intolerance.[33] The data sited here, however, are from plasma studies, and therefore extrapolation to the brain needs to be done with caution.

We hypothesize that an increase in 2-hydroxybutyrate in the CSF supports the concept of insulin resistance and uncontrolled glucose metabolism[34-36] in a *M. tb*-infected brain, resulting in an inability of glucose to enter the cells, and subsequently leading to reduced cellular glycolysis and ATP deprivation. A decrease in cellular glucose leads to increased ketone synthesis by upregulating monocarboxylate transporter expression, to allow more lactate and ketone bodies to enter the cells in order to provide more energy substrates for the astrocytes and neurons. This process ultimately leads to the destabilization of the blood–brain barrier (BBB). Our hypothesis, however, is speculative. Nonetheless, the role of 2-hydroxybutyrate in

the CSF as a metabolic marker of TBM, and possibly ischaemia, is one that deserves attention.

A common trend emerging in the literature is that chronic inflammation is associated with insulin resistance. Reduced insulin levels and uncontrolled glucose metabolism are typically associated with type 2 diabetes – an inflammatory disease.[37] Insulin resistance during uncontrolled glucose metabolism can lead to the transient oxidation of glucose via glucose oxidase (EC 1.1.3.4), a reaction that requires oxygen (non-hypoxic conditions). Oxidation of glucose leads to the production of gluconolactone, an inflammatory marker found in pulmonary TB.[38] Furthermore, glucose oxidation leads to increased levels of hydrogen peroxide.[38] Myeloperoxidase (EC 1.11.1.7), an immunological marker of TBM identified by Manyelo et al.,[29] interacts with hydrogen peroxide and activates various oxidative stress pathways.[39-41] This action is proposed to be needed by microglia to respond to the invading *M. tb* pathogen, which supports our hypothesis that 2-hydroxybutyrate is a metabolite marker of uncontrolled glucose metabolism in a *M. tb*-infected brain.

It is important to note some possible, alternative hypotheses regarding uncontrolled glucose metabolism. Ischaemia is potentially a major driver of uncontrolled glucose metabolism. However, in our study we were unable to assess ischaemia in the brain. The Warburg–Crabtree effect – involving increased glycolysis and glucose-induced repression of respiratory flux under hypoxic conditions, in the presence of oxygen[42] – is another phenomenon to consider. Based upon emerging studies regarding uncontrolled glucose metabolism, such as in diabetes[37] and marathon runners,[43] it can be seen that dysregulated glucose metabolism (upregulated glycolytic flux) is not always related to ischaemia. Indeed, several studies have shown no correlation between CSF lactate levels and cerebral blood flow,[44-46] suggesting that increased CSF lactate is not linked to ischaemia in the brain.

#### 4.1.5.2 Detoxification

Significantly elevated ($p < 0.001$) levels of L-carnitine were detected in the CSF of the TBM patients. L-Carnitine primarily transports long-chain fatty acids into the mitochondria, for breakdown into acetyl-CoA via β-oxidation.[47] The latter serves as a substrate for the Krebs cycle, and ultimately ATP production in the mitochondria. Furthermore, L-carnitine can form conjugates with various toxic compounds, improving on their water solubility and excretion from the body.[48] It has been reported that oxidative stress can be alleviated by L-carnitine, preventing oxidative damage and thus providing a degree of neuroprotection.[49]

#### 4.1.5.3 Proline metabolism

Using the more sensitive analytical platform of gas chromatography–mass spectrometry, amino acid profiling was conducted on the CSF of a paediatric population with TBM, as a result of which five important amino acids were previously identified.[50] Proline was one of these five amino acids, and was also identified as significantly elevated in our study ($p < 0.001$). Proline is a proteinogenic amino acid, hence its elevated levels in CSF in our subjects are not surprising since elevated protein is a classic hallmark of TBM. Proline is catabolised to pyrroline-5-carboxylic acid (P5C) via proline dehydrogenase (EC 1.5.5.2), which is in spontaneous equilibrium with its tautomer glutamate-5-semialdehyde (G5A). From here, G5A can be metabolised to either glutamate or arginine, which is incorporated into creatine metabolism. Both the glutamate and creatine pathways are discussed below.

#### 4.1.5.4 Creatine metabolism

Four metabolites of the creatine metabolic pathway were identified as statistically significant in our paediatric cohort with TBM, namely, guanidinoacetate, creatine, creatine phosphate and creatinine. Guanidinoacetate, a precursor of creatine, is biosynthesized by glycine conjugation with arginine through its interaction with the enzyme glycine amidinotransferase (EC 2.1.4.1). A transfer of a methyl group from S-adenosylmethionine to guanidinoacetate by guanidinoacetate N-methyltransferase (EC 2.1.1.2) leads to the formation of S-adenosylhomocysteine and creatine. Guanidinoacetate was significantly ($p = 0.002$) decreased in the TBM cases, indicating a need for significantly elevated creatine/creatinine ($p < 0.001$ and $p = 0.023$, respectively) to be present in a *M. tb*-infected brain.

Creatine can be converted into creatine phosphate through the enzyme creatine kinase b-type (EC 2.7.3.2). Creatine phosphate then undergoes irreversible cyclization and dehydration to form creatinine. Creatine phosphate is an intracellular store of high energy phosphate that is essential for brain function.[51] Creatinine is a catabolic by-product of creatine phosphate that is produced in muscle at a fairly constant rate during homeostasis, and has a slow diffusion rate across the BBB. Creatinine also is correlated with the CSF monoamine metabolites homovanillic acid and 5-hydroxyindoleacetic acid, which are associated with neurodegenerative conditions like schizophrenia and depression.[52-54] The consequences of altered creatinine levels in TBM patients are unclear, but are likely to be linked proportionally to the progression of neuronal injury.[16] An increase in creatine concentrations may be caused by an altered creatine transporter activity,[55] known to be associated with various neurological complications.[56] Apart of its well-known function of as an ‘energetic buffer’ through the creatine/creatine phosphate/creatine kinase system allowing the regeneration of ATP,

creatine has also been suggested as a potential neuromodulator with neuroprotective capabilities.[57]

#### 4.1.5.5 Disrupted glutamate-glutamine cycle and BBB

In our study, we found both glutamate and glutamine to be significantly elevated ($p < 0.001$) in the CSF of the TBM cases, implying a disruption of the glutamate–glutamine cycle. Glutamate, the main excitatory amino acid neurotransmitter in the brain, is released from glutamatergic neuronal vesicles through a calcium-dependent mechanism[58] into the extracellular space along the glutamate transporter EAAT3 (excitatory amino acid transporter 3), which is exclusively located in neurons. Glutamate is taken up by the astrocytes via the glutamate transporters EAAT1 and EAAT2. The transport of glutamate is driven by a sodium gradient, with a stoichiometry of three $Na^+$ ions co-transported with every one glutamate molecule. Within the astrocytes, the enzyme glutamine synthetase (EC 6.3.1.2) uses ATP to attach one ammonium ion to glutamate. Glutamine is released from astrocytes via the system N amino acid transport system into the extracellular fluid, and is then taken up by neurons via the system A amino acid transport system, where it is deaminated by glutaminase (EC 3.5.1.2) to regenerate glutamate, allowing rapid neurotransmitter replenishment in neuronal compartment(s).[59] Hence, neurons rely upon astrocytes for the constant recycling of glutamate.

Cerebral capillary endothelial cells form the BBB that is an inherent feature of the entire central nervous system. Tight junctions connect endothelial cells and separate the BBB into luminal and abluminal domains. Molecules entering or leaving the brain must thus pass through two membranes, each of which has distinct properties. Facilitative carriers exist only in the luminal membranes, and $Na^+$-dependent glutamate cotransporters (EAATs) exist exclusively in abluminal membranes. The EAATs are secondary transporters that couple the $Na^+$ gradient between the extracellular fluid and the endothelial cells, to move glutamate against the existing electrochemical gradient. Thus, the EAATs in the abluminal membrane shift glutamate from the extracellular fluid to the endothelial cells, where glutamate is free to diffuse into the blood on facilitative carriers. This organization does not allow net glutamate entry to the brain, rather, it promotes the removal of glutamate and the maintenance of low glutamate concentrations in the extracellular fluid. This explains studies that show that the BBB is impermeable to glutamate, even when in high concentrations.[60]

The glutamate–glutamine cycle and the BBB function together to regulate the levels of glutamate within the brain, and to prevent excessive glutamate and its associated excitotoxicity.[61] Glutamatergic neurotransmissions are paradoxical as glutamate is essential

for normal brain activity and development, but excess amounts of glutamate but excessive glutamate can lead to neuronal death; however, neuronal death is a multifactorial process, not simply a cause of excitotoxicity caused by glutamate accumulation.[62] Inhibition of glutamate-mediated synaptic transmission may be neuroprotective by increasing the resistance of neurons to other deleterious mechanisms (e.g. inadequate energy supply) that are not directly related to glutamatergic transmission.[63]

During ischaemic conditions there is an energy deficit due to the brain cells not receiving enough energy. This results in an inability of these cells to maintain their ionic gradients necessary for optimal physiological functioning. Neurons are especially affected by states of low available energy and experience excessive depolarization and increased release of excitatory neurotransmitters, along with a reduced ability to re-uptake neurotransmitters. During this process an influx of $Ca^{2+}$ and other positive ions occurs, stimulating various cellular responses – such as disturbed mitochondrial potential – that lead to either apoptotic or necrotic neuronal death.[64] The release of excess glutamate by ischaemic neurons and the consequent difficulty for energy-deprived neurons to re-establish the ionic membrane gradient has been well studied in research on traumatic brain injury.[65,66] Rohlwink et al.[1] suggest that TBM-induced infarction and ischaemia could potentially stimulate glutamate release, which then leads to the excessive binding of glutamate to the *N*-methyl-D-aspartate receptors on neurons, leading to an influx of $Ca^{2+}$ and other positive ions into the neurons, and a cascade of injurious events. Hence, the potential role of ischaemia in glutamate accumulation cannot be ruled out.

Since both glutamate and glutamine were elevated in our study, we postulate that there is reduced transporter functioning in both astrocytes and neurons. Furthermore, elevated levels of CSF proline contribute to the raised levels of glutamate in the CSF. The mechanisms underlying the penetration of the BBB are poorly understood;[67] however, it has been shown that glutamate induces BBB permeability through activation of *N*-methyl-D-aspartate receptors,[68] and via altered expression of tight junction proteins in brain endothelial cells.[69]

A summary of our findings is given in Fig. 5, which illustrates the proposed metabolic pathways involved in a *M. tb*-infected brain. It is important to state that the comparison made in our study was between a well-defined cohort of TBM cases and ‘healthy’ controls without any neurological symptoms. The refinement of the cohorts studied here distinguishes our study from previous investigations, and allowed us to identify eight new metabolites associated with a *M. tb*-infected brain. Since these eight metabolites are novel – that is, not previously identified within a *M. tb*-infected brain – our interpretation of their roles in the CSF is speculative, but supported by the literature where indicated. These findings therefore may not represent TBM specifically but rather an infectious, or indeed an inflammatory, state in the

brain. Furthermore, until any of the data in this manuscript are shown to be TBM specific by a comparative study with a control group of patients with infection of a non-TB origin we do not believe we can conclusively state the specificity of any of this data to the *M. tb*-infected brain.

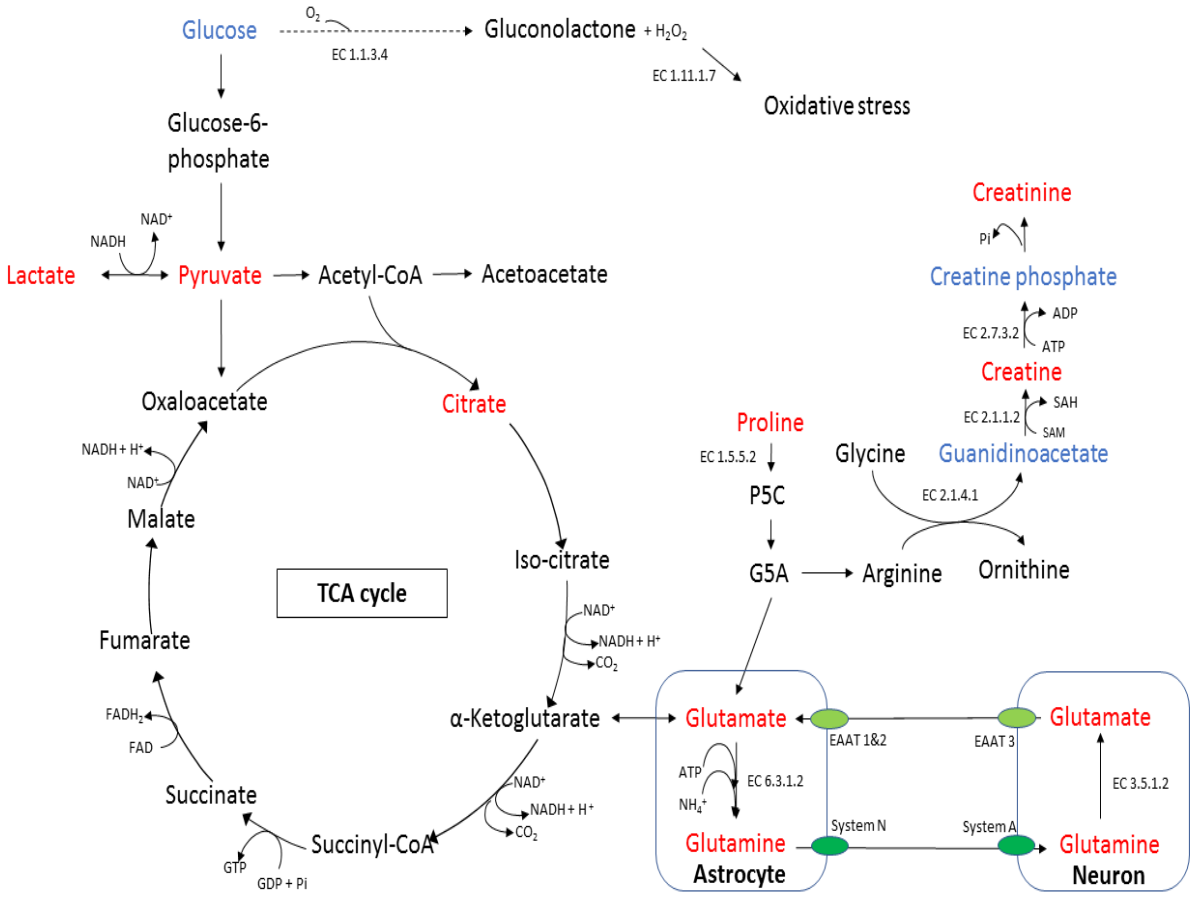


**Figure 4-5** **Illustration of metabolic pathways perturbed within a *M. tb*-infected brain. Metabolites in red, which increased, and blue, which decreased, as a result of *M. tb* infection are the important metabolites identified in our study. The dashed line from glucose to gluconolactone indicates a transient pathway that is activated during insulin resistance. Key: P5C, pyrroline-5-carboxylic acid; G5A, glutamate-5-semialdehyde; SAM, S-adenosylmethionine; SAH, S-adenosylhomocysteine; EAAT, glutamate transporter.**

### 4.1.6 Conclusion

This study identified 20 metabolites that differentiated well-defined TBM cases from 'healthy' controls in their respective CSF profiles. The main novel metabolic pathways reported here were: uncontrolled glucose metabolism, upregulated proline and creatine metabolism, and disruption of the glutamate–glutamine cycle in the TBM cases. Associated with oxidative stress and chronic neuroinflammation, our findings collectively contribute to recognising destabilization of the BBB in the infected state. This is manifested by progressive BBB permeability, which is associated with increased intra-cranial pressure – a clinical hallmark of advanced meningitis, particularly in TBM. The metabolic insights gained from this investigation improve our understanding of TBM, and contribute to the metabolic characterization of TBM to aid future diagnostic and possibly therapeutic research. In the future, we recommend the identification of the statistically significant variables identified in our study as unknowns 1-4, as well as loosening the exclusion criteria to see how various concomitant factors ($TB^+$ controls and $HIV^+$ patients) affect the metabolic characterization of the CSF profile of TBM cases.

### 4.1.7 Declarations

*Conflict of interest*

The authors declare no conflict of interest

*Funding*

This research did not receive any specific grant from funding agencies in the public, commercial, or not-for-profit sectors.

*Ethics approval*

The study was approved by the Health Research Ethics Committee (HREC) of Stellenbosch University, Tygerberg Hospital (ethics approval no. N16/11/142), the Western Cape Provincial Government, as well as by the HREC of North-West University, Potchefstroom campus (ethics approval no. NWU-00063-18-S1).

*Author contributions*

SM conceptualized the manuscript. CDWvZ, DTL, MvR and SM planned the outline of the manuscript. CDWvZ did the experimental work and wrote the manuscript. SM supervised CDWvZ in the writing of the manuscript by providing critical feedback. MvR conducted the statistical analyses and provided insights and explanations. RS supervised sample collection

and associated meta-data and provided essential clinical input and context. All co-authors critically read each draft and approved the final draft for submission.

### 4.1.8 References


1. Rohlwink, UK, Figaji A, Wilkinson KA, et al. Tuberculous meningitis in children is characterized by compartmentalized immune responses and neural excitotoxicity. *Nat Commun* 2019;**10**(1):3767–74.
2. Van, TT, Farrar J. Tuberculous meningitis. *J Epidemiol Community Health* 2014;**68**(3):195–6.
3. Gil-Santana L, Cruz LA, Arriaga MB, et al. Tuberculosis-associated anemia is linked to a distinct inflammatory profile that persists after initiation of antitubercular therapy. *Sci Rep* 2019;**9**(1):1–8.
4. Gantz NM. *Manual of clinical problems in infectious diseases.* 5th ed. Lippincott Williams & Wilkins, Hagerstown, MD; 2006:170–223.
5. Grobbelaar M, van Toorn R, Solomons R. Lumbar cerebrospinal fluid evolution in childhood tuberculous meningitis. *J Child Neurol* 2018;**33**(11):700–7.
6. Bennett JE. Chronic meningitis. *Principles and practice of infectious diseases.* 7th ed. Philadelphia. Churchill Livingstone; 2010:1237–42.
7. Helbok R, Broessner G, Pfausler B, Schmutzhard E. Chronic meningitis. *J Neurol* 2009;**256**(2):168–75.
8. Rich A, McCordock H. The pathogenesis of tuberculous meningitis. *Bull Johns Hopkins Hosp* 1933;**52**:2–37.
9. Thwaites GE, Tran TH. Tuberculous meningitis: many questions, too few answers. *Lancet Neurol* 2005;**4**(3):160–70.
10. Rock RB, Olin M, Baker CA, Molitor TW, Peterson PK. Central nervous system tuberculosis: pathogenesis and clinical aspects. *Clin Microbiol Rev* 2008;**21**(2):243–61.
11. Rock RB, Hu S, Gekker G, Sheng WS, May B, Kapur V, Peterson PK. Mycobacterium tuberculosis-induced cytokine and chemokine expression by human microglia and astrocytes: effects of dexamethasone. *J Infect Dis* 2005;**192**(12):2054–8.
12. Chatterji T, Singh S, Sen M, et al. Comprehensive $^{1}$H NMR metabolic profiling of body fluids for differentiation of meningitis in adults. *Metabolomics* 2016;**12**(8):130–43.
13. Coen M, O'Sullivan M, Bubb WA, Kuchel PW, Sorrell T. Proton nuclear magnetic resonance-based metabonomics for rapid diagnosis of meningitis and ventriculitis. *Clin Infect Dis* 2005;**41**(11):1582–90.
14. Himmelreich U, Malik R, Kuhn T, Daniel HM, Somorjai RL, Dolenko B, Sorrell TC. Rapid etiological classification of meningitis by NMR spectroscopy based on metabolite profiles and host response. *PLoS One* 2009;**4**(4):e5328.
15. Li Z, Du B, Li J, et al. Cerebrospinal fluid metabolomic profiling in tuberculous and viral meningitis: screening potential markers for differential diagnosis. *Clin Chim Acta* 2017;**466**:38–45.

16. Mason S, van Furth AM, Mienie LJ, Engelke UF, Wevers RA, Solomons R, Reinecke CJ. A hypothetical astrocyte-microglia lactate shuttle derived from a $^{1}$H-NMR metabolomics analysis of cerebrospinal fluid from a cohort of South African children with tuberculous meningitis. *Metabolomics* 2015;**11**(4):822–37.
17. Zhang P, Zhang W, Lang Y, Qu Y, Chen J, Cui L. $^{1}$H nuclear magnetic resonance-based metabolic profiling of cerebrospinal fluid to identify metabolic features and markers for tuberculosis meningitis. *Infect Genet Evol* 2019;**68**:253–64.
18. Oliver SG, Winson MK, Kell DB, Baganz F. Systematic functional analysis of the yeast genome. *Trends Biotechnol* 1998;**16**(9):373–8.
19. Fiehn O. Metabolomics—the link between genotypes and phenotypes. In *Functional Genomics*. Springer, Dordrecht; 2002:155–71.
20. Donald PR, Cotton MF, Hendricks MK, Schaaf HS, de Villiers JN, Willemse TE. Pediatric meningitis in the Western Cape Province of South Africa. *J Trop Ped* 1996;**42**:256–61.
21. Marais S, Thwaites G, Schoeman JF, et al. Tuberculous meningitis: a uniform case definition for use in clinical research. *Lancet Infect. Dis.* 2010;**10**(11):803–12.
22. Mason S, Terburgh K, Louw R. Miniaturized $^{1}$H-NMR method for analyzing limited-quantity samples applied to a mouse model of Leigh disease. *Metabolomics* 2018;**14**(6):74–85.
23. Cui X, Churchill GA. Statistical tests for differential expression in cDNA microarray experiments. *Genome Biol* 2003;**4**(4):210–9.
24. De Meyer T, Sinnaeve D, Van Gasse B, et al. NMR-based characterization of metabolic alterations in hypertension using an adaptive, intelligent binning algorithm. *Anal Chem* 2008;**80**(10):3783–90.
25. van den Berg RA, Hoefsloot HCJ, Westerhuis JA, Smilde AK, van der Werf MJ. Centering, scaling, and transformations: improving the biological information content of metabolomics data. *BMC Genom* 2006;**7**(1):142.
26. Mason S, Reinecke CJ, Solomons R, Wevers RA, Engelke UFH. $^{1}$H NMR spectral identification of medication in cerebrospinal fluid of pediatric meningitis. *J Pharm Biomed Anal* 2017;**143**:56–61.
27. Connolly DT. Vascular permeability factor: a unique regulator of blood vessel function. *J Cell Biochem* 1991;**47**:219–23.
28. Yancopoulos GD, Davis S, Gale NW, Rudge JS, Wiegand SJ, Holash J. Vascular-specific growth factors and blood vessel formation. *Nature* 2000;**407**:242–8.
29. Manyelo CM, Solomons RS, Snyders CI, et al. Application of cerebrospinal fluid host protein biosignatures in the diagnosis of tuberculous meningitis in children from a high burden setting. *Mediat Inflamm* 2019:7582948.
30. Mason S. Lactate shuttles in neuroenergetics—homeostasis, allostasis and beyond. *Front Neurosci* 2017;**11**:43.

31. Mason, S. (2020). A novel, multi-faceted perception of lactate in neurology. *Front. Neurosci*. **14**:460.
32. Laursen, M. R., Hansen, J., Elkjær, C., Stavnager, N., Nielsen, C. B., Pryds, K., et al. (2017). Untargeted metabolomics reveals a mild impact of remote ischemic conditioning on the plasma metabolome and α-hydroxybutyrate as a possible cardioprotective factor and biomarker of tissue ischemia. *Metabolomics* **13**(6):67–79.
33. Cobb, J., Eckhart, A., Motsinger-Reif, A., Carr, B., Groop, L., & Ferrannini, E. (2016). α-Hydroxybutyric acid is a selective metabolite biomarker of impaired glucose tolerance. *Diabetes Care* **39**(6):988–995.
34. Gall, W. E., Beebe, K., Lawton, K. A., Adam, K. P., Mitchell, M. W., Nakhle, P. J., et al. (2010). α-Hydroxybutyrate is an early biomarker of insulin resistance and glucose intolerance in a nondiabetic population. *PLoS One* **5**(5):e10883.
35. Gu, Y., Zang, P., Li, L Q., Zhang, H. Z., Li, J., Li, J. X.., et al. (2019). A non-targeted metabolomics study on different glucose tolerance states. *Int. J. Diabetes Dev. Ctries.* **39**(3):478–485.
36. Sari, H., Esen, B., Yildirim, S., Pilten, S., & Aydin, H. (2017). Serum α-hydroxybutyrate: a candidate marker of insulin resistance is associated with deterioration in anthropometric measurements in individuals with low diabetes risk. *J. Appl. Lab. Med.* **1**(5):562–567.
37. American Diabetes Association. (2017). Classification and diagnosis of diabetes. *Diabetes Care* **40**(Supplement 1):S11–S24.
38. Preez, I. D., Luies, L., & Loots, D. T. (2017). Metabolomics biomarkers for tuberculosis diagnostics: current status and future objectives. *Biomark. Med.* **11**:179–194.
39. Hampton, M. B., Kettle, A. J., & Winterbourn, C. C. (1998). Inside the neutrophil phagosome: oxidants, myeloperoxidase, and bacterial killing. *Blood* **92**:3007–3017.
40. Klebanoff, S. J. (2005). Myeloperoxidase: friend and foe. *J. Leukoc. Biol.* 77:598–625.
41. Podrez, E. A., Abu-Soud, H. M., & Hazen, S. L. (2000). Myeloperoxidase generated oxidants and atherosclerosis. *Free Rad. Biol. Med.* **28**:1717–1725.
42. Hammad, N., Rosas-Lemus, M., Uribe-Carvajal, S., Rigoulet, M., & Devin, A. (2016). The Crabtree and Warburg effects: do metabolite-induced regulations participate in their induction? *Biochim. Biophys. Acta – Bioenergetics* **1857**(8):1139–1146.
43. Stander, Z., Luies, L., Mienie, L. J., Keane, K. M., Howatson, G., Clifford, T., et al. (2018). The altered human serum metabolome induced by a marathon. *Metabolomics* **14**:150–160.
44. Brodersen, P., & Jorgensen, E. O. (1974). Cerebral blood flow and oxygen uptake, and cerebrospinal fluid biochemistry in severe coma. *J. Neurol. Neurosurg. Psychiatr.* **37**:384–391.
45. DeSalles, A. A., Kontos, H. A., Becker, D. P., Yang, M. S., Ward, J. D., Moulton, R., et al. (1986). Prognostic significance of ventricular CSF lactic acidosis in severe head injury. *J. Neurosurg.* **65**:615–624.

46. DeSalles, A. A., Muizelaar, J. P., & Young, H. F. (1987). Hyperglycemia, cerebrospinal fluid lactic acidosis, and cerebral blood flow in severely head-injured patients. *Neurosurgery* **21**:45–50.
47. Jones, L. L., McDonald, D. A., & Borum, P. R. (2010). Acylcarnitines: role in brain. *Prog. Lipid Res.* **49**(1):61–75.
48. Walter, J. H. (1996). L-Carnitine. *Arch. Dis. Child.* **74**(6):475–478.
49. Ferreira, G. C., & McKenna, M. C. (2017). L-Carnitine and acetyl-L-carnitine roles and neuroprotection in developing brain. *Neurochem. Res.* **42**(6):1661–1675.
50. Mason, S., Reinecke, C. J., & Solomons, R. (2017). Cerebrospinal fluid amino acid profiling of pediatric cases with tuberculous meningitis. *Front. Neurosci.* **11**:534.
51. Adeva-Andany, M., Souto-Adeva, G., Ameneiros-Rodríguez, E., Fernández-Fernández, C., Donapetry-García, C., & Domínguez-Montero, A. (2018). Insulin resistance and glycine metabolism in humans. *Amino Acids* **50**(1):11–27.
52. Agren, H., & Niklasson, F. (1988). Creatinine and creatine in CSF: indices of brain energy metabolism in depression. *J. Neural Transm.* **74**:55–59.
53. Levine, J., Panchalingam, K., Rapoport, A., Gershon, S., McClure, R. J., & Pettegrew, J. W. (2000). Increased cerebrospinal fluid glutamine levels in depressed patients. *Biol. Psychiatry* **47**:586–593.
54. Swahn, C. G., & Sedvall, G. (1988). CSF creatinine in schizophrenia. *Biol. Psychiatry* **23**(6):586–594.
55. Tachikawa, M., Fujinawa, J., Takahashi, M., Kasai, Y., Fukaya, M., Sakai, K., et al. 2008. Expression and possible role of creatine transporter in the brain and at the blood-cerebrospinal fluid barrier as a transporting protein of guanidinoacetate, an endogenous convulsant. *J. Neurochem.* **107**(3):768–778.
56. Barichello, T., Silva, G. Z., Savi, G. D., Torquato, J. M., Batista, A. L., Scaini, G., et al. (2009). Brain creatine kinase activity after meningitis induced by Streptococcus pneumoniae. *Brain Res. Bull.* **80**(1-2):85–88.
57. Béard, E., & Braissant, O. (2010). Synthesis and transport of creatine in the CNS: importance for cerebral functions. *J. Neurochem.* **115**(2):297–313.
58. Fillenz, M. (1995). Physiological release of excitatory amino acids. *Behav. Brain Res.* **71**(1-2):51–67.
59. Souza, D. G., Almeida, R. F., Souza, D. O., & Zimmer, E. R. (2019). The astrocyte biochemistry. In *Seminars in Cell & Developmental Biology*. Academic Press.
60. Hawkins, R.A., 2009. The blood-brain barrier and glutamate. *Am. J. Clin. Nutr.* **90**(3):867S–874S.
61. Lipton, S. A., & Rosenberg, P. A. (1994). Excitatory amino acids as a final common pathway for neurologic disorders. *NEJM* **330**(9):613–622.

62. Lewerenz, J., & Maher, P. (2015). Chronic glutamate toxicity in neurodegenerative diseases—what is the evidence? *Front. Neurosci.* **9**:469.
63. Obrenovitch, T. P., Urenjak, J., Zilkha, E., & Jay, T. M. (2000). Excitotoxicity in neurological disorders—the glutamate paradox. *Int. J. Dev. Neurosci.* **18**(2–3):281–287.
64. Szydlowska, K., & Tymianski, M. (2010). Calcium, ischemia and excitotoxicity. *Cell Calcium* **47**(2):122–129.
65. Barkhoudarian, G., Hovda, D. A., & Giza, C. C. (2016). The molecular pathophysiology of concussive brain injury–an update. *Phys. Med. Rehabil. Clin.* **27**(2):373–393.
66. Giza, C. C., & Hovda, D. A. (2001). The neurometabolic cascade of concussion. *J. Athl. Train.* **36**(3):228.
67. Vazana, U., Veksler, R., Pell, G. S., Prager, O., Fassler, M., Chassidim, Y., et al. (2016). Glutamate-mediated blood–brain barrier opening: implications for neuroprotection and drug delivery. *J. Neurosci.* **36**(29):7727–7739.
68. Xhima, K., Weber-Adrian, D., & Silburt, J. (2016). Glutamate induces blood–brain barrier permeability through activation of N-methyl-D-aspartate receptors. *J. Neurosci.* **36**(49):12296.
69. Andras, I. E., Hayashi, K., Hennig, B., & Toborek, M. (2006). Glutamate-induced alterations of tight junction protein expression and distribution in brain endothelial cells. *FASEBJ* **20**(4):A378–A378.

# CHAPTER 5 METABOLIC CHARACTERISATION OF VIRAL MENINGITIS IN A SOUTH-AFRICAN PAEDIATRIC POPULATION USING $^{1}$H-NMR METABOLOMICS

## 5.1 Introduction

Viral meningitis (VM) is an acute form of meningitis as discussed in Chapter 2.2., which is in contrast to TBM – a chronic form of meningitis. Viral meningitis, also known as aseptic meningitis, is defined as patients presenting with symptoms (e.g., headache, arthralgia, nausea and photo-sensitivity) and signs (e.g., fever, neck stiffness and vomiting) of meningitis where the bacterial cultures of CSF are negative. As shown in the summary figure (Figure 2.1) at the end of **Chapter 2**, the CSF glucose and lactate concentrations reported in previous studies of VM are within the normal reference ranges; whereas, for TBM, CSF glucose is decreased and CSF lactate is highly elevated. Here, we used $^{1}$H-NMR metabolomics to determine the CSF metabolic characteristics of VM.

## 5.2 Patients and methods

**Chapter 4** described the comparison between TBM against controls. Here, we compared VM against controls (workflow given in Figure 5.1) and VM against TBM (workflow given in Figure 5.2). The exact same methods described in Chapter 4.1.3 were used here, with the addition of a VM experimental group. Application of the exclusion criteria, shown in Figure 5.1 and Figure 5.2, resulted in a well-defined group of 16 ‘definite’ VM cases, used for statistical analysis.

A ‘definite’ case definition of VM includes: 1) clinical evidence of acute meningitis, such as fever, headache, vomiting, bulging fontanelle, nuchal rigidity or other signs of meningeal irritation and CSF pleocytosis (>5 leucocytes/mm$^3$ if older than 2 months of age, or >15 leucocytes/mm$^3$ if younger than 2 months of age (Hristea *et al.*, 2012)), and 2) absence of any microorganism on gram stain of CSF and negative routine bacterial culture of CSF if antibiotics were not administered prior to the first LP.

A summary of the pertinent clinical demographics of the cases used for metabolic characterization in this Chapter is given in Table 5.1.

**Table 5-1 Summary of mean/median ranges of various clinical results of cases investigated**

| | TBM (N=23) Mean (median) ± SD | VM (N=16) Mean (median) ± SD | Control (N=33) Mean (median) ± SD |
|---|---|---|---|
| Age (months) | 52.5 (46) ± 34.6 | 66.5 (67.5) ± 49.6 | 42.3 (28) ± 42.2 |
| Gender | Male = 12<br>Female = 11 | Male = 12<br>Female = 4 | Male = 23<br>Female = 10 |
| CSF Leucocytes (cells/uL) | 223.43 (93) ± 411.01 | 153.62 (102.5) ± 170.00 | 1.48 (0) ± 4.13 |
| CSF Lymphocytes (cells/uL) | 193.48 (86) ± 313.07 | 68.06 (32) ± 80.09 | 1.38 (0.5) ± 3.38 |
| CSF PMN's (cells/uL) | 33.52 (8) ± 87.08 | 85.56 (58.5) ± 109.40 | 0.16 (0) ± 0.72 |
| CSF Glucose (mmol/L) | 2.18 (1.85) ± 1.48 | 3.40 (3.55) ± 1.05 | 3.71 (3.9) ± 1.04 |

*PMN’s = polymorphonuclear cells. CSF Glucose determined on-site during diagnosis via glucose oxidase assay.

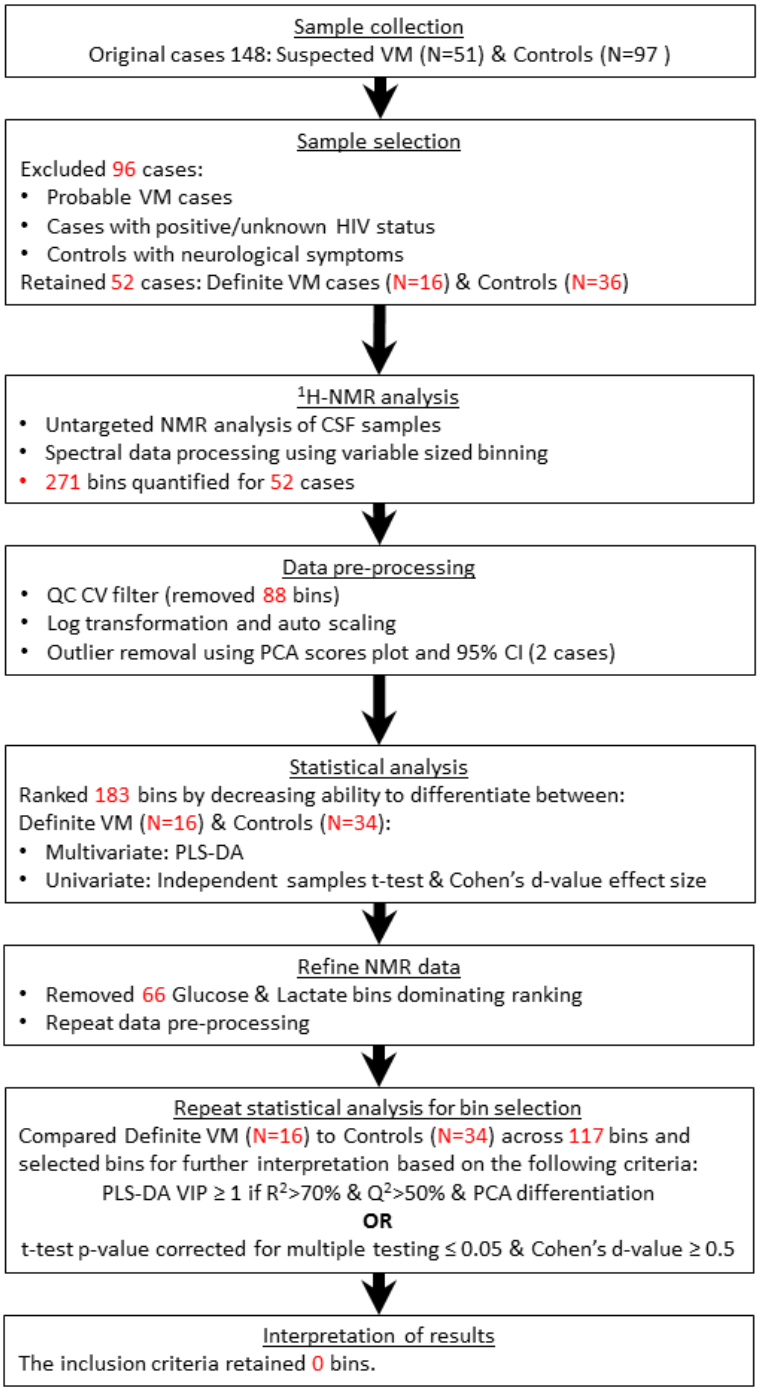


**Figure 5-1** **Schematic workflow of $^{1}$H-NMR metabolomics experimental design for VM vs control.**

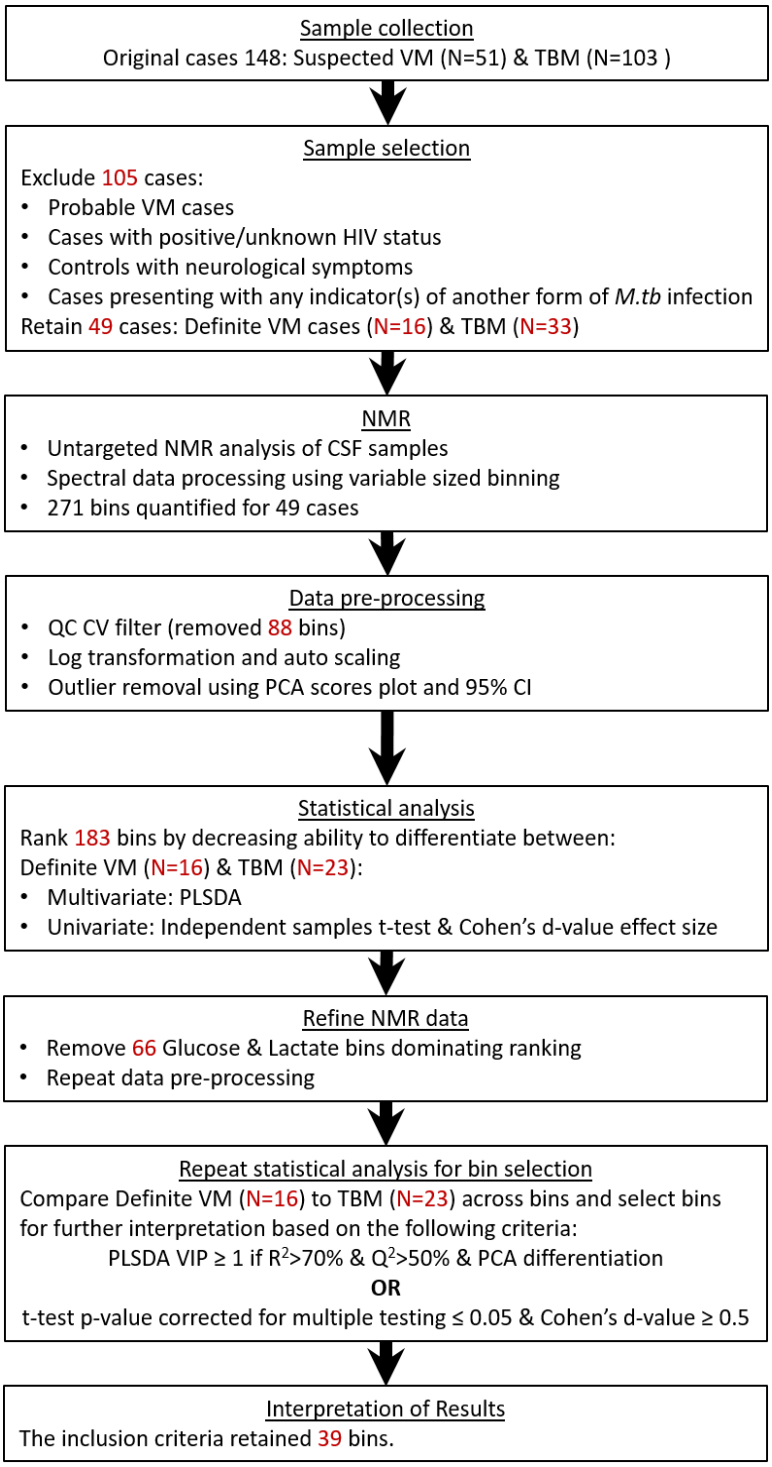


**Figure 5-2 Schematic workflow of $^{1}$H-NMR metabolomics experimental design for VM vs TBM**

## 5.3 Results and Discussion

### 5.3.1 Comparing CSF metabolite profile of viral meningitis to controls using $^{1}$H-NMR metabolomics

A 3D PCA scores plot of controls vs VM, excluding glucose and lactate (117 bins), with ellipsoids of 90% CI, is shown in Figure 5.3.

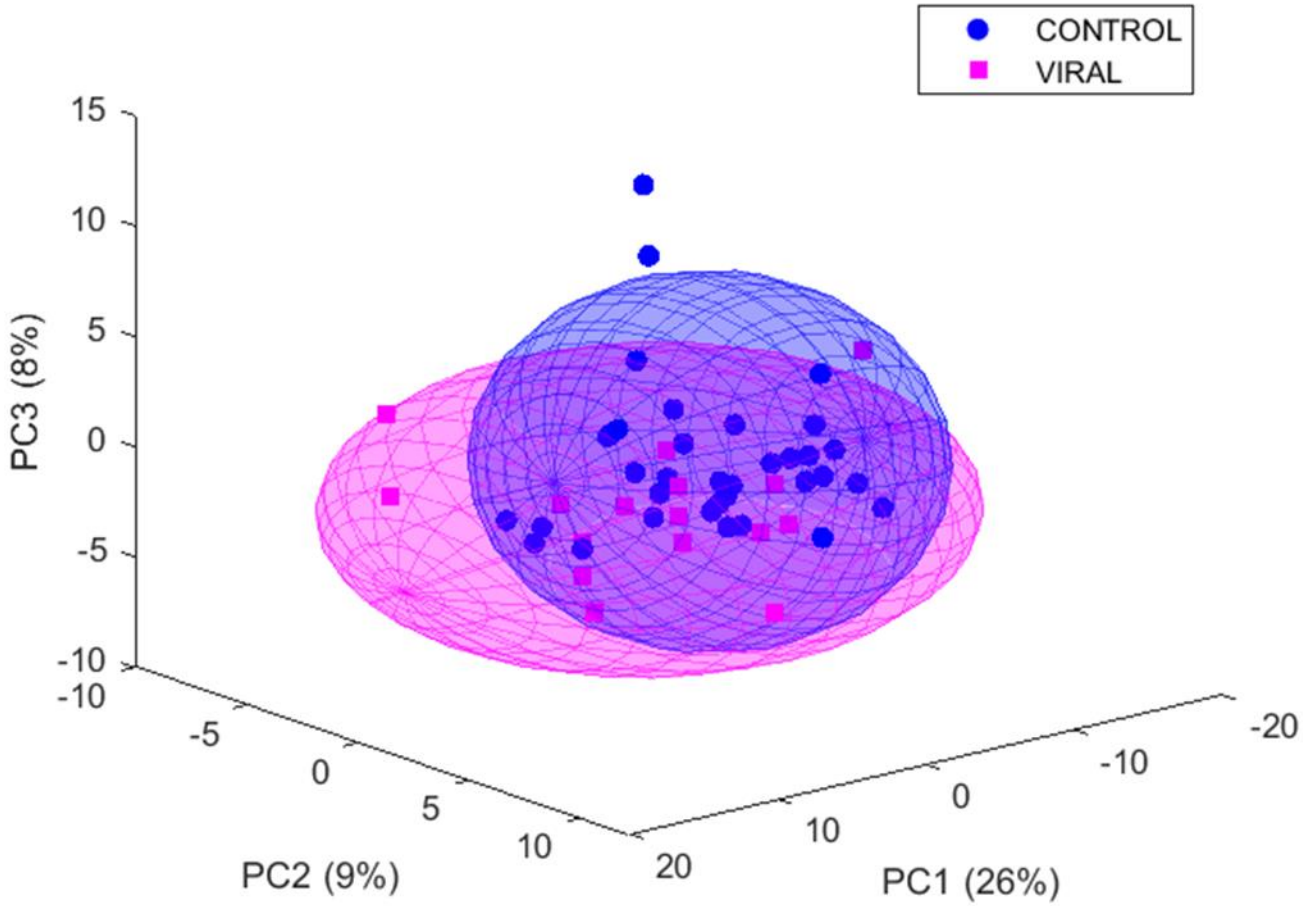


**Figure 5-3 3D PCA scores plot of controls vs VM, excluding glucose and lactate (117 bins), with ellipsoids of 90% CI**

Unsupervised PCA did not separate VM from controls as they overlap very closely. This indicates that they share a similar metabolic profile, and that there are likely no metabolites that distinguish VM from controls.

To confirm these results, a PLS-DA and univariate analysis was also done. It was found that no metabolites were found to be of statistical significance in the differentiation between VM

and controls. The reason for these results is most likely because VM is an acute form of meningitis, which is characterised by a rapid onset which quickly dissipates upon treatment. Hence, cerebral infarctions and hydrocephalus, that take time to form and are common to chronic meningitis such as TBM, do not occur in VM. Furthermore, VM cases do not typically display any long-term neurological complications post-treatment. As discussed in Chapter 4.1, the control group consisted of paediatric patients that were suspected to have meningitis based upon clinical symptoms but proven to be negative for meningitis upon final diagnosis (see Annexure 1 for final diagnosis of all controls). Hence, most of our controls were sick in some way (obtaining CSF samples from healthy infants is ethically not possible). Thus, it is not surprising to see that our VM group did not differentiate from the controls

A postulation can thus be made that in our paediatric cohort VM has the same CSF metabolic profile as the controls.

### 5.3.2 Comparing CSF metabolite profile of viral meningitis to tuberculous meningitis using $^{1}$H-NMR metabolomics

The metabolic comparison between TBM and controls, was done in Chapter 4.1 and it was found that there were 20 metabolites differentiating these 2 groups from one another. Since there were no metabolites differentiating VM and controls, and it is postulated that VM has the same CSF metabolic profile as controls, it was necessary to investigate if there would be a similar 20 metabolites differentiating TBM from VM. Thus the same methodology was followed as indicated in Figure 4.1. The original VM cases were N = 51 and the TBM cases were N = 103. After exclusion criteria was applied and statistical outliers were removed the cases were reduced to VM = 16 cases and TBM = 23 cases.

A 3D PCA scores plot of TBM vs VM, excluding glucose and lactate (117 bins), with ellipsoids of 90% CI is shown in Figure 5.4.

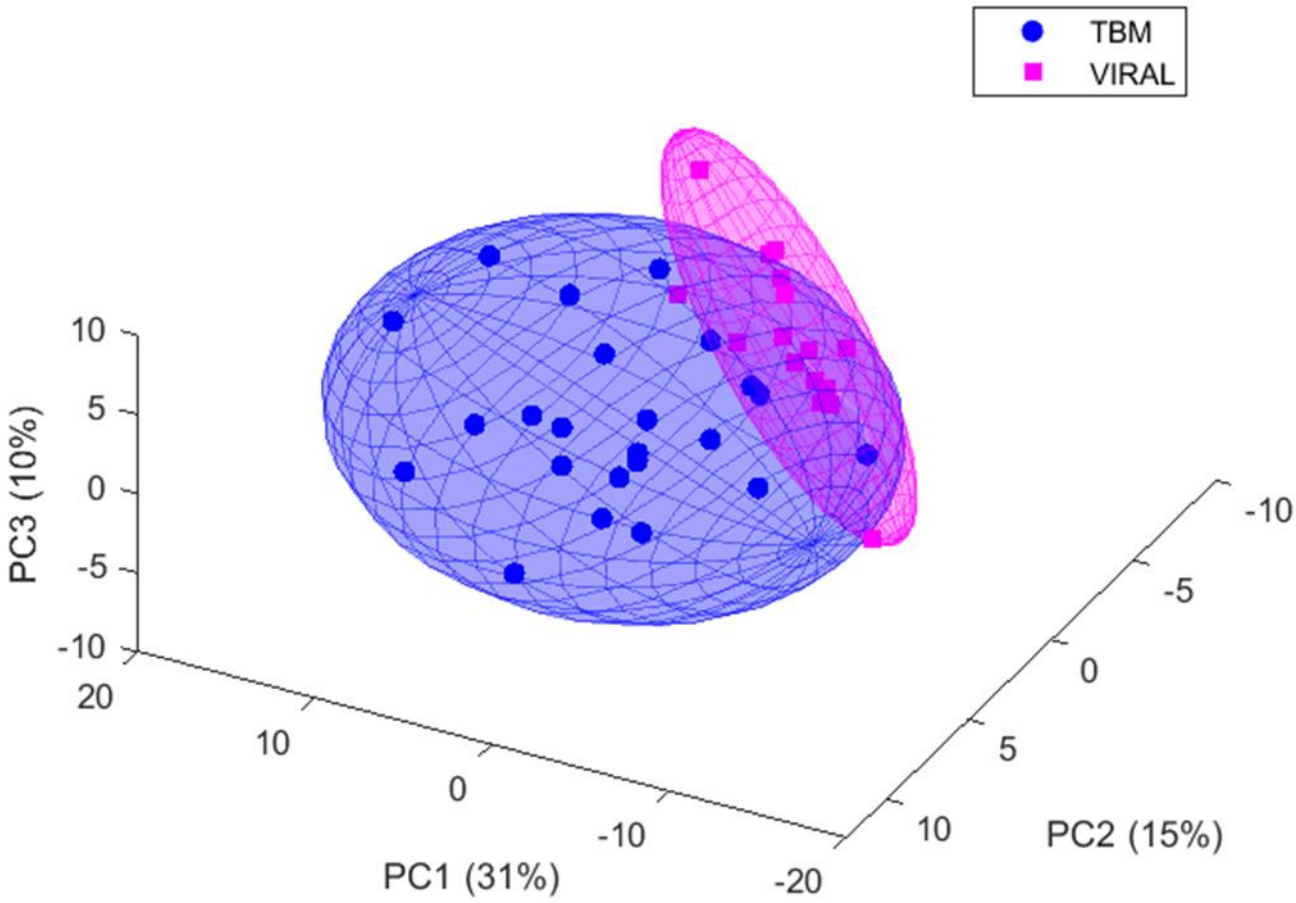


**Figure 5-4** **3D PCA scores plot of TBM vs VM, excluding glucose and lactate (117 bins), with ellipsoids of 90% CI**

The same PLS-DA and univariate analysis as described in Chapter 4, with the same cut-off values were applied here. The metabolites identified from the statistical significant bins, when comparing TBM to VM, were very similar to that detected when comparing the metabolite profiles of the TBM and control samples in Chapter 4, after the removal of glucose and lactate bins. The metabolites differentiating TBM from VM were: valine, alanine, glutamine, lysine, choline, carnitine, creatine, isoleucine, proline, myo-inositol and guanadinoacetate, and the same unknown variables – unknowns 1, 2, 3 and 4. The explanation and elucidation of these important metabolites are thus the same as in the discussion of TBM vs controls and can be found in Chapter 4.1.5.

The findings from the comparison between VM and TBM are thus in support of the conclusion from the comparison between VM and controls, in that VM has the same metabolic profile as controls, as very similar metabolites were identified to be of statistical significance when cross comparison was done.

## 5.4 References

Hristea, A., Olaru, I.D., Baicus, C., Moroti, R., Arama, V. & Ion, M. (2012). Clinical prediction rule for differentiating tuberculous from viral meningitis. Int J Tuberc Lung Dis, 16(6):793-798.

# CHAPTER 6 FINAL CONCLUSIONS AND FUTURE PROSPECTS

## 6.1 Addressing objective 1 of this thesis

Objective 1 of this study was to determine analyst competency by creating a synthetic CSF quality control sample and performing repeat analyses.

The creation of a synthetic quality control was successful and representative of CSF by containing several ions and nine metabolites commonly found in CSF. Three concentration ranges (high, medium and low) were established to determine analyst repeatability across varying sample concentrations. I then analysed ten samples of each concentration per day, over three days, resulting in a total of 90 samples analysed. The absolute concentration of each metabolite and their respective CV values, linearity and standard errors were calculated, in order to assess analyst repeatability. It was determined that the CV values were acceptable, linearity was good, accompanied by low standard errors, proving that I am a competent NMR analyst able to produce repeatable metabolomics data. Thus, objective 1 was achieved with the confidence that analytically reliable and accurate results were obtained throughout this study.

## 6.2 Addressing objective 2.1 of this thesis

Objective 2.1 of this study was to characterize the CSF metabolic profile of TBM, a chronic form of meningitis, by the use of univariate and multivariate statistics.

The characterization of TBM CSF metabolic profile was done by analysing CSF samples from a South Africa paediatric population with a $^{1}$H-NMR analytical platform. From an original sample set of 200 (TBM = 103, controls = 97), 61 cases were identified to be included for analysis after strict exclusion criteria were applied to ensure a homogenous control group and well-defined TBM group. Univariate and multivariate statistical methods where then used to identify important metabolites. Twenty metabolites were identified to be of statistical significance in differentiating TBM from controls, several of which overlap and have been previously described in two separated instances (Mason *et al.*, 2015; Zhang *et al.*, 2019). Eight metabolites are unique to this study, have been written up, and described in Chapter 4.1.5, along with a schematic illustrating the perturbed metabolic pathways in a *M.tb*-infected brain.

The main unique metabolic findings were: uncontrolled glucose metabolism, elevated carnitine, upregulated proline and creatine metabolism and disrupted glutamate-glutamine cycle of the host.

The uncontrolled glucose mechanism is a result of a sustained metabolic burst which in indicated by the high concentrations of lactate and reduced glucose concentration in the CSF. The rapid use of glucose stimulates glycolysis indicating a high energy demand, the need for. alternative energy pathways, and a consequence of insulin levels. A support for this is the increase of 2-hydroxybutyrate in the CSF, which leads to an insulin resistant state (Gall *et al.*, 2010; Gu *et al.*, 2019; Sarı *et al.*, 2019), thus glucose is unable to enter the cell to undergo glycolysis resulting in less ATP being produced. The decrease in glucose leads to upregulation of other metabolic pathways in an effort to recover the energy deficit, leading to an influx of lactate and ketones into the cells, which causes a destabilization of the blood brain barrier.

Carnitine concentration is increased in an effort to aid in the energy deficit, as it is a transporter for long chain fatty acids into the mitochondria, where the long chain fatty acids are broken down to acetyl-CoA via β-oxidation (Jones *et al.*, 2010). Carnitine can also detoxify various compounds by forming conjugates with them, making them more water soluble, thus carnitine can provide a degree of neuroprotection (Yu *et al.*, 1997).

Creatine is synthesized from guanidinoacetate. Guanidinoacetate was significantly decreased in TBM cases indicating an increased need of creatine/creatinine (both elevated in TBM). Creatinine is associated with neurodegenerative conditions like schizophrenia and depression (Agren and Niklasson, 1988; Levine *et al*., 2000; Swahn and Sedvall, 1988). Creatine has also been suggested as a potential neuromodulator with neuroprotective capabilities (Béard and Braissant, 2010).

Glutamate and glutamine was found to be significantly elevated in TBM cases, pointing to a disrupted glutamate-glutamine cycle. Increase in glutamate can disrupt the BBB permeability through the activation of N-methyl-D-aspartate receptors (Xhima *et al.*, 2016), and via alterations of tight junction protein expression in brain endothelial cells (Andras *et al.*, 2006).

Associated with oxidative stress and chronic neuroinflammation, our findings cumulatively contribute toward destabilization of the BBB; hence, increasing BBB permeability, which is associated with increased intra-cranial pressure – a clinical hallmark of advanced meningitis, particularly in TBM.

Thus, objective 2.1 was successfully completed by identifying unique metabolites using $^{1}$H-NMR metabolomics. The metabolic insights gained from this investigation improve upon our understanding of TBM, and contribute toward the metabolic characterization of TBM to aid in future diagnostic and possibly therapeutic research.

## 6.3 Addressing objective 2.2 of this thesis

Objective 2.2 of this study was to characterise CSF metabolic profile for acute (VM) meningitis by comparison to that of a control CSF sample set and that of a TBM sample set.

Comparing the CSF metabolic profile of VM to that of control CSF revealed that no metabolites were of statistical significance in the differentiation of VM and controls. This led to the postulation that VM and controls in our paediatric cohort have a very similar CSF metabolic profile. The findings from the comparison between VM and TBM were in support of the postulation that VM and controls in our paediatric cohort have a very similar CSF metabolic profile, in that very similar metabolites were identified to be of statistical significance if differentiating VM from TBM when cross comparison was done. Thus, objective 2.2 was successfully completed.

## 6.4 Conclusion

In conclusion, this study successfully achieved all the objectives set out in Chapter two. By the successful completion of all the set objectives, the aims of this study were met by providing valuable new insights into the characterisation of various types of meningitis by using $^{1}$H-NMR metabolomics platform. These new insights can possibly help improve upon early differential diagnosis of meningitis cases and provides experimental evidence that $^{1}$H-NMR metabolomics can possibly be a valuable future diagnostic aid.

## 6.5 Directives for future research

This study opened up a vast number of future directives, and can be followed up by various studies namely:

(1) Further $^{1}$H-NMR investigation into the unknown variables identified to be characteristic of TBM in this study. This would involve additional NMR experiments (e.g. $^{13}$C-NMR, $^{15}$N-NMR, 2D HSQC NMR, 2D TOCSY NMR, and diffusion NMR), and the use of other analytical platforms (e.g. GC-MS and LC-MS systems). Furthermore, once isolated, structure elucidation of the unknown variables would need to be done to aid in their identification, and, eventually, describe their role in the metabolism of a *M.tb* -infected brain.

(2) $^{1}$H-NMR metabolomics of all HIV-negative cases with the inclusion of TBM cases given a ‘probable’ TBM diagnosis, probable VM cases, and controls cases with the inclusion of TB cases and neurological symptoms. With this more diverse and larger sample group, a robust diagnostic profile could then be determined.

(3) $^{1}$H-NMR metabolomics with the inclusion of HIV-positive cases to determine confounding factors. Investigate if/how an HIV co-infection affects the CSF metabolic profile, which is a situation many clinicians face on a daily basis, as this comparison would better represent patients in hospitals in sub-Saharan Africa.

(4) Use of a more sensitive analytical platform such as 2D gas chromatography-mass spectrometry coupled with a time-of-flight (GCxGC-TOF-MS). Such an untargeted metabolomics approach would identify metabolites that may be significant but that are below the detection limit of the $^{1}$H-NMR analytical platform, and/or not detectable via $^{1}$H-NMR. This additional metabolomics analyses could be extended to include LC-MS/MS. Ultimately, providing a greater scope of the CSF metabolome and acting as complementary to each other.

(5) Targeted, in-depth metabolomics studies to quantify and validate potential biomarkers/biosignature of TBM. Such targeted analyses would involve extraction methods to isolate specific classes of metabolites, such as amino acids, carnitines and organic acids.

## 6.6 References

Ågren, H. & Niklasson, F. 1988. Creatinine and creatine in CSF: indices of brain energy metabolism in depression. Journal of Neural Transmission, 74(1):55-59.

Andras, I.E., Hayashi, K., Hennig, B. & Toborek, M. 2006. Glutamate-induced alterations of tight junction protein expression and distribution in brain endothelial cells. The FASEB Journal, 20(4):A378-A378.

Béard, E. & Braissant, O. 2010. Synthesis and transport of creatine in the CNS: importance for cerebral functions. Journal of Neurochemistry, 115(2):297-313.

Gall, W.E., Beebe, K., Lawton, K.A., Adam, K.-P., Mitchell, M.W., Nakhle, P.J., Ryals, J.A., Milburn, M.V., Nannipieri, M., Camastra, S., Natali, A., Ferrannini, E. & Group, R.S. 2010. alpha-hydroxybutyrate is an early biomarker of insulin resistance and glucose intolerance in a nondiabetic population. PloS one, 5(5):e10883-e10883.

Gu, Y., Zang, P., Li, L.-q., Zhang, H.-z., Li, J., Li, J.-x., Yan, Y.-y., Sun, S.-m., Wang, J. & Zhu, Z.-y. 2019. A non-targeted metabolomics study on different glucose tolerance states. International Journal of Diabetes in Developing Countries, 39(3):478-485.

Jones, L.L., McDonald, D.A. & Borum, P.R. 2010. Acylcarnitines: role in brain. Prog Lipid Res, 49(1):61-75.

Levine, J., Panchalingam, K., Rapoport, A., Gershon, S., McClure, R.J. & Pettegrew, J.W. 2000. Increased cerebrospinal fluid glutamine levels in depressed patients. Biological Psychiatry, 47(7):586-593.

Mason, S., van Furth, A.M., Mienie, L.J., Engelke, U.F., Wevers, R.A., Solomons, R. & Reinecke, C.J. 2015. A hypothetical astrocyte-microglia lactate shuttle derived from a (1)H NMR metabolomics

analysis of cerebrospinal fluid from a cohort of South African children with tuberculous meningitis. Metabolomics, 11(4):822-837.

Sarı, H., Esen, B., Yıldırım, S., Pilten, S. & Aydın, H. 2019. Serum α-Hydroxybutyrate: A Candidate Marker of Insulin Resistance Is Associated with Deterioration in Anthropometric Measurements in Individuals with Low Diabetes Risk. The Journal of Applied Laboratory Medicine, 1(5):562-567.

Swahn, C.-G. & Sedvall, G. 1988. CSF creatinine in schizophrenia. Biological Psychiatry, 23(6):586-594.

Xhima, K., Weber-Adrian, D. & Silburt, J. 2016. Glutamate Induces Blood-Brain Barrier Permeability through Activation of N-Methyl-D-Aspartate Receptors. J Neurosci, 36(49):12296-12298.

Yu, Z., Iryo, Y., Matsuoka, M., Igisu, H. & Ikeda, M. 1997. Suppression of pentylenetetrazol-induced seizures by carnitine in mice. Naunyn-Schmiedeberg's Archives of Pharmacology, 355(4):545-549.

Zhang, P., Zhang, W., Lang, Y., Qu, Y., Chen, J. & Cui, L. 2019. (1)H nuclear magnetic resonance-based metabolic profiling of cerebrospinal fluid to identify metabolic features and markers for tuberculosis meningitis. Infect Genet Evol, 68:253-264.

# ANNEXURES

## ANNEXURE 1

**Supplementary Information:**

# Metabolic characterization of tuberculous meningitis in a South African paediatric population using $^{1}$H-NMR metabolomics

Christiaan De Wet van Zyl[1], Du Toit Loots[1], Regan Solomons[2], Mari van Reenen[1], Shayne Mason[1*]

[1] Human Metabolomics, Faculty of Natural and Agricultural Sciences, North-West University, Potchefstroom, South Africa,

[2] Department of Pediatrics and Child Health, Faculty of Medicine and Health Sciences, Stellenbosch University, Tygerberg, South Africa.

Table S1: Alternative diagnoses ascribed to control cases that were shown to be negative for meningitis.

| Control case | Alternative diagnosis |
|---|---|
| C1 | N/A |
| C2 | Mastitis |
| C3 | Seizures eci |
| C4 | Gastro enteritis |
| C5 | N/A |
| C6 | Gastro enteritis |
| C7 | Febrile seizure |
| C8 | Viral pneumonia |
| C9 | Gastro enteritis |
| C10 | Gastro enteritis |
| C11 | Forticollis |
| C12 | Pneumonia |
| C13 | Virus or flu |
| C14 | Pulmonary TB, Pneumonia, Conjunctivitis, Chlamydia, HIV |
| C15 | N/A |
| C16 | MTB, Pneumonia, Gastro enteritis |
| C17 | N/A |
| C18 | Flu |
| C19 | Pulmonary TB, Measles |
| C20 | N/A |
| C21 | Seizures |
| C22 | Convulsions |
| C23 | PTB |
| C24 | UTI, Pneumonia, Rash, HIV |
| C25 | Flu |
| C26 | N/A |
| C27 | N/A |
| C28 | RVD positive |
| C29 | UTI |
| C30 | Pneumonia |
| C31 | N/A |
| C32 | Bronchopneumonia, Encephalopathy |
| C33 | RML Pneumonie, Gastro enteritis |

| | |
|---|---|
| C34 | Hemilplegia (left), Aneamia, Sinus renalis trombosis, Hypoalbumineamia with oedema. |
| C35 | LRTI |
| C36 | LRTI |
| C37 | Generalised clonic tonic seizures |
| C38 | Pneumonie |
| C39 | Seizures |
| C40 | Convulsions |
| C41 | URTI |
| C42 | Poisoning |
| C43 | Richetsial infection, Macular papital rash |
| C44 | Hydrocephalus |
| C45 | Viral respiratory infection |
| C46 | Viral URTI, Febrile convulsions |
| C47 | Focal Seizures |
| C48 | Milliary TB |
| C49 | Milliary TB |
| C50 | Viral Infection |
| C51 | Focal seizures |
| C52 | Convulsions |
| C53 | Organophosphate poisoning |
| C54 | Focal seizures |
| C55 | Febrile convulsions, URTI |
| C56 | Febrile convulsions, Strabism non paralytic |
| C57 | Copmplex febrile seizures |
| C58 | Drug ingestion, Acute dystonic reaction |
| C59 | Bilateral puj.obstruction, Right pyeloplasty |
| C60 | Seizures |
| C61 | Pontine lesion, Acute gastro enteritis |
| C62 | Seizures |
| C63 | N/A |
| C64 | Hypoglycaemia |
| C65 | Delayed milestones, Focal seizures, FFT |
| C66 | Tonsillitis |
| C67 | Seizures, Failure to thrive, URTI |
| C68 | Pulmonary TB, Kwashiokor |
| C69 | Hallucinations |

| | |
|---|---|
| C70 | Bronchiolitis, 2nd degree URTI |
| C71 | TB right ear, Mastoidectomy |
| C72 | N/A |
| C73 | Right otitis media, Pulmonary TB |
| C74 | Tonsillitis |
| C75 | Glomerulonephrititis with hypertension, Focal seizures |
| C76 | Cerebral oedema |
| C77 | N/A |
| C78 | Focal seizures, Myoclonic jerks, Encephalopathy |
| C79 | Febrile Convulsions |
| C80 | Pulmonary TB |
| C81 | Varicella zoster infection |
| C82 | Focal seizures |
| C83 | Focal seizures, Developmental delay |
| C84 | Gastro enteritis |
| C85 | Tuberculoma |
| C86 | Viral Pneumonia, SAM, Nosocomial sepsis |
| C87 | Chicken Pox, Febrile seizure |
| C88 | Febrile Seizure, Acute gastro enteritis |
| C89 | Guilain Barre |
| C90 | Gastroenteritis Cx by shock |
| C91 | Febrile Seizure |
| C92 | Cerebral infarction - right MCA |
| C93 | Developmental regression |
| C94 | N/A |
| C95 | Mastitis |
| C96 | Seizures eci |
| C97 | Gastro enteritis |

Table S2: Chemical information and shifts for $^{1}$H-NMR spectra of the 20 statistically significant CSF metabolites identified for TBM. Multiplicity: s − singlet; d − doublet; t – triplet; dd − double doublet; q – quartet; m – multiplet; AB – AB system. ND = not determined.

| Metabolite name | Chemical structure | HMDB ID | Chemical formula | δ (ppm), multiplicity (J coupling) | Chemical group | Atom(s) |
|---|---|---|---|---|---|---|
| Glucose | 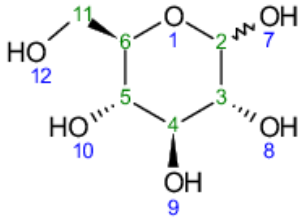 | HMDB0000122 | $C_6H_{12}O_6$ | 3.25 dd (J = 9.3 Hz) | CH | 3 |
| | | | | 3.39–3.50 m | | 3,4,5,6,11 |
| | | | | 4.65 d (J = 7.9 Hz) | CH | 2 |
| | | | | 5.22 d (J = 3.6 Hz) | CH | 2 |
| Lactate | 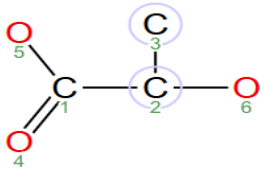 | HMDB0000190 | $C_3H_6O_3$ | 1.33 d (J = 6.9 Hz) | $CH_3$ | 3 |
| | | | | 4.12 q | $CH_2$ | 2 |

| | | | | | | |
|---|---|---|---|---|---|---|
| | | | | (J = 6.8 Hz) | | |
| 2-Hydroxybutyrate | 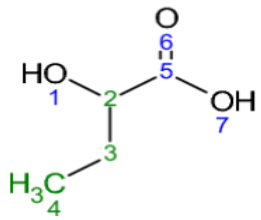 | HMDB0000008 | $C_4H_8O_3$ | 0.89 t<br>(J = 7.47 Hz) | $CH_3$ | 4 |
| | | | | 1.66 m | $CH_2$ | 3 |
| | | | | 1.73 m | $CH_2$ | 3 |
| | | | | 3.99 dd<br>(J = 6.56, 4.52 Hz) | CH | 2 |
| Isoleucine | 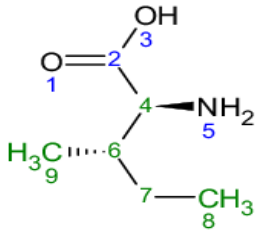 | HMDB0000172 | $C_6H_{13}NO_2$ | 0.94 t<br>(J = 7.3 Hz) | $CH_3$ | 8 |
| | | | | 1.01 d<br>(J = 7.3 Hz) | $CH_3$ | 9 |
| Valine | 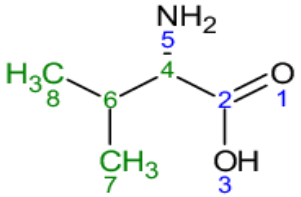 | HMDB0000883 | $C_5H_{11}NO_2$ | 0.99 d<br>(J = 7.0 Hz) | $CH_3$ | 8 |
| | | | | 1.04 d | $CH_3$ | 7 |

| | | | | | | |
|---|---|---|---|---|---|---|
| | | | | (J = 7.0 Hz) | | |
| Alanine | 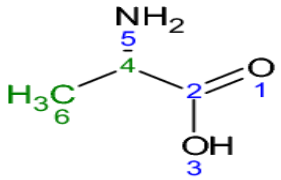 | HMDB0000161 | $C_3H_7NO_2$ | 1.48 d<br>(J = 7.2 Hz) | $CH_3$ | 6 |
| Lysine | 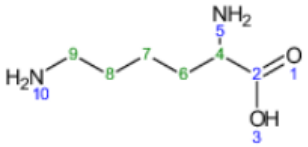 | HMDB0000182 | $C_6H_{14}N_2O_2$ | 1.72 m | $CH_2$ | 8 |
| | | | | 3.02 t<br>(J = ND) | $CH_2$ | 9 |
| Proline | 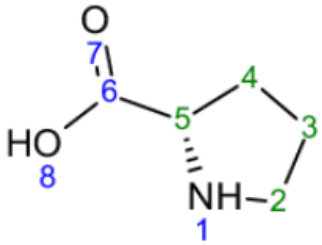 | HMDB0000162 | $C_5H_9NO_2$ | 1.98 m | $CH_2$ | 3 |
| | | | | 2.03 m | $CH_2$ | 4 |
| Acetate | 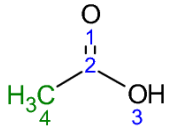 | HMDB0000042 | $C_2H_4O_2$ | 1.92 s | $CH_3$ | 4 |

| | | | | | | |
|---|---|---|---|---|---|---|
| Pyruvate | 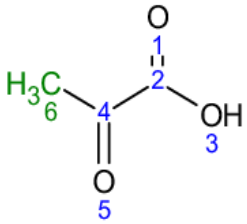 | HMDB0000243 | $C_3H_4O_3$ | 2.37 s | $CH_3$ | 6 |
| Glutamate | 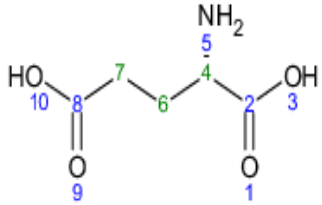 | HMDB0000148 | $C_5H_9NO_4$ | 2.11 m | $CH_2$ | 6 |
| | | | | 2.35 m | $CH_2$ | 7 |
| Glutamine | 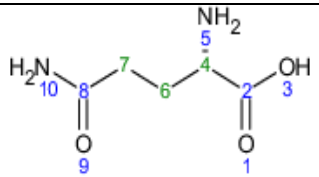 | HMDB0000641 | $C_5H_{10}N_2O_3$ | 2.11 m | $CH_2$ | 6 |
| | | | | 2.45 m | $CH_2$ | 7 |
| Citrate | 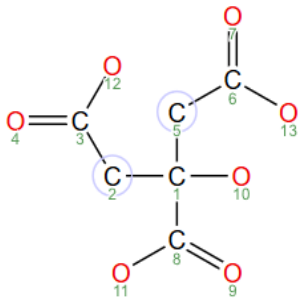 | HMDB0000094 | $C_6H_8O_7$ | 2.61 AB<br>(J = 15.3 Hz) | $(CH_2)_2$ | 2,5 |

| | | | | | | |
|---|---|---|---|---|---|---|
| Creatine | 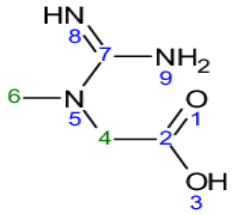 | HMDB0000064 | $C_4H_9N_3O_2$ | 3.03 s | $CH_3$ | 6 |
| | | | | 3.93 s | CH | 4 |
| Creatine phosphate | 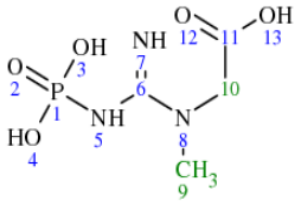 | HMDB0001511 | $C_4H_{10}N_3O_5P$ | 3.04 s | $CH_3$ | 9 |
| | | | | 3.96 s | CH | 10 |
| Creatinine | 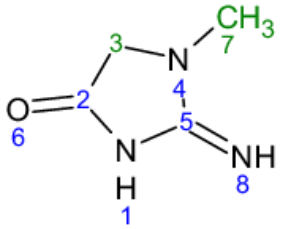 | HMDB0000562 | $C_4H_7N_3O$ | 3.04 s | $CH_3$ | 7 |
| | | | | 4.06 s | $CH_2$ | 3 |
| Choline | 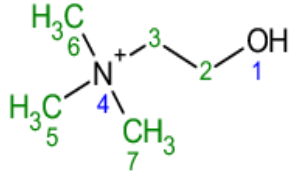 | HMDB0000097 | $C_5H_{14}NO$ | 3.20 s | $(CH_3)_3$ | 5,6,7 |

| | | | | | | |
|---|---|---|---|---|---|---|
| Carnitine | 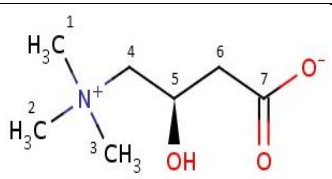 | HMDB0000062 | $C_7H_{15}NO_3$ | 3.22 s | $(CH_3)_3$ | 1,2,3 |
| Guanidinoacetate | 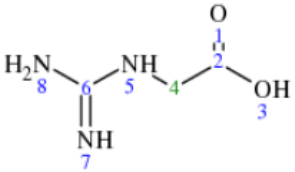 | HMDB0000128 | $C_3H_7N_3O_2$ | 4.81 s | $CH_2$ | 4 |
| myo-Inositol | 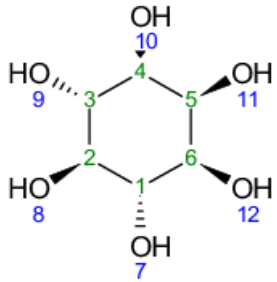 | HMDB0000211 | $C_6H_{12}O_6$ | 4.07 t<br>(J = 2.9 Hz) | CH | 5 |
| TSP | 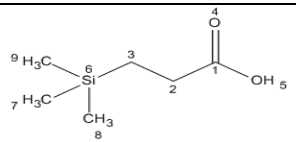 | N/A | $C_6H_{14}O_2Si$ | 0.00 s | $Si-(CH_3)_3$ | 7,8,9 |

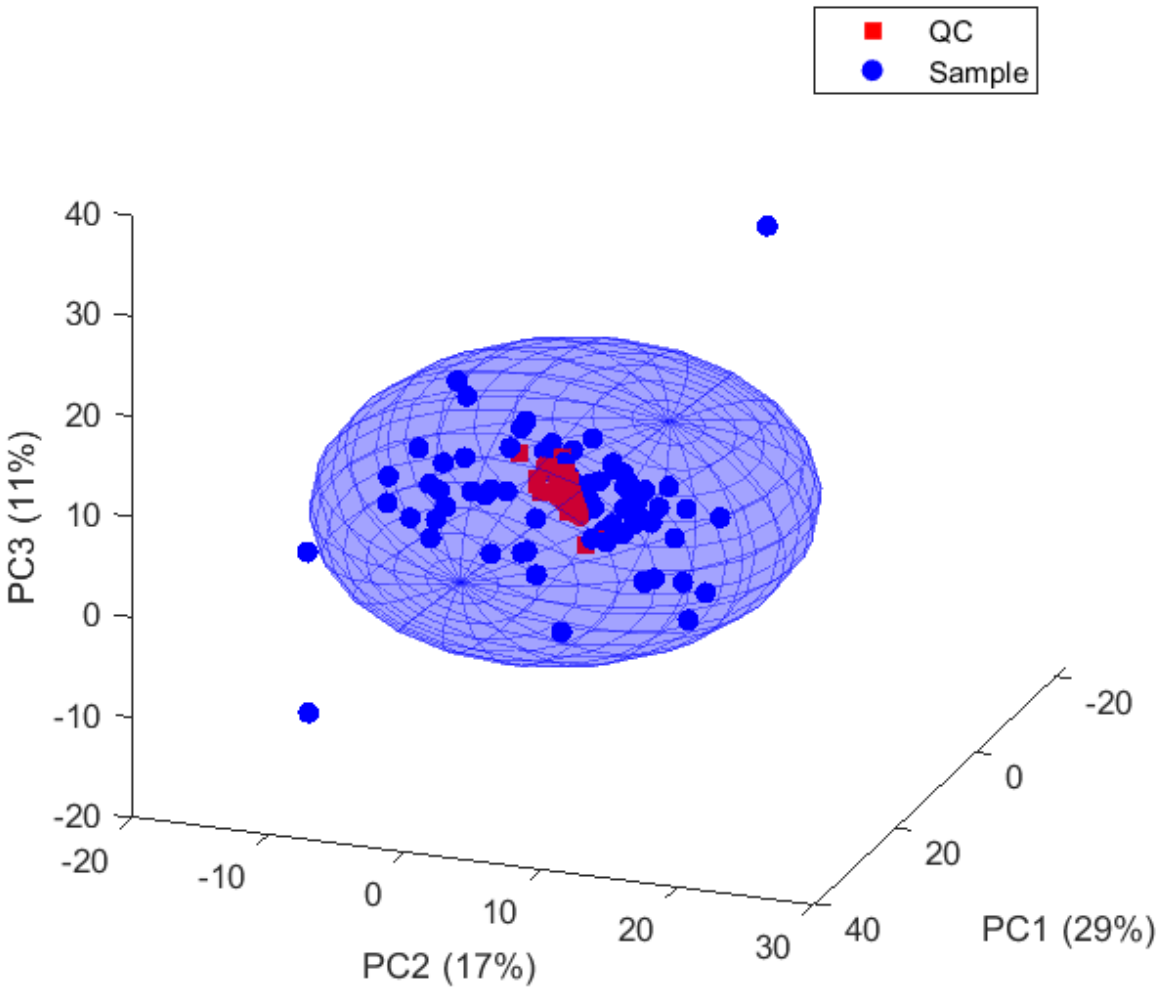


Figure S1: 3D PCA plot comparing all experimental samples analysed to QC samples. The QC samples cluster closely together and show far less variation compared to the experimental samples indicating consistency in NMR analysis and data collection.

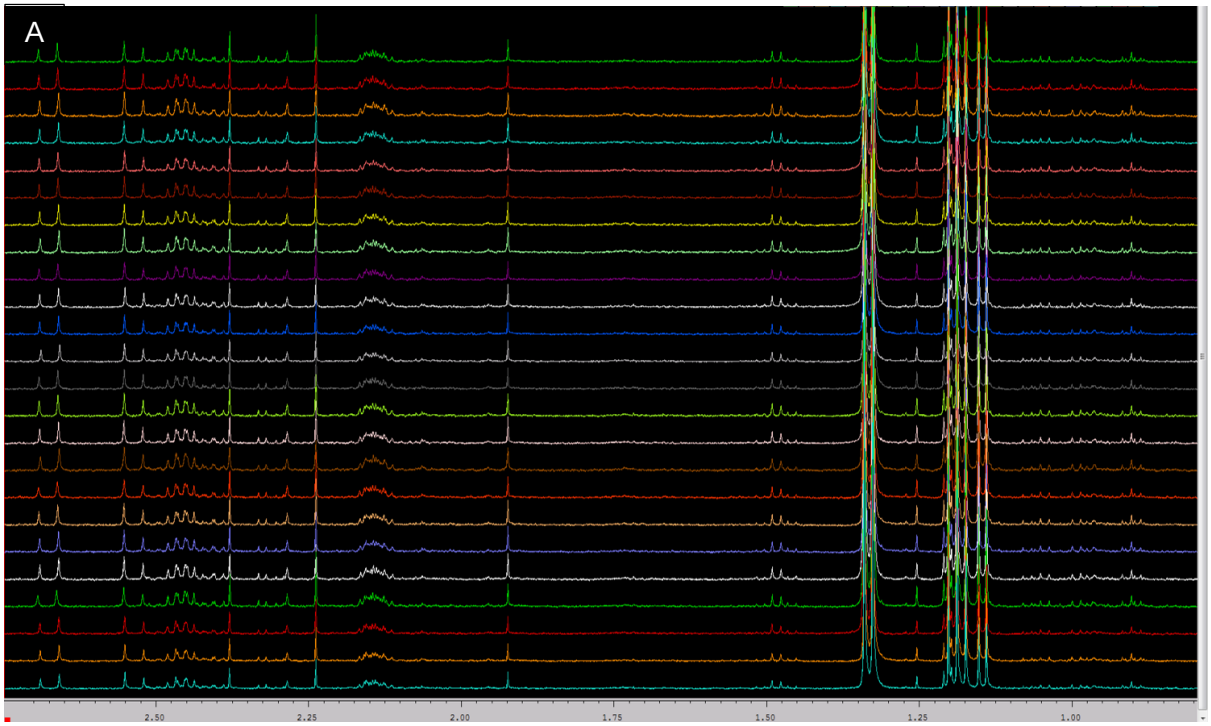
A
2.50
2.25
2.00
1.75
1.50
1.25
1.00

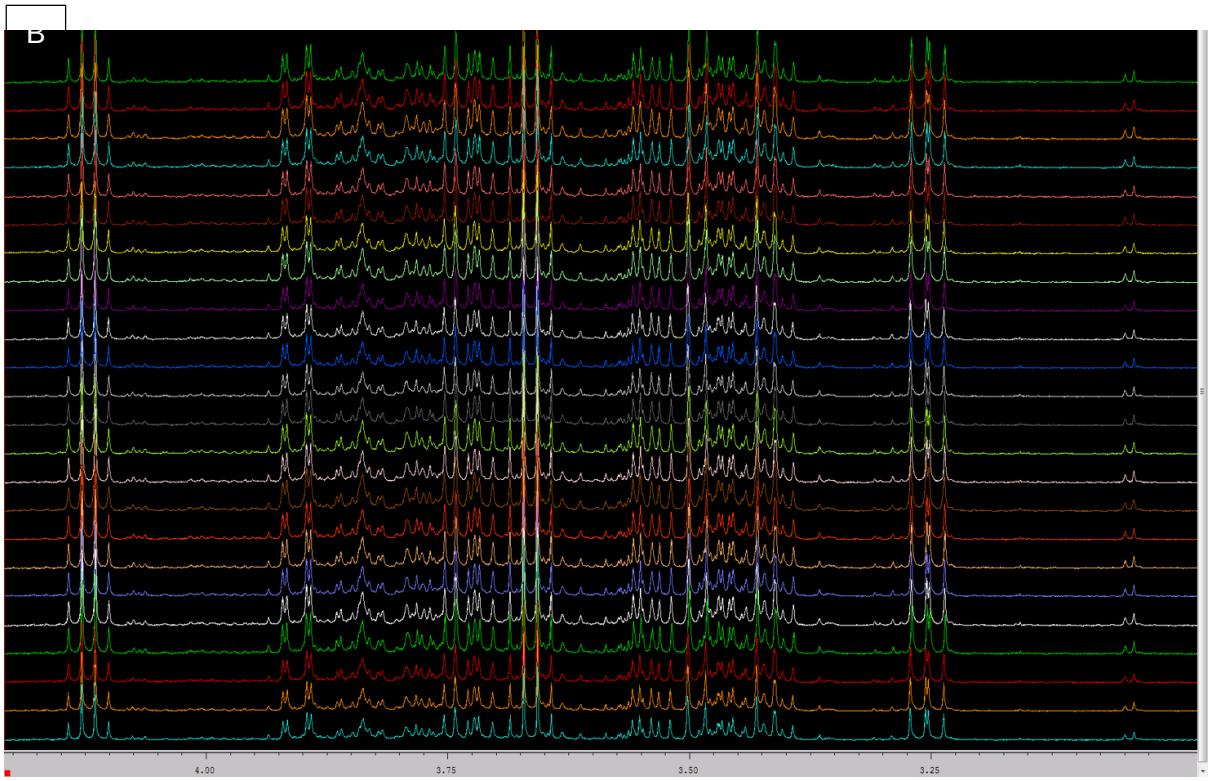
B
4.00
3.75
3.50
3.25

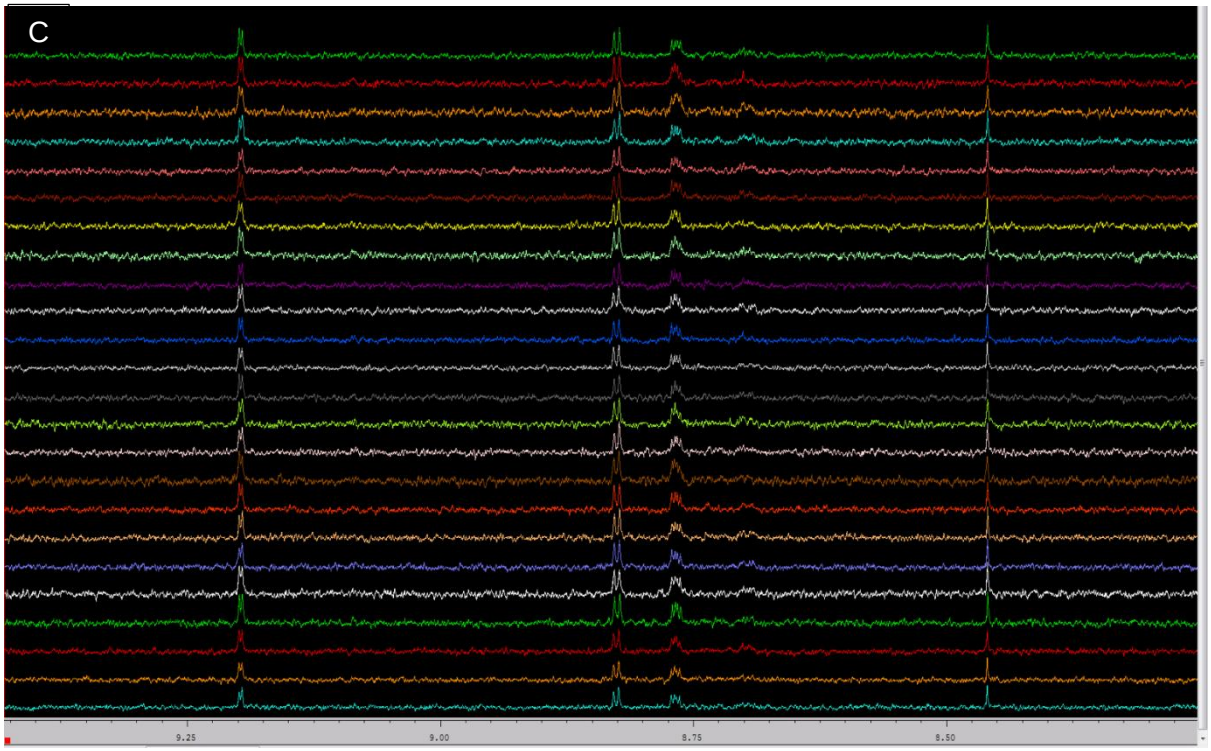


Figure S2: Overlay of the $^{1}$H-NMR spectra of all 24 QC samples, indicating qualitatively that all QCs produced repeatable results. A: spectra region 0.80–2.80 ppm; B: spectral region 2.80–4.20 ppm; C: spectral region 8.25–9.45 ppm.

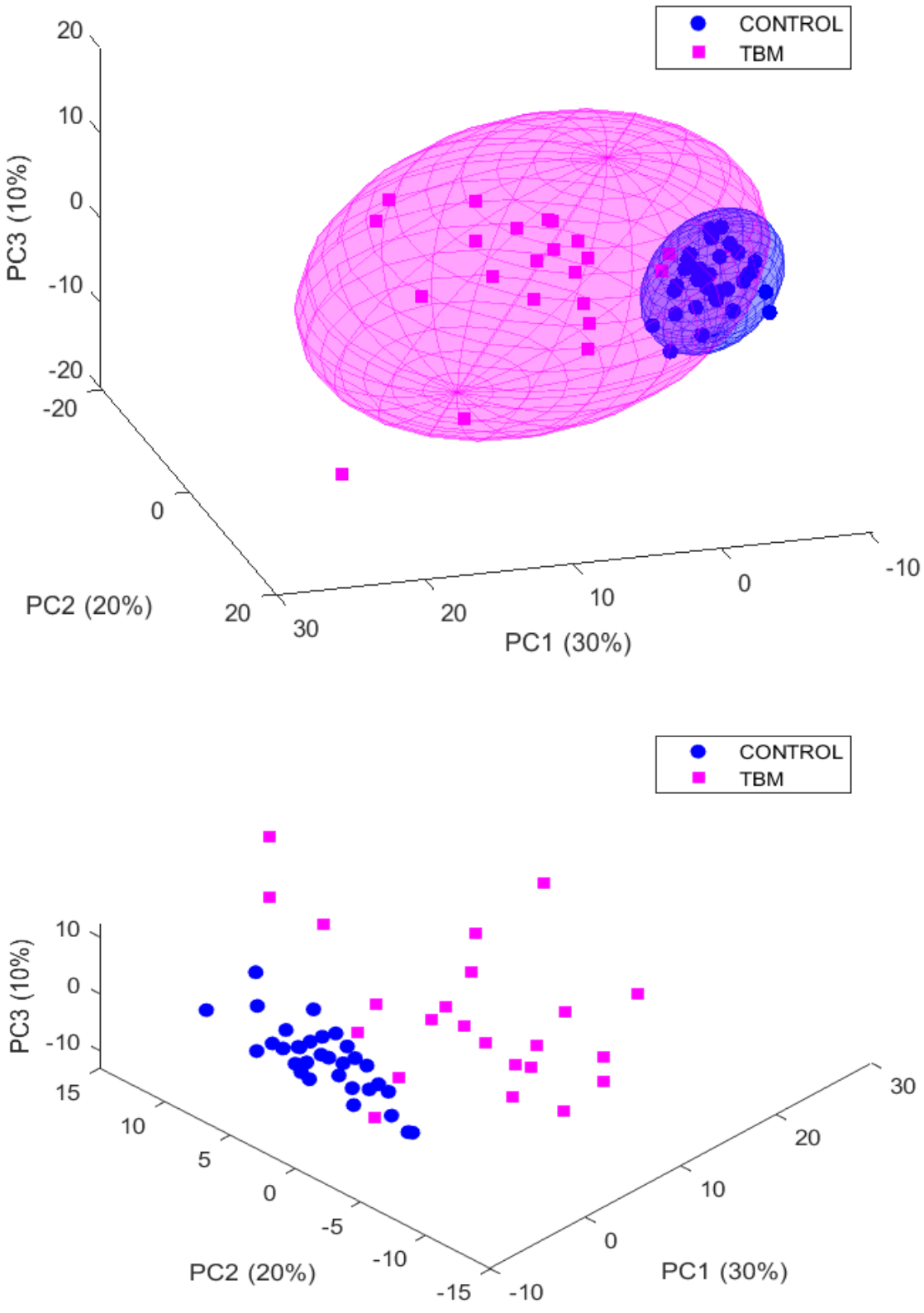


Figure S3: 3D PCA scores plot of Controls vs TBM, glucose and lactate included (183 bins).

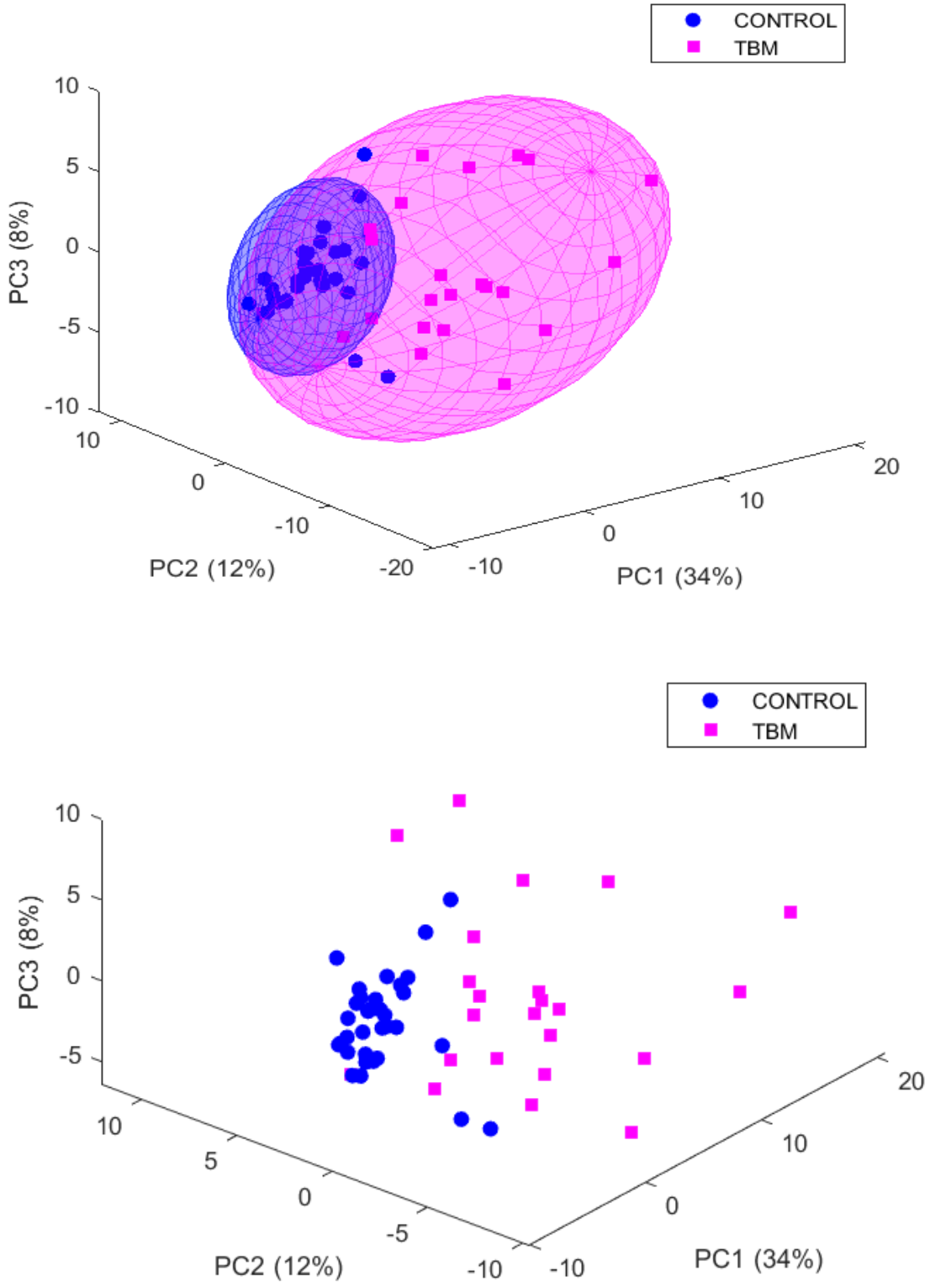


Figure S4: 3D PCA scores plot of Controls vs TBM, excluding glucose and lactate (117 bins).

## ANEXURE 2

Proof of submission

**ANEXURE 3**

Journal of Infection pre-proof of Chapter 4 manuscript accepted for publication on 27 June 2020.

Journal Pre-proof


# Metabolic characterization of tuberculous meningitis in a South African paediatric population using $^{1}$H-NMR metabolomics

Christiaan De Wet van Zyl , Du Toit Loots , Regan Solomons , Mari van Reenen , Shayne Mason

PII: S0163-4453(20)30494-1
DOI: https://doi.org/10.1016/j.jinf.2020.06.078
Reference: YJINF 4758

To appear in: *Journal of Infection*

Accepted date: 27 June 2020

Please cite this article as: Christiaan De Wet van Zyl , Du Toit Loots , Regan Solomons , Mari van Reenen , Shayne Mason , Metabolic characterization of tuberculous meningitis in a South African paediatric population using $^{1}$H-NMR metabolomics, *Journal of Infection* (2020), doi: https://doi.org/10.1016/j.jinf.2020.06.078

**ANEXURE 4**

Response to reviewer of the Journal of infection

Reviewer #1: Overall comment

I think this study has a strong methodology in terms of patient phenotype, metabolomic analysis and data analysis. However, the weakness is the interpretation of the data. The authors over-reach in the interpretation of their data and their focus on tenuous explanations for the data rather than looking at the basic pathophysiology which we know to be at play in TBM. They also need to more clearly delineate how this study differs from previous work from their group. No limitations are discussed, the study has several, some I have mentioned below. Importantly the fact that this is a comparison between a TBM cohort and a 'healthy' cohort and the associated limitations needs to be clearly stated.

Background

* 1st paragraph the authors refer to 'exudate microglia' I would remove the word 'exudate' as the text refers to microglia that are general to the CNS

Response:

Removed the word exudate

"The microglia, whose many functions include immune regulation, are the primary cerebral cells infected by *M.tb*., however, astrocytes and neurons are also affected (Rock et al., 2005)."

Results

* Figure 4: the axes are difficult to read, please increase the font size. The legend says 20 statistically significant metabolites but not all p values are <0.05, or does this significance refer to different analysis?

Response:

Rewrote legend

"Figure 4: Box plots of the absolute concentrations (µM) of the 20 CSF metabolites identified by untargeted $^{1}$H-NMR metabolomics in our paediatric cohort. Mann-Whitney p-values given on the bottom of each box plot."

Figure 4 was also redone to make the font size on the axes bigger. It is now easier to read.

Discussion

* The authors refer to a previous study conducted using unbiased metabolomics in paediatric TBM patients Mason 2015 (n=63) and adult patients Zhang 2019 (n=61) and then they refer to yet another paediatric cohort n=200 - it is not clear which study this last one with 200 patients refers to, please clarify

* The authors refer to their previous study (Mason 2015) which found largely the same outputs, except for 8 unique metabolites found in this study, why do the authors think that this study elucidated these additional metabolites? What makes this study different to the previous one? Or is this study meant as a validation cohort?

Response:

Thank you for identifying for these points. This study had a better defined cohort, in terms of more metadata, resulting in better defined case phenotypes. We have made some edits to more clearly delineate the current study from previous studies, as well as to indicate that the current study supports previous findings. We have made edits to provide clarity to the reader with regard to the Reviewer's comments

Edits made to manuscript:

"In the current study, however, the original paediatric cohort consisted of 200 cases (TBM=103, Controls=97). Utilizing the comprehensive meta-data accompanying the CSF samples, we were able to better define our cohort, as defined under *Experimental group definition*. Hence, in the current study, due our strict data filtering methods, we were able to utilize a more-defined TBM group (n=33) and homogenous control group (n=33), in order to better characterize the CSF metabolic profile of TBM."

"The experimental results of our current NMR metabolomics study support the data for the AMLS hypothesis given by Mason et al. (2015). The increased lactate, together with ketones and gluconeogenic amino acids, derived from astrocytes, is directed from the neurons preferentially into microglia…"

Further, based on one the Reviewer's later comments, we included the following at the end of our discussion, highlighting that the refinement of the cohorts delineates our study from previous studies, and allowed us to identify eight new metabolite associated with a Mtb-infected brain:

"It is important to state that the comparison done in our study was between a well-defined definite TBM cohort and a 'healthy' control cohort without any neurological symptoms. The refinement of the cohorts studied here delineates our study from previous studies, and allowed us to identify eight new metabolites associated with a *M.tb*-infected brain. Since these eight metabolites are novel (i.e. not previously identified within a *M.tb*-infected brain), our interpretation of them in the CSF is speculative, but is supported by literature where indicated. Therefore these findings may not represent TBM specifically but rather an infectious state in the brain, or indeed an inflammatory state in the brain."

* The authors provide various possible explanations for dysregulated glucose metabolism, but the scientific and physiological basis for many of these is questionable. For example, TBM is not a chronic inflammatory process, it is rather sub-acute with an acute presentation and therefore the connection to chronic inflammation and insulin resistance is too tenuous.

Response:

Uncontrolled glucose metabolism was definitely one of the main findings of our experiment. In our interpretation in the discussion we link this dysregulated glucose metabolism to other chronic inflammatory diseases (e.g. diabetes). There is indeed an argument that can be made that TBM is rather sub-acute with an acute presentation and we respect that argument; however, we base our interpretation on TBM being defined as a chronic inflammatory disease. Hence, we have made this definition clearer at the onset of our manuscript – in the introduction (with additional references added):

"M.tb is known to cause characteristic persistent granulomatous inflammation (Gil-Santana et al., 2019), and is one of the most common infectious causes of chronic meningitis (Gantz, 2006; Grobbelaar et al., 2018), defined here as at least 4 weeks of symptoms with signs of inflammation in the cerebrospinal fluid (CSF) (Bennett, 2010; Helbrok et al., 2009)."

Further, while it is possible that the bacteria and immunologically active microglia may contribute to increased glycolysis it is more likely that the main driver of dysregulated glucose metabolism is

ischaemia, which is a major disease process underlying TBM and the consequent brain injury, yet ischaemia is only briefly discussed.

Response:

The Reviewer makes a very valid point here – we did not discuss the role of ischaemia. Ischaemia is indeed a major process underlying TBM and the consequent brain injury. Since we were only able to obtain cerebrospinal fluid through a lumbar puncture and were unable to measure/assess the oxygen in the brain, we could not incorporate any strong data on ischaemia into our discussion. What we do know is that within pulmonary TB (PTB), in one of our previous studies (Preez et al., 2017), that gluconolactone was identified as an inflammatory marker of PTB. This metabolite is only formed via the oxidation of glucose (O2 is required for this reaction to occur). This was stated in the manuscript, but we have edited it to incorporate the discussion of ischaemia.

"Insulin resistance during uncontrolled glucose metabolism can lead to the transient oxidation of glucose via glucose oxidase (EC 1.1.3.4), a reaction that requires oxygen (non-hypoxic conditions). Oxidation of glucose leads to the production of gluconolactone, an inflammatory marker found in pulmonary TB (Preez et al., 2017)."

Further to this edit, we have now added the following (including references) to the manuscript:

"Furthermore, we acknowledge that ischaemia is a variable; however, in our study we were unable to determine oxygen levels in the brain. The Warburg-Crabtree effect – increased glycolysis and glucose-induced repression of respiratory flux under hypoxic conditions, in the presence of oxygen (Hammad et al., 2016) – is another phenomenon to consider. We can only speculate based upon other studies regarding uncontrolled glucose metabolism, such as in diabetes (American Diabetes Association, 2017) and marathon runners (Stander et al., 2018), that dysregulated glucose metabolism (upregulated glycolytic flux) is not always related to ischaemia. Indeed, several studies have shown no correlation between CSF lactate levels and cerebral blood flow (Brodersen and Jorgensen, 1974; DeSalles et al., 1986; De Salles et al., 1987)."

The discussion around 2-hydroxybutyrate is interesting, but the data sited is from plasma studies, and therefore extrapolation to the brain needs to be done with caution and I would suggest that the authors look for some data in the brain to support their hypothesis, and if none exist then reword the hypothesis to make clear that this is purely conjecture, not fact.

Response:

The reviewer is absolutely correct. Our discussion around 2-hydroxybutyrate is novel in that this metabolite, to the best of our knowledge, has never been identified as a metabolite of interest in a *M.tb*–infected brain. Data from literature that identifies 2-hydroxybutyrate as metabolite biomarker of glucose intolerance is based upon plasma studies. We have thus reworded this part of our discussion to clearly lineate what is data from literature and that our hypothesis is speculative:

"A significantly elevated (p=0.004) CSF metabolite identified in the TBM cases was 2-hydroxybutyrate. In the literature, 2-hydroybutyrate in the plasma metabolome was found to be a more sensitive marker of transient tissue ischemia than lactate (Laursen et al., 2017), and a selective metabolite biomarker of impaired glucose intolerance (Cobb et al., 2016). To our knowledge, 2-hydoxybutyrate has never been identified as a metabolite of interest in the CSF of a *M.tb*–infected brain. The data sited here is from plasma studies, and therefore extrapolation to the brain needs to be done with caution. Hence, our hypothesis is purely speculative at this point; namely, an increase in 2-hydroxybutyrate in the CSF supports the concept of insulin resistance and uncontrolled glucose metabolism (Gall et al., 2010; Sari et al., 2017; Gu et al., 2019) in a *M.tb*–infected brain, resulting in an inability of glucose to enter the cells, and subsequently reduced cellular glycolysis and ATP depravation. A decrease in cellular

glucose leads to increased ketone synthesis by up-regulating monocarboxylate transporter expression, to allow more lactate and ketone bodies to enter the cells in order to provide more energy substrates for the astrocytes and neurons. This process ultimately leads to the destabilization of the blood-brain barrier (BBB). Hence, the role of 2-hydroxybutyrate in the CSF as a metabolic marker of TBM, and possibly ischaemia, is one that deserves attention.

Furthermore, glucose oxidation leads to increased levels of hydrogen peroxide (H2O2) (Preez et al., 2017). Myeloperoxidase (EC 1.11.1.7), an immunological marker of TBM identified by Manyelo et al. (2019), interacts with H2O2 and activates various oxidative stress pathways (Hampton et al., 1998; Podrez et al., 2000; Klebanoff, 2005) proposed to be needed by microglia to respond to the invading *M.tb* pathogen, supporting our hypothesis that 2-hydroxybutyrate is metabolite marker of uncontrolled glucose metabolism in a *M.tb*–infected brain.

* In the discussion on L-Carnitine the authors suggest that its role in transporting long chain fatty acids may provide a source of substrate for energy production, however, the paper they cite by Yu et al clearly states that the brain does not use long chain fatty acids for energy metabolism. Further, Yu et al suggest that the beneficial role of L-Carnitine in a seizure model may be because it alters GABAergic systems, there is no data in that paper to support its role in oxidative stress as suggested by the authors of this manuscript.

Response:

Thank you to the Reviewer for identifying this. The reference Yu et al. used in the manuscript was incorrect. The reference has been changed to Ferreira & McKenna 2017, which discusses the neuroprotective role of L-carnitine in the brain.

* Importantly these data are a comparison between a diseased state and a healthy state, therefore these findings may not represent TBM specifically but rather an infectious state in the brain, or indeed an inflammatory state in the brain. In the discussion on creatinine the authors state that significantly elevated creatinine and creatine are needed in the Mtb-infected brain. Until any of the data in this manuscript are shown to be TBM specific by a comparative study with a control group of patients with infection of a non-TB origin I do not believe we can conclusively state the specificity of any of this data to the Mtb infected brain.

Response:

The Reviewer is correct in stating the above. We have now included the following to the manuscript to explicitly highlight this:

“It is important to state that the comparison done in our study was between a well-defined definite TBM cohort and a ‘healthy’ control cohort without any neurological symptoms. The refinement of the cohorts studied here delineates our study from previous studies, and allowed us to identify eight new metabolites associated with a *M.tb*-infected brain. Since these eight metabolites are novel (i.e. not previously identified within a *M.tb*-infected brain), our interpretation of them in the CSF is speculative, but is supported by literature where indicated. Therefore these findings may not represent TBM specifically but rather an infectious state in the brain, or indeed an inflammatory state in the brain.”

* The authors discuss glutamate and glutamine at length, but they do not make mention of data which points to the release of excess glutamate by ischaemic neurons and the consequent difficulty for energy deprived neurons to re-establish the ionic membrane gradient, this has been well studied in research on traumatic brain injury, ( see Giza CC, Hovda DA. The Neurometabolic Cascade of Concussion. J Athl Train. 2001;36(3):228-235; Szydlowska K, Tymianski M. Calcium, ischemia and excitotoxicity. Cell Calcium. 2010;47(2):122-129; Barkhoudarian G, Hovda DA, Giza CC. The Molecular Pathophysiology of Concussive Brain Injury - an Update. Phys Med Rehabil Clin N Am.

2016;27(2):373-393). Data on neuroexcitotoxicity in TBM are also available and may be of interest (Rohlwink, U.K., Figaji, A., Wilkinson, K.A., Horswell, S., Sesay, A.K., Deffur, A., Enslin, N., Solomons, R., Van Toorn, R., Eley, B. and Levin, M., 2019. Tuberculous meningitis in children is characterized by compartmentalized immune responses and neural excitotoxicity. Nature communications, 10(1), pp.1-8.)

Response:

The Reviewer is correct in that the potential role of ischaemia cannot be ruled out. We have incorporated the suggested literature into the revised manuscript through the addition of the following paragraph:

"During ischaemic conditions there is an energy deficit resulting in the brain cells not receiving enough energy, resulting in an inability of cells to maintain their ionic gradients necessary for their optimal physiological functions. Neurons are especially affected during low available energy states and experience excessive depolarization and increased release of excitatory neurotransmitters, along with a reduced ability to re-uptake neurotransmitters. During this process an influx of $Ca^{2+}$ and other positive ions occurs, stimulating various cellular responses (such as disturbed mitochondrial potential) that lead to either apoptotic or necrotic neuronal death through death (Szydlowska and Tymianski, 2010). The release of excess glutamate by ischaemic neurons and the consequent difficulty for energy deprived neurons to re-establish the ionic membrane gradient, has been well studied in research on traumatic brain injury (Barkhoudrian et al., 2016; Giza and Hovda, 2001). Rohlwink et al. (2019) suggest that TBM-induced infarction and ischaemia could potentially stimulate glutamate release, which then leads to the excessive binding of glutamate to the *N*-methyl-D-aspartate receptors on neurons, leading to an influx of $Ca^{2+}$ and other positive ions into the neuron, and a cascade of injurious events. Hence, the potential role of ischaemia cannot be ruled out."

* Figure 5 is a very nice demonstration of the interplay between the various metabolic pathways

Response:

Thank you for this comment. We have slightly adjusted the figure to indicate which metabolites were increased (in red) and decreased (in blue) in our study.

* There are a few typos in throughout the manuscript.

Response:

An independent language editor has now worked through the entire revised manuscript in order to improve upon the language.

**ANEXURE 5**

Ethics document

Private Bag X6001, Potchefstroom
South Africa 2520

Tel: 018 299-1111/2222
Web: http://www.nwu.ac.za

**Health Sciences Ethics Office for Research, Training and Support**

**Health Research Ethics Committee (HREC)**
Tel: 018-285 2291
Email: Wayne.Towers@nwu.ac.za

Dr SW Mason
Biochemistry
Centre for Human Metabolomics

26 November 2018

Dear Dr Mason

# APPROVAL OF YOUR APPLICATION BY THE HEALTH RESEARCH ETHICS COMMITTEE (HREC) OF THE FACULTY OF HEALTH SCIENCES

Kindly use the ethics reference number provided above in all future correspondence or documents submitted to the administrative assistant of the Health Research Ethics Committee (HREC) secretariat.

**Study leader: Dr SW Mason**
**Student: CD van Zyl-22130438**
**Application type: Larger study**

**Risk level: Medium (monitoring report required six-monthly)**

**Expiry date: 30 November 2019 (monitoring reports are due at the end of May and November annually until completion)**

You are kindly informed that after review by the HREC, Faculty of Health Sciences, North-West University, your ethics approval application has been successful and was determined to fulfil all requirements for approval. Your study is approved for a year and may commence from 26/11/2018. Continuation of the study is dependent on receipt of the annual (or as otherwise stipulated) monitoring

report and the concomitant issuing of a letter of continuation. A monitoring report should be submitted two months prior to the reporting dates as indicated

i.e. annually for minimal risk studies, six-monthly for medium risk studies and three-monthly for high risk studies, to ensure timely renewal of the study. A final report must be provided at completion of the study or the HREC, Faculty of Health Sciences must be notified if the study is temporarily suspended or terminated. The monitoring report template is obtainable from the Faculty of Health Sciences Ethics Office for Research, Training and Support at Ethics-HRECMonitoring@nwu.ac.za. Annually, a number of studies may be randomly selected for an internal audit.

The HREC, Faculty of Health Sciences requires immediate reporting of any aspects that warrants a change of ethical approval. Any amendments, extensions or other modifications to the proposal or other associated documentation must be submitted to the HREC, Faculty of Health Sciences prior to implementing these changes. These requests should be submitted to Ethics-HRECApply@nwu.ac.za with a cover letter with a specific subject title indicating, “Amendment request: NWU-XXXXX-XX-XX”. The letter should include the title of the approved study, the names of the researchers involved, the nature of the amendment/s being made (indicating what changes have been made as well as where they have been made), which documents have been attached and any further explanation to clarify the amendment request being submitted. The amendments made should be indicated in yellow highlight in the amended documents. The *e-mail*, to which you attach the documents that you send, should have a *specific subject line* indicating that it is an amendment request e.g. “Amendment request: NWU-XXXXX-XX-XX”. This e-mail should indicate the nature of the amendment. This submission will be handled via the expedited process.

Any adverse/unexpected/unforeseen events or incidents must be reported on either an adverse event report form or incident report form to Ethics-HRECIncident-SAE@nwu.ac.za. The *e-mail*, to which you attach the documents that you send, should have a specific subject line indicating that it is a notification of a serious adverse event or incident in a specific project e.g. “SAE/Incident notification: NWU-XXXXX-XX-XX”. Please note that the HREC, Faculty of Health Sciences has the prerogative and authority to ask further questions, seek additional information, require further modification or monitor the conduct of your research or the informed consent process.

The HREC, Faculty of Health Sciences complies with the South African National Health Act 61 (2003), the Regulations on Research with Human Participants (2014), the Ethics in Health Research: Principles, Structures and Processes (2015), the Belmont Report and the Declaration of Helsinki (2013).

We wish you the best as you conduct your research. If you have any questions or need further assistance, please contact the Faculty of Health Sciences Ethics Office for Research, Training and Support at Ethics- HRECApply@nwu.ac.za.

Yours sincerely

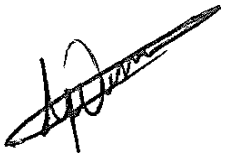

Prof Wayne Towers

HREC Chairperson

Prof Minrie Greeff

Ethics Office Head

Current details: (23239522) G:\My Drive\9. Research and Postgraduate Education\9.1.5 Ethics\NWU-00063-18-S1\9.1.5.4.1_AN_NWU-00063-18-S1_26-11-2018.docm 26 November 2018

File reference: 9.1.5.4.1

Ethics monitoring report

Private Bag X6001, Potchefstroom
South Africa 2520

Tel: +2718 299-1111/2222
Web: http://www.nwu.ac.za

**Faculty of Health Sciences Ethics Office for Research, Training and Support**

Tel: 018 299 2092
Email:minrie.greeff@nwu.ac.za

30 November 2019

Dr SW Mason
Centre for Human Metabolomics

Dear Dr Mason

## FEEDBACK ON NWU-HREC ANNUAL MONITORING REPORT: NWU-00063-18-A1

We would like to thank you for submitting the annual monitoring report for your project entitled, **"*Investigation of metabolic biomarkers for early diagnosis and treatment of tuberculous meningitis in children*"**, to the North-West University Health Research Ethics Committee (NWU-HREC) in a timely manner. Please find below the decision of the NWU-HREC regarding the continuation of your project.

| **Classification** | **Mark with X** | **Comment** | |
|---|---|---|---|
| ***Clarification*** | | | |
| ***Completion (Final report)*** | | | |
| ***Suspended*** | | | |
| ***Continuation*** | **X** | **Date of next monitoring report:** | 31 May 2020 |
| ***Termination*** | | | |

Should you have any further queries, please feel free to contact Mr Buti Majola at your earliest convenience (E-mail: Ethics-HRECMonitoring@nwu.ac.za; Tel: 018 299 2197). We wish you well in your future endeavours.

Yours sincerely

Date: 2019.12.05

12:47:14 +02'00'

Chairperson: NWU-HREC

Current details: (20536690) G:\My Drive\9. Research and Postgraduate Education\9.1.5.5 HREC Monitoring\NWU-00063-18-A1\9.1.5.5.4_Cont_NWU-00063-18-A1_30-11- 2019.docm

30 November 2019

File reference: 9.1.5.5.4



1